UNIVERSITEIT VAN PRETORIA
UNIVERSITY OF PRETORIA
YUNIBESITHI YA PRETORIA

Anti-mycolic acid gallibodies as labelling tools in tuberculosis-related biological samples

by

Mosa Jennifer Molatseli

Student number: 14119189

Submitted in partial fulfilment of the degree:

Magister Scientiae Biochemistry

in the Faculty of Natural and Agricultural Sciences

Department of Biochemistry, Genetics and Microbiology

University of Pretoria

November 2019

DECLARATION OF ORIGINALITY UNIVERSITY OF PRETORIA

The Department of Biochemistry, Genetics and Microbiology places great emphasis upon integrity and ethical conduct in the preparation of all written work submitted for academic evaluation.

While academic staff teach you about referencing techniques and how to avoid plagiarism, you too have a responsibility in this regard. If you are at any stage uncertain as to what is required, you should speak to your lecturer before any written work is submitted.

You are guilty of plagiarism if you copy something from another author's work (e. g a book, an article or a website) without acknowledging the source and pass it off as your own. In effect you are stealing something that belongs to someone else. This is not only the case when you copy work word-for-word (verbatim), but also when you submit someone else's work in a slightly altered form (paraphrase) or use a line of argument without acknowledging it. You are not allowed to use work previously produced by another student. You are also not allowed to let anybody copy your work with the intention of passing if off as his/her work.

Students who commit plagiarism will not be given any credit for plagiarized work. The matter may also be referred to the Disciplinary Committee (Students) for a ruling. Plagiarism is regarded as a serious contravention of the University's rules and can lead to expulsion from the University.

The declaration which follows must accompany all written work submitted while you are a student of the Department of Biochemistry. No written work will be accepted unless the declaration has been completed and attached.

Full names of student: Mosa Jennifer Molatseli

Student number: 14119189

Topic of work: Anti-mycolic acid gallibodies as labelling tools in tuberculosis-related biological samples.

1. I understand what plagiarism is and am aware of the University's policy in this regard.
2. I declare that this dissertation is my own original work. Where other people's work has been used (either from a printed source, Internet or any other source), this has been properly acknowledged and referenced in accordance with departmental requirements.
3. I have not used work previously produced by another student or any other person to hand in as my own.
4. I have not allowed, and will not allow, anyone to copy my work with the intention of passing it off as his or her own work.

SIGNATURE: 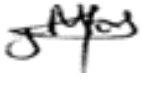 **DATE: November 2019**

ACKNOWLEDGMENTS

1. To God, the source of my joy and the strength of my life. Unto Him be all the glory, the honour and adoration. Romans 8:28 “For we know that all things work together for the good to those who love God, to those who are called according to His purpose.”

2. To my mother who has been my pillar of strength. She believed in me when I no longer believed in myself and she was a constant source of encouragement. She prayed for me daily and reassured me of my capabilities.

3. To my husband for being patient with me throughout my degree and for his amazing love.

4. To my supervisors, Prof. Anton Stoltz, Prof. Jan Verschoor and Dr Yolandy Lemmer for giving me an opportunity to work on a project I really enjoyed and for their guidance, patience and encouragement. A special thank you to Prof Jan Verschoor for availing himself to see me through my degree.

5. To Dr Jeanni Fehrsen and Ms Susan Wemmer for hosting me at the Agricultural Research Council-Onderstepoort Veterinary Institute, and their insightful scientific assistance that helped me gain a deeper understanding about my research work. And as well to Mrs Sandra van Wyngaardt and Ms Sonýa September at the University of Pretoria for their technical assistance.

6. To my colleagues Ms Arthessa Ragavaloo and Ms Heena Ranchod for making every moment memorable.

7. To all my friends, and a special thank you to Ms Ordender Mashele, Mr Kutlwano Sesing, Mr Themba Mfecane, Mr Court Chiramba and Mr Kevin Pule for helping me to keep the faith and for making this journey more enjoyable.

8. To the National Research Foundation for their financial support of this project.

TABLE OF CONTENTS

SUMMARY

Tuberculosis (TB) is a curable infectious disease, but remains a persistent scourge of mankind. It is caused by *Mycobacterium tuberculosis* (*M. tb*) that is a master of survival in the human host, where it can lie dormant for decades, build up resistance to antibiotics and await conditions for relapsing into active disease. It demands a global strategy to manage the epidemic, of which the single most important element is fast and affordable accurate diagnosis. To date, the only reliable diagnosis of active disease depends on sputum samples, which consequently leads to misdiagnosis of extrapulmonary TB, paediatric TB and TB in immune compromised populations such as HIV infected individuals. Because of this, the World Health Organization (WHO) and Foundation for Innovative New Diagnostics (FIND) called for a non-sputum-based triage test for the diagnosis of active tuberculosis (TB) with specific target product profiles (TPP) to eradicate TB by 2035. Our TB research group is focused on the development of TB diagnostics based on the detection of surrogate marker anti-mycolic acids (anti-MA) antibodies in patient blood samples at the point of care level. Mycolic acids (MA) are cell wall waxes from the mycobacterial infectious agent. The group has created recombinant monoclonal antibodies against MA, selected from a semi-synthetic chicken phage displayed antibody gene library, which was found to have inadequate avidity for application in sensitive TB diagnosis. In this study, attempts were made to increase avidity of the recombinant antibodies by creation of oligomers of their antigen binding short chain variable (scFv) fragments. Two strategies were applied to this end: first, shortening the synthetic linker between the heavy and light variable domains of the anti-MA scFv's and second, fusing the scFv genes with the core streptavidin gene that can be expressed to generate spontaneous non-covalent tetramers. Both approaches yielded oligomeric antigen binding proteins with significantly improved avidity for MA binding compared to that of scFv. The best of these were selected to demonstrate their utility in an originally designed lateral flow immunoassay, which opens the way for its further development into that much needed diagnostic device for point of care screening for active TB in disease burdened communities and health centres.

LIST OF FIGURES

LIST OF TABLES

LIST OF ABBREVIATIONS

2XTY	2X Tryptone-yeast
AHSV	African horse sickness virus
AmB	Amphotericin B
Anti-MA scFv SA	Anti-mycolic acids scFv streptavidin
Anti-MA scFv SL	Anti-mycolic acids short-linker scFv's
BCG	Bacillus Calmette-Guerin
BSA	Bovine serum albumin
BTV	Bluetongue virus
CCD	Counter Current Distribution
CD	Cluster of differentiation
CDR	Complementarity determining regions
CPC	Cetylpyridinium chloride
$dddH_2O$	Triple distilled water
DNA	Deoxyribonucleic acid
ELISA	Enzyme-linked immunosorbent assay
Fab	Fragment of antigen binding
EDTA	Ethylenediaminetetraacetic acid
FIND	Foundation for Innovative New Diagnostics
Fv	Variable fragment
HCl	Hydrochloric acid
HIV	Human immunodeficiency virus
HRP	Horseradish peroxidase
H_2SO_4	Sulphuric acid
IB	Inclusion bodies
Ig	Immunoglobulin
IGRA	Interferon gamma release assay
INF- γ	Interferon gamma
IPTG	Isopropyl β-D-1 thiogalactopyranoside
LAM	Lipoarabinomannan
LFIA	Lateral flow indirect immunoassay
LTBI	Latent tuberculosis infection
MA	Mycolic acids
MALIA	Mycolic Acid Lateral Flow Immunoassay
MARTI	Mycolic Acid Real Time Inhibition assay
MDR	Multidrug resistant
$MgCl_2$	Magnesium chloride
MHC	Major histocompatibility complex
M. tb	*Mycobacterium tuberculosis*
mRNA	Messenger ribonucleic acid
m/v	Mass per volume
NaCl	Sodium chloride
Na_2HPO_4	Disodium hydrogen phosphate

NaSCN	Sodium thiocyanide
PBS	Phosphate buffered saline
PCR	Polymerase chain reaction
POC	Point of care
PP	Periplasmic space
PPD	Purified protein derivative
scFv	Short chain variable fragments
SDS-PAGE	Sodium dodecyl sulphate polyacrylamide gel electrophoresis
SEC	Size exclusion chromatography
SDS	Sodium dodecyl sulphate
SOC	Super optimal broth with catabolite repression
SOE	Splicing by overlap extension
SN	Supernatant
SPR	Surface plasmon resonance
TAE	Tris-acetate EDTA
TB	Tuberculosis
TGS	Tris glycine SDS
TMB	Tetramethyl Benzidine
TPP	Target product profiles
TST	Tuberculin skin test
V_H	Heavy chain variable
V_L	Light chain variable
v/v	Volume per volume
WHO	World Health Organization
XDR	Extremely drug resistant

CHAPTER 1: Literature Review

1.1 INTRODUCTION

1.1.1 The burden of TB

Tuberculosis (TB), a chronic infectious disease caused by *Mycobacterium tuberculosis* (*M. tb*) claims the lives of millions of people globally every year (Cole *et al*., 1998). The mortality rates reported by the World Health Organization (WHO) in 2018 were 1.3 million among human immunodeficiency virus (HIV) negative patients and over 300 000 in the HIV co-infected population. The global annual mortality rates of TB still remain at approximately 1.2 to 2.4 million (WHO, 2018). TB is curable with antibiotic treatment that includes first-line defence drugs such as Isoniazid which is bactericidal to rapidly dividing mycobacteria through inhibition of cell wall synthesis (Zhang *et al*., 1992) and Rifampicin that inhibits bacterial transcription (Rosenthal *et al*., 2007, Chopra and Brennan, 1998). Nonetheless, the global burden of TB is exacerbated by HIV co-infection that leads to immunocompromised patients and by the emergence of multidrug resistant (MDR) and extremely drug resistant (XDR) strains that render the first-line defence drugs impotent (Wright *et al*., 2009, Aziz *et al*., 2006). In 2017, an estimated 3.5% of new cases and 18% of previously treated cases globally had MDR-TB. Moreover, over 500 000 people were reported to have developed Rifampicin resistant TB. The countries reported to have the largest numbers of MDR-TB cases are China, India and the Russian Federation (WHO, 2017). Furthermore, about 23% of the world population has latent TB that can develop into active TB. The highest incidence and prevalence rates of TB are in developing countries with Southern Africa being the most affected region (Hamasur *et al*., 2001, Winkler *et al*., 2005). Figure 1-1 depicts global mortality rates excluding death rates among the HIV positive population, with 22 000 reported deaths from South Africa.

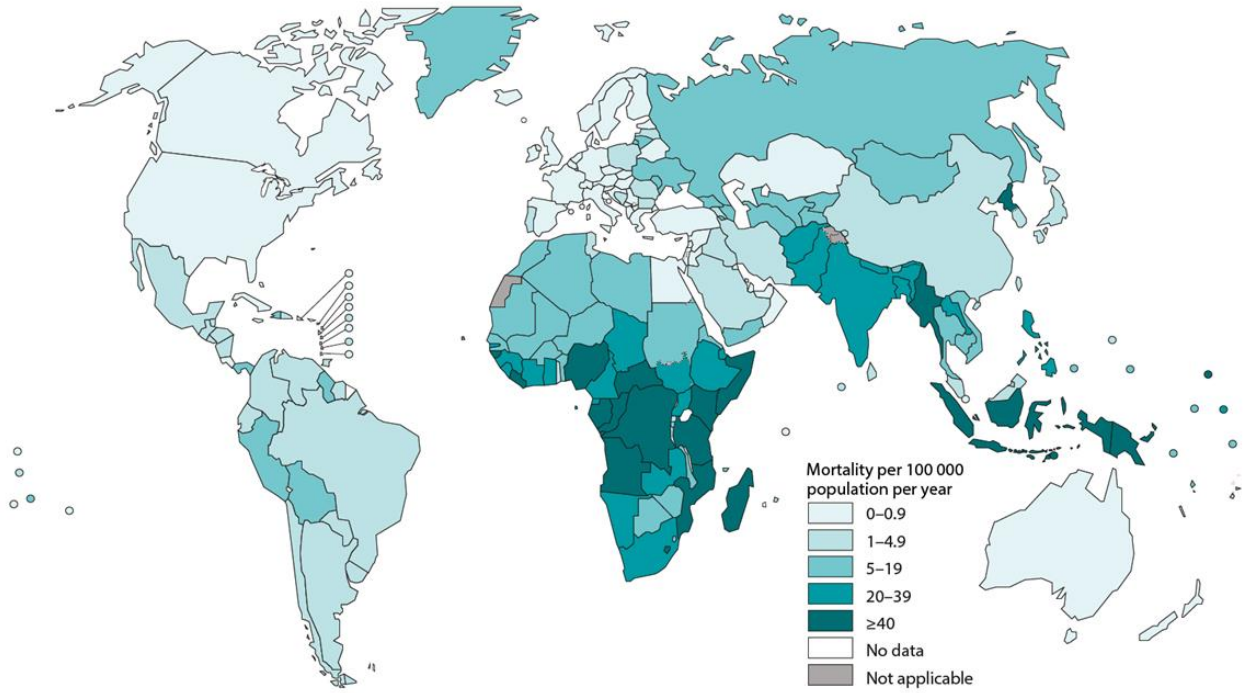

Figure 1-1: The WHO report on global mortality rates. Global mortality rates excluding death rates among HIV positive population. The increase in the intensity of the blue colour indicates an increase in the mortality rates (WHO, 2018).

1.1.2 The etiology of TB

The rod-shaped structure of *M. tb* was first described by the Nobel Prize winner, Robert Koch, who also underlined the urgency of regarding TB as a deadly infectious disease (Koch, 1982). *M. tb* is an acid-fast human pathogen that is spread by aerosol transmission of micro-droplets from the coughing of an infected individual (Smith and Moss, 1994). Once seeded in the lungs through the respiratory tract, the bacilli are engulfed by macrophages where they replicate to induce the innate immune response for the formation of granulomas (Dannenberg Jr and Rook, 1994). The formation of these granulomas at the site of infection is imperative for the containment of the infection and the concentration of immune response to combat the infection (Silva Miranda *et al*., 2012). While the architecture of TB granulomas differs individually, the granulomas are mainly composed of infected, uninfected and foamy macrophages, multinucleated giant cells, epithelioid cells and a perimeter of lymphocytes as shown in Figure 1-2 (Guirado and Schlesinger, 2013). In these well-organized dynamic structures, infected

macrophages and T cells play a fundamental role in maintaining elevated levels of chemokines and cytokines for recruitment of more inflammatory cells at the site of infection as well as clearing of the infection (Marakalala *et al*., 2016). Evasion of the immunity by the pathogen leads to propagation of the bacteria and therefore development of active TB (Marakalala *et al*., 2016). Active TB is characterized by prolonged coughs, phlegm secretion, weight loss and profuse night sweats. Successful containment of the infection due to the immune response fulfilling its role leads to latent TB infection (LTBI) which is clinically asymptomatic (Sterling *et al*., 2010).

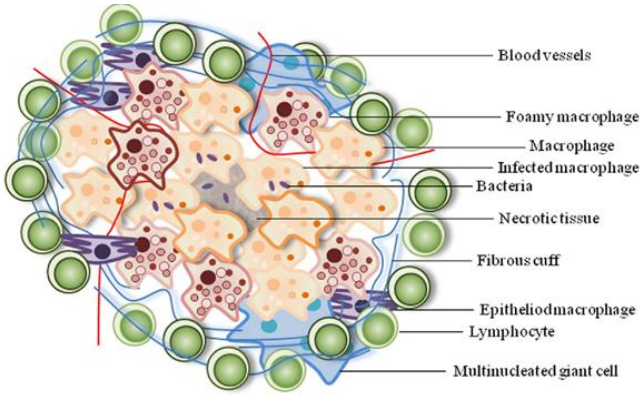

Figure 1-2: The architecture of TB granuloma. Infected, uninfected and foamy macrophages, multinucleated giant cells, epithelioid cells and a perimeter of lymphocytes (Guirado and Schlesinger, 2013).

Granulomas are also renowned for harbouring TB even in a latent state (Guirado and Schlesinger, 2013, de Noronha *et al*., 2008). Granulomas can become a point of dissemination of the bacilli. The ability of *M. tb* to manipulate and evade the host immune system allows the tubercle to persist in granulomas (Silva Miranda *et al*., 2012). Reactivation and escape of the bacilli from the host immune system causes the dissemination of the bacilli outside the lungs by hematogenous spread resulting in extra-pulmonary TB development (Dannenberg Jr and Rook, 1994). While people with LTBI cannot transmit the disease, reactivation of the infection, although poorly understood, can lead to clinical symptoms. Reactivation of LTBI occurs 80% of the time leading to active TB (Silva Miranda *et al*., 2012). Moreover, the possible rupture of the macrophages leads to dissemination of the bacteria, and consequently transmission. Pulmonary

TB remains the most common in both the paediatric and adult population. However, extra-pulmonary TB can establish should the infection escape from the lungs (Cruz and Starke, 2007, de Noronha *et al*., 2008).

The lipid rich cell wall of the bacilli and the ability to manipulate both the innate and acquired immune response are characteristic of the pathogen and are essential for its survival. The cell wall of *M. tb* is composed of complex lipids that include mycolic acids (MAs). MAs are α-alkyl, β-hydroxy mycobacteria-specific 60-90 long carbon chain fatty acids (Beukes *et al*., 2010). MAs exist in three main subclasses in *M. tb*. Alpha-MAs are non-oxygenated (Figure 1-3 A), whereas keto- (Figure 1-3 C) and methoxy-MAs (Figure 1-3 B and 1-3 D) are oxygenated (Pan *et al*., 1999). MAs are presented on cluster of differentiation 1b (CD1b) proteins which are antigen-presenting proteins of dendritic cells that recognize bacterial lipids and stimulate CD4/CD8 double negative T cell line response in contrast to protein antigens that elicit a cellular response of CD8 cytotoxic T cells, $CD4^+$ T helper cells that are targeted by HIV, as well as a humoral response of cytokines.

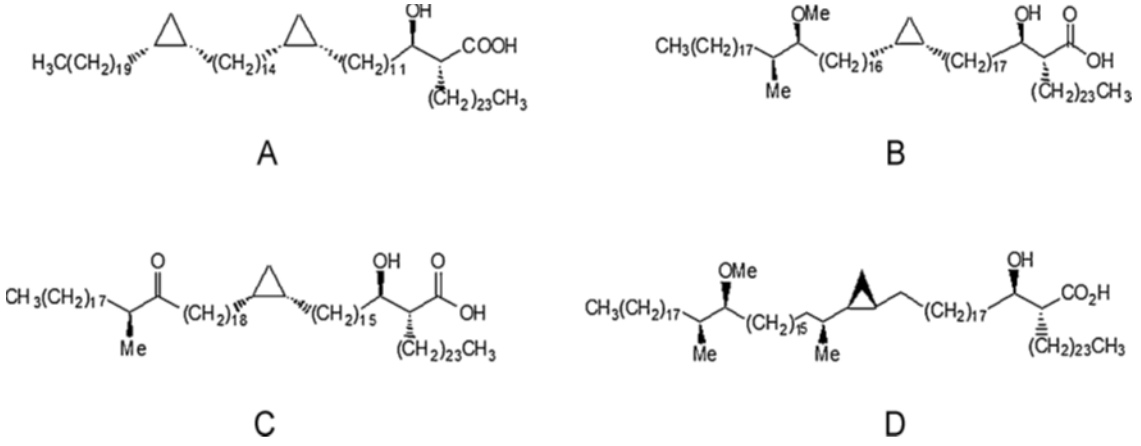

Figure 1-3: The three subclasses of mycolic acids. (A) Alpha-MAs. (C) Keto-MAs. (B and D) Cis- and Trans methoxy-MAs (Beukes *et al*., 2010).

Cholesterol also plays a role in the etiology of TB. Cholesterol is a component of the eukaryotic cell membrane that mediates fluidity. The presence of cholesterol affects the etiology of TB. In *M. tb*, MAs that are bound to the cell wall of the bacillus form an outer membrane that attract

cholesterol into the zone surrounding the cell wall MA layer (Peyron *et al*., 2000) and enables phagocytosis of the bacilli by macrophages (Zhang *et al*., 2010). Cholesterol is also used by the bacilli as an energy and carbon source promoting its survival, replication and persistence in the host (Pandey and Sassetti, 2008).

1.1.3 The global management of TB

TB has been treated effectively using first-line defence drugs since the 1940's (Dye *et al*., 1999). Nonetheless, long drug treatment led to patient non-compliance as many people found it difficult to complete the six to nine months of treatment, consequently contracting drug resistance by non-compliance (Addington, 1979). The long-term treatment of TB is to ensure complete bacilli obliteration as the antibiotics are active against proliferating bacilli, and a short-term treatment can miss persistent, slow growing and dormant mycobacteria which may become genetically or phenotypically antibiotic resistant (Connolly *et al*., 2007). A control strategy called Directly observed treatment, short-course (DOTS) was initiated and endorsed by the WHO to combat TB globally and encourage patient compliance. The DOTS programme aims at monitoring TB treatment closely to improve completion rates through enforcing government commitment; detecting cases by sputum smear microscopy; standardizing treatment regimens directly for six to nine months with observation by a healthcare worker or community health worker for at least the first two months; supplying first-line defence drugs (Isoniazid, Rifampicin, Pyrazinamide and Ethambutol) and standardizing the recording and reporting system that allows for assessment of treatment. Following up on DOTS, a STOP TB initiative was launched in 2006 to dramatically reduce the burden of TB by 2015 (Raviglione and Uplekar, 2006, Copp, 2006) While a lot of countries improved their compliance rates through DOTS (Volmink and Garner, 2007) the global TB mortality rates are still in millions to date.

Vaccination against TB has existed for over 80 years (Luca and Mihaescu, 2013). Bacillus Calmette-Guerin (BCG) vaccine is the primarily used vaccine made from an attenuated strain of *Mycobacterium bovis*. While BCG was shown to be effective against meningitis and disseminated TB in children it unfavourably does not prevent primary infection in adults and more importantly, does not prevent reactivation of latent pulmonary infection (Colditz *et al*.,

1995, Roy *et al*., 2014). A positive impact of BCG vaccination on transmission of *M. tb* is thus restricted.

As a measure to aid effective and rapid treatment of TB, an accurate point of care (POC) TB diagnostics test is essential. A regular TB screening of people at high risk, such as health workers, miners, sex workers and immune compromised people such as those infected with HIV is required. The biggest hindrance to efficient TB control is the lack of an accurate, affordable POC diagnostic test (WHO, 2014). Target product profiles (TPP) exist for this test to facilitate the eradication of TB by 2035. This test must be a highly sensitive test that is based on a biological sample other than sputum such as urine, blood, saliva, or exhaled air, suitable for implementation at lower levels of care to help shorten the delay of diagnosis and enable early treatment. Importantly, a non-sputum-based diagnostic test will enable the diagnosis of extrapulmonary TB, paediatric TB and TB in patients who do not have a productive cough to provide sputum (Denkinger *et al*., 2015b, Denkinger *et al*., 2015a, Warsinske *et al*., 2019).

1.1.4 Current diagnostic methods of TB

Sampling in TB plays a huge role in the reliability of the test results. The inability to obtain quality samples from patients contributes to misdiagnosis of TB. Sputum sampling is quite invasive, requiring taking numerous deep breaths and coughing (Grant *et al*., 2012). In some instances, sputum collection is carried out using physiotherapy-assisted pressure on the chest accompanied by slow expiration. Moreover, the procedure to obtain sputum puts the health care worker that receives the sample from a deep coughing patient at risk. Also, a volume of about 2-10 mL of sputum is required from the patients (Datta *et al*., 2017). Blood and urine samples on the other hand are easy to obtain (Ahmed *et al*., 1998, Kafwabulula *et al*., 2002), can be self-acquired without clinical or health worker assistance and much less volume samples are required for tests. Moreover, the bacilli cannot be acquired by inhalation from blood and urine samples, decreasing the risks for health care workers. For this reason, blood and urine samples are favourable to use in a POC test.

Thus far, the only reliable diagnosis of active disease depends on sputum samples. Sputum-based tests measure the whole or part of the pathogen in the body. Smear microscopy involves direct

smear examination for the presence of acid-fast bacilli using Ziehl-Neelsen staining for the diagnosis of TB (Villeneuve *et al*., 2005). Smear microscopy is employed in most low-income countries as it is inexpensive, quick and easy to use, but its low sensitivity is a major drawback of the technique (Villeneuve *et al*., 2005, Kivihya-Ndugga *et al*., 2004). In an attempt to improve sensitivity, fluorescent stains have been used.

Another sputum-based test is the sputum-based polymerase chain reaction (PCR) that involves the hybridisation of amplified nucleic acids using fluorescently labelled probes that span the DNA of interest (Forbes and Hicks, 1993). While the technique is sensitive and specific, it requires skilled personnel and can therefore not be translated into a POC test (Forbes and Hicks, 1993).

GeneXpert is an automated test that detects *M. tb* DNA using sputum as a sample and in parallel also detects the pathogen's susceptibility to the most effective TB antibiotic, Rifampicin to simultaneously direct the clinician into which type of antibiotic regime to prescribe to the patient. This test detects *M. tb* in less than 2 h, although the process to obtain the sample takes about 24 h. The drawback of GeneXpert is that it is expensive and fails to detect TB in HIV co-infected patients because of low specificity. GeneXpert can generate false positives due to RNA from *M. tb* from previous infections still hiding in the body (Ioannidis *et al*., 2011). Moreover, sputum at three different time points is obligatory to ensure that *M. tb* is not missed. GeneXpert is also an expensive technology.

The current gold standard in TB diagnosis is the highly sensitive technique of bacterial culture of *M. tb* from patients' sputum for 4-8 weeks (Samanich *et al*., 2000). The technique's sensitivity abates in HIV co-infected and paediatric populations as it is difficult to obtain quality sputum samples at adequate volumes from extremely ill patients and children (Ghodbane *et al*., 2014). Sputum based tests are thus, prone to misdiagnosis of extrapulmonary TB, paediatric TB and TB in immune compromised populations such as HIV infected individuals. Moreover, sputum-based tests cannot predict the progression of LTBI to active TB, as active TB is defined as the presence of the bacilli (WHO, 2014).

Other TB tests measure the specific host response to the pathogen. Chest X-ray is a rapid imaging technique that is widely used to identify lung abnormalities. Additionally, the technique

provides an alternative method for diagnosing TB in patients who have difficulty producing good sputum. The downside of the technique is that it is not specific to *M. tb* (Van Cleeff *et al*., 2005, Burrill *et al.*, 2007). Other infectious lymphoproliferative disorders may lead to similar lung abnormalities. Moreover, in HIV/AIDS patients, the sensitivity of chest X-ray is low (Jaeger *et al*., 2014). Also, the technique cannot differentiate old lung lesions from previously cured infections. Tuberculomas are persistent lesions which can be seen in both primary TB and reactivated TB. These pulmonary tuberculomas however, are also seen in patients with healed primary TB (Bhalla *et al*., 2015).

TB Tuberculin skin test (TST) is one the first discovered TB diagnostic tests that is based on the intradermal injection of a purified protein derivative (PPD) which is an extract of *M. tb*. TST TB positive test results are characterized by a red, lumpy dermal reaction after 48-72 h (Doherty *et al*., 2002). The disadvantages of TST is not only the inability to differentiate between exposure and infection with TB, but also the likelihood of false positive results in patients who received BCG vaccine (Chan *et al*., 2000, Ewer *et al*., 2003) TST is therefore used to indicate the absence of TB, rather than to diagnose active TB.

Interferon gamma release assay (IGRA) like TST measure the specific response of a human host to the active infection with *M. tb*. IGRA is a blood-based diagnostic method based on the release of a cytokine interferon gamma (INF-γ) from T-lymphocytes in the blood primed by TB specific antigens (Castro *et al*., 2010). A volume of 1 mL of blood sample is required to carry out the test. Two IGRA methods exist where one IGRA method utilizes a single mixture of synthetic peptides representing the *M. tb* antigenic peptides ESAT-6, CFP-10 and TB7.7, while the other method uses separate mixtures of synthetic peptides representing ESAT-6 and CFP-10. The former IGRA method that is known as QFT-GIT measures the concentration of the INF-γ released whereas the latter measures the number of INF-γ producing cells and is commonly known as T spot. Like TST, however, IGRA fails to distinguish LTBI from active TB (Kardos and Kimball, 2012). Moreover, IGRA is expensive, costing more than $68 per test. Additionally, errors in collecting, transporting and storing the blood specimens, or in running the assay can decrease the accuracy of IGRAs (Lalvani and Pareek, 2010). IGRA cannot be utilize as a POC diagnostic test.

Lateral flow tests have also been used for the diagnosis of TB. Lateral flow tests require little amount of sample and are amenable to be translated into a POC test. Lipoarabinomannan (LAM) is a cell wall lipopolysaccharide *M. tb* antigen (Sada *et al*., 1990) that can be detected from urine samples. High tissue concentrations of LAM at the sites of infection promote the entry of the antigen into the systemic circulation allowing LAM to be detected in serum and urine samples from patients. The LAM POC TB test is therefore non-invasive and has been shown to be specific and sensitive in HIV-associated TB (Lawn *et al*., 2012). The LAM POC test requires 60 µL of urine sample, the test result is obtained after 25 minutes and it costs $3.50 per test (WHO, 2015). The disadvantage of the LAM POC test is low sensitivity in patients who are not at an advanced HIV/AIDS stage (Lawn, 2012, Lawn *et al.*, 2012).

Autopsies are regarded as the universal gold standard for identification of the cause of death and confirmation of the accuracy of clinical diagnosis (Gupta *et al*., 2015). With diagnosis of TB being particularly challenging in HIV co-infected populations, autopsies remain crucial in identifying TB as the cause of death in HIV burdened populations (Gupta *et al*., 2015). Moreover, autopsies reveal clinically undiagnosed diseases in almost 80% of post-mortems done, including extrapulmonary TB that is quite often missed before death (Roulson *et al*., 2005). An accurate POC TB diagnostic test accordingly has the potential to decrease the number of undiagnosed TB cases.

Current technologies hence, accurately diagnose TB but predominantly from sputum samples. Thus, paediatric TB, extrapulmonary TB and TB in immune compromised patients are missed (Oberhelman *et al*., 2015, Lawn and Nicol, 2011). Moreover, none of the TB diagnostic tests to date are amenable to reliable POC field testing for active TB. For field testing, sampling should preferably be safe and non-invasive, typically utilizing blood or urine as samples. Existing tests from blood and urine do not meet the requirements of accuracy (Warsinske *et al*., 2019) and cannot distinguish between active and latent TB (Lawn, 2012, Lawn *et al.*, 2012). Consequently, the WHO and Foundation for Innovative New Diagnostics (FIND) have called for a non-sputum-based triage test for the diagnosis of active tuberculosis (TB). TPPs of the triage test include 90% sensitivity and 70% specificity for the eradication of TB by 2035 (WHO, 2014). Such a test will have the potential to rapidly diagnose active TB and consequently, early treatment can be commenced, thereby decreasing the number of undiagnosed cases revealed by autopsies.

MAs mentioned in 1.2 are also attractive antigens to use in a POC TB diagnostic test. These MAs have a few advantages. The MAs exist as various mixtures with different chain lengths on the cell wall and the different class mixtures of MAs (alpha-, keto- and methoxy MAs) present in the mycobacterial strains afford the different strains a fingerprint, consequently allowing for the specific diagnosis of *M. tb* (Butler and Guthertz, 2001, Song *et al.*, 2009). The negative perception about the use of protein antigens is that no single protein antigen or combinations of protein antigens produce a sufficiently sensitive signal for accurate diagnosis (Dowdy *et al*., 2011). The use of lipid antigens such as MAs may be applied to overcome this problem. This is because the MAs elicit an immune response independent of the major histocompatibility complex (MHC) and T cells owing to their lipid nature (Thanyani *et al*., 2008) with the oxygenated MAs, in particular methoxy MA, eliciting a greater immune response (Beukes *et al*., 2010). An immune response independent of the MHC is therefore critical for the success of reliable TB detection in HIV/AIDS co-infected individuals (Thanyani *et al*., 2008, Verschoor *et al*., 2012). The B-cells of the immune system produce antibodies against MAs in large quantities which can be detected in immunoassays, making them a plausible biomarker in TB infected patients.

1.1.5 Natural anti-mycolic acid and anti-cholesterol antibodies

TB patients produce immunoglobulin G (IgG) and immunoglobulin M (IgM) antibodies against MAs (Roberts, 2008). The examination of the reactivity of human sera from tuberculosis patients through the detection of anti-MA antibodies was first published in 1999 (Pan *et al*., 1999), who suggested that the oxygenated methoxy- and keto-MAs were more antigenic than alpha-MA. Both self-prepared and commercially available (Sigma-Aldrich) natural MA preparations have compositions of around 50% alpha-MA and 50% oxygenated MA. Of the latter, the ratio of keto- to methoxy-MA is around 1:2 for Sigma MA and 1:4 for self-prepared MA (Ndlandla *et al*., 2016). Human CD1b elicit cytolytic and IFN-γ responses by presenting mycobacterial lipids to CD4/CD8 double negative T cells (Schofield *et al.*, 1999). The stimulation of polyclonal B-cells leads to the production of anti-mycolic acid (anti-MA) antibodies that can be detected in large amounts in serodiagnostic tests (Schleicher *et al*., 2002). Although MAs seem to be an attractive antigen for the detection of biomarker anti-MA antibodies in TB patients, cholesterol gives rise

to cross-reactivity in TB detection. Human sera contain variable levels of natural anti-cholesterol antibodies (Alving and Wassef, 1999, Horváth and Bíró, 2003). IgM and IgG isotypes against cholesterol were first reported in 1988 (Swartz *et al.*, 1988). The human anti-cholesterol antibodies recognize MAs, thus, yield false TB positive results in TB negative patients. The antigenic similarity between MAs and cholesterol explains the cross-reactivity of TB negative sera containing anti-cholesterol antibodies binding equally well to MAs (Benadie *et al*., 2008). Studies have shown the indistinctive binding of Amphotericin B (AmB) - a cholesterol binding anti-fungal drug - to MAs, indicating that the packed structure of MAs is similar to that of cholesterol (Benadie *et al.*, 2008). Serum concentrations of anti-cholesterol antibodies also increase with HIV infection and other pulmonary pathogens probably due to the release of phospholipids and cholesterol from the exposure to certain micro-organisms (Horváth *et al.*, 2001). Human anti-cholesterol antibodies thereby complicate TB detection when antigenic MAs are used, and even more so in HIV co-infected populations (Alving and Wassef, 1999). For this reason, it is important to have recombinant antibodies available that have greater avidity for binding MA than natural human anti-cholesterol antibodies to be used in lateral flow immunoassays as labelled anti-MA antibodies for competitive binding with serum anti-MA antibodies to MAs in the POC TB test.

1.1.6 Mycolic Acid Real Time Inhibition assay (MARTI)

In light of anti-MA antibodies being plausible surrogate markers for TB infection, Mycolic Acid Antibody Real Time Inhibition (MARTI) assay was developed and patented in 2005 by the University of Pretoria (Verschoor *et al*., 2012). This assay accurately detects low affinity anti-MA antibodies in patients for TB diagnosis (Verschoor *et al*., 2012). In the MARTI test, an ESPRIT-based surface plasmon resonance (SPR) biosensor is used to detect the anti-MA antibodies (Lemmer *et al*., 2009). In the test, MAs are immobilized on sensor discs with a hydrophobic surface in cuvettes. The hydrophobic surfaces are activated by treatment with a cationic detergent, cetylpyridinium chloride (CPC) before adsorbing the antigen. The detergent saponin, is then used to block unbound sites, followed by an extensive washing with phosphate buffered saline (PBS) to obtain a stable baseline. An inhibition study is then undertaken by first exposing a high dilution serum (1:4000) to the MA coated surfaces. A more concentrated serum

(1:500) that was preincubated with empty liposomes (control) or MA containing liposomes is then exposed to the MA coat. For TB positive patients, the binding of serum antibodies to MAs contained in liposomes reduces the quantity of the serum antibodies present that can bind to the MAs immobilized on the hydrophobic surface. A TB positive patient's MARTI profile will therefore display a high degree of difference of antibody binding to immobilized MAs in comparison to the control, owing to inhibition by serum anti-MA antibodies. A TB negative profile will display a similar degree of antibody binding to immobilized MAs as the control due to lack of inhibition (Lemmer *et al*., 2009). A typical SPR profile is shown in Figure 1-4 with the different steps. MARTI uses a drop of blood from a finger prick, eliminating the need for sample freezing or storing. Although quite accurate, it is too sophisticated, slow and expensive to predict its implementation in any other environment than reference laboratories. However, MARTI aspires to be used in the field as a POC test.

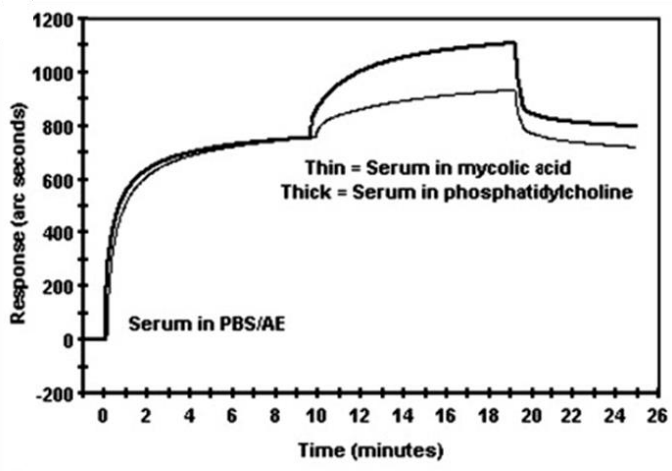

Figure 1-4: A representative MARTI biosensor test read-out. Biosensor read-out for detecting anti-MA antibodies as surrogate markers of active TB. Inhibition of human TB positive patient serum antibody binding with MA liposomes (thin) or empty liposomes (thick) on a cuvette surface coated with immobilized MA liposomes (Thanyani *et al*., 2008).

1.1.7 Mycolic Acid Lateral Flow Immunoassay (MALIA)

Having encountered the challenges brought about by MARTI, a Mycolic acid lateral flow immunoassay (MALIA) test was developed and patented by the University of Pretoria (Verschoor and Beukes, 2011) on the basis of the first success at being able to select and apply

chicken monoclonal antibody fragment (scFv) proteins in an immunoassay. This test is designed to be a negative predictor test and has the potential to be used as a POC device for the detection of TB in less than 1 h using labelled gallibodies, i.e. anti-MA scFv's recombinantly grafted onto the Fc domains of chicken IgG (Ranchod *et al.*, 2018). Moreover, MALIA does not rely on electricity, making the test an ideal POC diagnostic test. The MALIA test is a competitive test between serum anti-MA antibodies and conjugate pad colloidal gold-labelled gallibodies for the binding of MAs immobilized on the control line. As shown in Figure 1-5, the colloidal gold-labelled gallibodies will be mixed with the patient blood sample (analyte) and moved by capillary flow towards the test and control lines for results visualization. On the control line, anti-chicken antibodies will be immobilized to capture excess gold-labelled gallibodies, resulting in a bright red line owing to aggregation of colloidal gold. On the test line, MAs will be immobilized to allow for competitive binding of gold-labelled gallibodies and serum anti-MA antibodies, which will result in a less red colour for a TB positive patient owing to competitive binding of serum anti-MA antibodies from the patient sample with the gold-labelled gallibodies on the MA coated test line (Ranchod *et al.*, 2018).

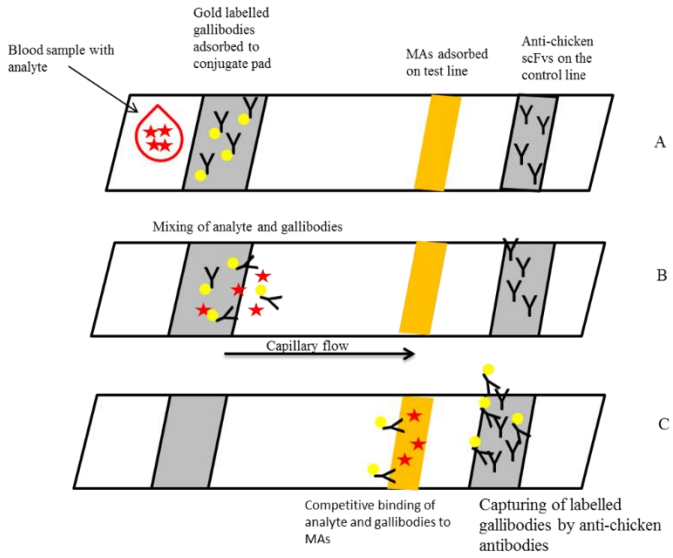

<u>Figure 1-5</u>: Graphic explanation of the design of the MALIA TB diagnostic test. (A) Patient sample adsorbed to the sample pad. (B) Capillary flow of patient sample to the conjugate pad and mixing of the patient sample with the gold-labelled gallibodies. (C) Competitive binding of serum anti-MA antibodies and gold-labelled antibodies to immobilized MAs on the test line. And eventually, the capturing of excess gold-labelled gallibodies by anti-chicken antibodies on the control line (Verschoor and Beukes, 2011).

The significance of the gallibodies for use as labelling tools is reliant on their monoclonal nature. Monoclonal antibodies are highly specific not only because they recognize a single epitope but also because there is reduced probability of cross-reactivity. The affinities and avidities of the gallibodies to the MAs are much higher as compared to their component chicken scFv's due to double valency of the gallibodies (Ranchod *et al*., 2018).

1.1.8 The Gallibody: anti-mycolic acid (anti-MA) antibodies

Gallibodies are chicken-based immunoglobulins with short chain variable fragments (scFv's). These gallibodies are anti-MA antibodies that were engineered for high affinity binding to MA from unstable, low affinity recombinant chicken scFv's obtained from a chicken phage library. The use of chicken scFv's was because chickens - like humans - present lipid antigens including MAs on CD1 proteins. Furthermore, recombinant antibodies can be rapidly and easily generated without relying on animal immunisation (Plückthun and Pack, 1997, Winter *et al*., 1994). The engineering of the recombinant chicken scFv's was into two types of IgY formats, one that is theoretically flexible (CH1-4) and the other that is more rigid (CH2-4) as shown in Figure 1-6 (Ranchod *et al*., 2018). The serological distinctiveness of these gallibodies from mammalian immunoglobulins makes the gallibodies suitable for utilization in immune tests. Notably, two of the gallibodies, 18CH1-4 and 18CH2-4 were shown to be specific to TB as there was no evidence of cross-reactivity with cholesterol, as thus making these gallibodies more favourable for use in serodiagnostic tests (Wemmer, 2008, Ranchod *et al*., 2018).

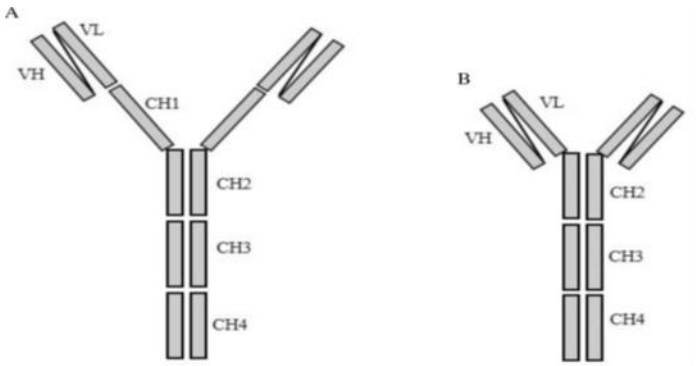

Figure 1-6: Structures of two types of IgY formats of engineered gallibodies. (A) scFvIgY (CH1-4), (B) scFvIgY (CH2-4) (Ranchod *et al*., 2018).

1.2 BACKGROUND OF THE STUDY

1.2.1 Phage display technology and recombinant anti-mycolic acid (anti-MA) antibodies

The research work reported in this dissertation builds on the initial successes of the TB biochemistry research group at the University of Pretoria to create recombinant anti-MA gallibodies derived from a phage display library of chicken antibody genes (Ranchod *et al*., 2018). Phage display technology is a technique that was first used in the display of foreign peptide fragments on the surface of M13 filamentous phage particles (Smith, 1985). Over the years, phage display technology has since evolved into a widely utilized technique for the expression of large amounts of proteins, peptides and antibodies of interest as fusion coat proteins. Phage display is currently the gold standard for the identification and isolation of monoclonal antibodies (Hamidon *et al*., 2018). For expression to occur, the gene encoding the protein of interest is inserted into the gene encoding phage coat protein III. A collection of the natural human heavy chain and light chain antibody repertoire can be replicated to form immune phage libraries; naïve phage libraries; synthetic and semi-synthetic phage libraries. These libraries are constructed from messenger ribonucleic acid (mRNA) IgG genes, mRNA of IgM genes from healthy non-immunized individuals, synthetic sequences or a mixture of synthetic and natural sequences respectively (Hamidon *et al*., 2018, Smith and Petrenko, 1997).

Phage display technology has several advantages over other antibody isolation methods. The technology is cheaper and allows for rapid production of monoclonal antibodies (Hamidon *et al*.,

2018). Moreover, the technique allows for more control over the selection process, affords the opportunity to design and manipulate the antibodies, and produces numerous clones for antibody expression (Hamidon *et al*., 2018). Additionally, the phage-bound antibodies can be displayed in various formats such as variable fragments (Fv), antigen binding fragments (Fab) and the scFv format as shown in Figure 1-7. The scFv format is a small recombinant antibody in which the heavy chain variable region (V_H) and the light chain variable region (V_L) are covalently joined by a flexible polypeptide linker of variable length (Bird *et al*., 1988, Huston *et al*., 1988, Holliger and Winter, 1997). To be put to useful utility, it is imperative for scFv's to possess adequate affinity and specificity for the antigen, stability over long periods of storage, and high expression yields. However, not all antibodies selected from a library will have these characteristics (Holliger and Winter, 1997). Therefore, antibody engineering methods can be applied to the genes coding for the antibodies to allow for the re-selection of fully functional antibodies with improved characteristics.

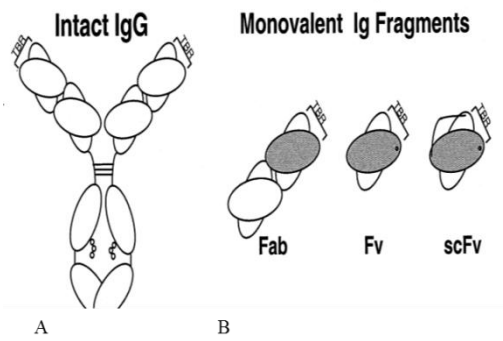

Figure 1-7: Structures of potential products from recombinant antibody of intact IgG. (A) Full antibody IgG; (B) Fragment for antigen binding (Fab). Variable fragment (Fv) and short chain variable fragment (scFv). TBR is the target binding region (Kortt *et al*., 2001).

1.2.2 The *Nkuku* library

The *Nkuku* library, in deference to its source of origin referring to the Zulu word for chicken, was created by the Onderstepoort Veterinary Institute (Van Wyngaardt *et al*., 2004). The library is a diverse semi-synthetic scFv library with 2 x 10^9 clones of veterinary and medical importance. Although large combinatorial libraries are based on human immunoglobulin genes,

chicken was used as an alternative to create the library as it beneficially utilizes two sets of primers to access its entire V_H and V_L chain repertoire in contrast to humans and other mammals. The library also has a flexible linker of 15 amino acids consisting of four glycine residues and a serine residue $(Gly_4Ser)_3$ (Van Wyngaardt *et al.*, 2004).

The library was found to be diverse enough to become a versatile source of antibody fragments. The viability of the *Nkuku* library was tested in the enzyme-linked immunosorbent (ELISA) assay against African horse sickness virus (AHSV); Bluetongue virus (BTV); Bluetongue antibodies; a 16 kDa protein mycobacterial protein; a 65 kDa heat shock protein from *Mycobacterium bovis* and MAs (Van Wyngaardt *et al.*, 2004, Beukes *et al.*, 2010, Wemmer, 2008, Ranchod *et al.*, 2018, Sixholo, 2008). The panning of the library against MAs provided three stable phage clones 12, 16 and 18 out of 270 clones from which scFv's could be expressed (Ndlandla *et al.*, 2016). Characterization of these anti-mycolic acid (anti-MA) scFv's portrayed that the scFv's from phage clones 12 and 16 recognized both cholesterol and MAs while the scFv from phage clone 18 was more specific to MAs. In the ELISA assay, the three anti-MA scFv's yielded low binding signals to MAs (Ndlandla *et al.*, 2016, Ranchod *et al.*, 2018). In this study, the same anti-MA scFv's from the *Nkuku* phage library were used as source materials to generate the oligomers from.

1.2.3 Increasing the affinity and avidity of anti-MA scFv's through oligomerization

The gallibodies mentioned in 1.8 and derived from the phage display library of chicken antibody genes were found to have adequate binding avidity to MAs (Ranchod *et al.*, 2018). The avidity of these gallibodies were however insufficient for the application in the MALIA test as the gallibodies lost functional binding to MAs upon standard gold-labelling (Alma Tryts, 2019). Subsequently, alternative methods to generate oligomeric anti-MA scFv's for the use in MALIA were deemed mandatory. The grafting of monovalent recombinant scFv's on their Fc domains by genetic engineering yields multivalent antibodies with increased functional binding avidity and decreased dissociation rates in antigen-antibody complexes (Cuesta *et al.*, 2010). While various methods exist to increase the affinity and avidity of monoclonal scFv's to their target antigens, this study will focus on two strategies; the shortening of the flexible polypeptide joining the V_H and V_L chains, and the production of recombinant scFv-streptavidin fusion proteins. Shortening

of the linkers of scFv's results in the non-covalent pairing of complementary V_H and V_L chains from adjacent scFv's to form oligomeric scFv's (Bie *et al*., 2010, Holliger *et al*., 1993, Holliger and Winter, 1997) whereas the fusion of scFv genes to streptavidin gene results in self-assembling non-covalent tetrameric proteins (Schultz *et al*., 2000). The anti-MA scFv's from the *Nkuku* library were engineered using both of these strategies in this study to prepare the desired multimeric scFv's, which were then characterised for their potential application in a prototype MALIA for eventual use in a POC TB diagnostic test.

1.3 AIM, HYPOTHESIS AND OBJECTIVES

1.3.1 Aim

The aim of this study is to increase the functional binding avidity of existing chicken monoclonal recombinant anti-mycolic acid (anti-MA) antibodies through multimer formation and test their utility in lateral flow immunoassay.

1.3.2 Hypotheses

H_1: Oligomeric scFv's from the scFv phage clones 12, 16 and 18 can be obtained by either shortening of the linker peptide between the V_H and V_L domains (SL), or by creating scFv-streptavidin fusion proteins (SA).

H_2: Prokaryotically expressed SL- and SA-oligomers of anti-MA scFv's derived from any of the scFv phage clones 12, 16 and 18 can be applied in the prototype lateral flow immunoassay to recognise immobilised MA.

1.3.3 Objectives

A. Increase of the avidity of the *Nkuku* library anti-MA scFv's through the formation of oligomers by shortening the polypeptide linker from between the V_H and V_L domains 15 amino acids to one glycine residue.
B. Increase of the avidity of the *Nkuku* library anti-MA scFv's through the formation of tetramers by the fusion of the anti-MA scFv's with streptavidin.
C. Investigate the cross-reactivity of the anti-MA oligomers to bind cholesterol.
D. Compare the performance of the oligomers from the two different oligomeric strategies in a typical lateral flow indirect immunoassay.

CHAPTER 2: Anti-mycolic acids short-linker scFv's (Anti-MA scFv SLs)

2.1 INTRODUCTION

The avidity of antibodies can be improved by increasing the number of binding sites to the antigen (Crothers and Metzger, 1972, Winter and Milstein, 1991). The variable heavy (V_H) and variable light (V_L) chains of short chain variable fragments (scFv's) are joined together by a flexible polypeptide called a linker (Holliger and Winter, 1997). The variable domains of the scFv's of the *Nkuku* library are linked together by a 15 residue polypeptide composed of four glycine residues and one serine residue $(Gly_4Ser)_3$ (Van Wyngaardt *et al*., 2004). Shortening of the linker of scFv's results in the non-covalent coupling of complementary V_H and V_L chains from two adjacent scFv's to form multimeric antibodies (Bie *et al*., 2010, Holliger *et al*., 1993, Holliger and Winter, 1997). Commonly, shortening the linker to less than 12 amino acid residues results in bivalent molecules called diabodies (Holliger and Winter, 1997). Further shortening of the linker can result in interactions between three or four scFv's, forming trimers and tetramers which are called triabodies and tetrabodies respectively as shown in Figure 2-1 (Kortt *et al*., 2001). The types of multibodies formed, however, are not only dependent on the number of amino acid residues removed, but also on the orientation of the variable domains. V_H-V_L and V_L-V_H orientations of the same scFv with an identical linker length and composition may lead to production of different oligomers as shown in Figure 2-1 (Kortt *et al*., 2001). For this reason, the types of multibodies formed can seldom be predicted.

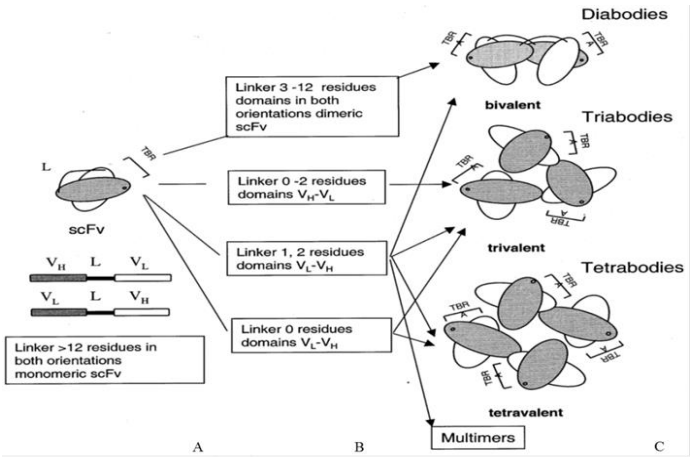

Figure 2-1: Combinations of V-domain orientation and peptide linker length. (A) Monomeric scFv with a 12 or more residue linker irrespective of V-domain orientation. (B) Combinations of V-domain orientations and linker lengths. (C) Resulting oligomers (Kortt *et al*., 2001).

Other studies have used the approach of shortening scFv linkers to increase the binding affinity and avidity of antibodies to the target for clinical diagnostic purposes. Most of these studies are on cancer cell research. In one study, dimeric scFv's were generated to target hepatocellular carcinoma tissue. In this study, immunohistochemistry was performed on hepatocellular carcinoma tissue and non-hepatocellular carcinoma tissue, and the results revealed specific binding to the hepatocellular carcinoma tissue (Bie *et al*., 2010). Some cancer-targeting scFv multimers from other studies like anti-HER2 C6.5 diabody and L19 dimer have undergone preclinical assessment (Adams *et al*., 1998, Viti *et al*., 1999). Other studies have used the strategy to target erythrocyte agglutination, plant fungi and viruses and influenza virus surface glycoproteins (Kortt *et al*., 1997, Saldarelli *et al*., 2005, Yajima *et al*., 2008). In this chapter, the *Nkuku* library anti-mycolic acids (anti-MA) scFv's with 15 amino acid residue linkers will be engineered to a glycine residue linker with the aim to form multimeric anti-MA scFv's with increased binding avidity to the antigenic mycolic acids (MAs).

2.1.1 Hypothesis

Oligomeric scFv's from the scFv phage clones 12, 16 and 18 can be obtained by shortening of the linker peptide between the V_H and V_L domains.

2.2 MATERIALS AND METHODS

2.2.1 Materials

A. Reagents

Phosphate buffered saline (PBS) 1X, pH 7.4: Sodium chloride (NaCl, 0.137 M), potassium chloride (KCl, 0.0027 M), disodium hydrogen phosphate (Na_2HPO_4, 0.01 M), and monopotassium phosphate (KH_2PO_4, 0.0018 M). All reagents obtained from Sigma-Aldrich, Missouri, USA. All reagents have quality of ≥99.0%. The PBS was autoclaved at 121ºC before use.

Mycolic acid from *Mycobacterium tuberculosis* (bovine strain): MAs (0.25 mg) dissolved in 1 mL hexane (≥99%, Sigma-Aldrich, Missouri, USA).

ELISA block buffer pH 7.4: Casein hydrolysate (4% (m/v), Oxoid, United Kingdom) dissolved in PBS pH 7.4.

ELISA dilution buffer pH 7.4: Casein hydrolysate (4% (m/v)) dissolved in PBS pH 7.4 and 0.05% (v/v) Tween20 (Sigma-Aldrich, Missouri, USA).

ELISA wash buffer pH 7.4: PBS (1 X) pH 7.4 and 0.1% (v/v) Tween20.

Anti-c-MYC Horseradish peroxidase (HRP): Mouse monoclonal anti-c-MYC antibody (clone 9E10) conjugated to peroxidase, (Roche Diagnostics GmbH, Germany).

Gallibody HRP: Goat anti-chicken Fc: HRP (AbD Serotic, Kidlington, UK).

ELISA Tetramethyl Benzidine (TMB) HRP substrate solution: TMB Single solution (Life Technologies, California, USA).

Blot test Tetramethyl Benzidine (TMB) HRP substrate solution: TMB for blot tests (Life Technologies, California, USA).

Tryptone-yeast (2XTY) media: Tryptone (1.6% (m/v)) (Sigma-Aldrich, Missouri, USA), 1% (m/v) yeast extract (Sigma-Aldrich, Missouri, USA) and 0.5% (m/v) NaCl in 1 L Triple distilled water ($dddH_2O$). Media was autoclaved at 121°C for 20 minutes.

Glucose (20% (m/v)): Glucose (20 g) (≥99.5%, Sigma-Aldrich, Missouri, USA), dissolved in 100 mL dddH_2O and autoclaved at 121ºC for 20 minutes.

Culture media (2XTY): 2XTY media (9 mL), 1 mL 20% (m/v) glucose and 10 µL ampicillin (Sigma-Aldrich, Missouri, USA).

Isopropyl β-D-1 thiogalactopyranoside (IPTG) media: 2XTY media (10 mL), 1 mM IPTG (≥99%) (Sigma-Aldrich, Missouri, USA) and 10 µM ampicillin (Sigma-Aldrich, Missouri, USA).

Dilution media (2XTY): 2XTY (45 mL), 5 mL 20% (m/v) glucose and 50 µL ampicillin.

Cell lysis solution: PBS (1X) pH 7.4, 1 M NaCl and 1 mM Ethylenediaminetetraacetic acid (EDTA) (Sigma-Aldrich, Missouri, USA).

Tris-buffered saline (TBS) 1X, pH 7.2: Tris (0.0025 M) (≥99.9%, Sigma-Aldrich, Missouri, USA) and 0.15 M NaCl.

Tris-acetate EDTA (TAE) buffer 50X, pH 8.3: EDTA (50 mM), 2 M Tris, 1 M glacial acetic acid (≥99.9%, Sigma-Aldrich, Missouri, USA).

Agarose gel: Agarose (1% (m/v)) dissolved 1X TAE with 1% (v/v) ethidium bromide (Sigma-Aldrich, Missouri, USA).

Agar plates: Tryptone (1% (m/v)), 0.5% (m/v) yeast extract, 0.8% (m/v) NaCl and 1.5% (m/v) agar in 1 L dddH_2O and autoclaved at 121°C for 20 minutes.

Agarose column wash buffer: TBS (1X) and 0.05% (v/v) Tween20 pH 7.2.

ScFv elution buffer: Glycine (0.1 M) (≥99%, Sigma-Aldrich, Missouri, USA) added to 0.02 M hydrochloric acid (HCl) (37%, Sigma-Aldrich, Missouri, USA) adjusted to pH 2.7.

Agarose column storage buffer: TBS (1X) and 0.05% (v/v) sodium azide (≥99%, Sigma-Aldrich, Missouri, USA).

ELISA Stop solution: Sulphuric acid (2 N) (H_2SO_4) (99.999%, Sigma-Aldrich, Missouri, USA).

Super optimal broth with catabolite repression (SOC) medium: Tryptone (2% (m/v)), 0.5% (m/v) yeast extract, 10 mM NaCl, 2.5 mM KCl, 10 mM Magnesium chloride ($MgCl_2$) (≥98%, Sigma-Aldrich, Missouri, USA), 10 mM Magnesium sulphate ($MgSO_4$) (≥95%, Sigma-Aldrich, Missouri, USA) and 20 mM glucose.

TGS buffer 1X, pH 8.3: Tris (0.025 M), 0.192 M glycine and 0.1% (w/v) Sodium dodecyl sulphate (SDS) (Sigma-Aldrich, Missouri, USA).

Towbin buffer 1X, pH 8.3: Tris (25 mM) and 192 mM glycine.

Western blot block buffer: Bovine serum albumin (BSA) (2% (m/v)) (≥98.0%, Sigma-Aldrich, Missouri, USA) dissolved in 1X PBS pH 7.4.

Western blot anti-c-MYC HRP conjugate: BSA (2% (m/v)) dissolved in PBS pH 7.4, 0.05% (v/v) Tween20, 1:1000 Mouse monoclonal anti-c-MYC antibody (clone 9E10) HRP conjugated to peroxidase.

Western blot wash buffer: PBS (1X) pH 7.4 and 0.05% (v/v) Tween20.

Anti-MA glycerol stocks: Anti-MA phage clones 12, 16 and 18 bacterial cultures diluted with 60% (m/v) glucose to a 15% (v/v) final glucose concentration. Stored at -80ºC. The stocks were obtained from Onderstepoort Veterinary Institute and were prepared according to Ranchod *et al.* (2018).

Affinity columns: Anti-c-MYC conjugated Pierce agarose (Thermo Scientific, Waltham, Massachusetts, USA). The agarose was packed in empty 15 mL disposable plastic drip columns with polyethylene frits (Thermo Scientific, Waltham, Massachusetts, USA). The bed volume used was 1 mL.

β-mercaptoethanol: ≥99.0% (Sigma-Aldrich, Missouri, USA).

SDS-PAGE gels: Pre-made Bio-Rad protean TGX gels (Thermo Scientific, Waltham, Massachusetts, USA) with a 4-15% gel concentration gradient.

Protein marker: Precision Plus protein marker (Bio-Rad, USA).

Western blotting filter papers: Western blotting cotton sheet filter papers (Thermo Scientific, Waltham, Massachusetts, USA).

Western blotting membrane: Invitrolon PVDF 0.45 µm pore size membrane (Thermo Scientific, Waltham, Massachusetts, USA).

Deoxyribonucleic acid (DNA) extraction kit: QIAquick miniprep kit (QIAGEN, Hilden, Germany).

Gel extraction kit: QIAquick gel extraction kit (QIAGEN, Hilden, Germany).

Polymerase chain reaction PCR clean up purification kit: QIAquick PCR purification kit (QIAGEN, Hilden, Germany).

DNA marker: Hyperladder 1 kbp (Bioline, London, UK).

Super optimal broth with catabolite (SOC) medium: Yeast extract (0.5% (m/v)), 2% (m/v) tryptone, 10 mM NaCl, 2.5 mM KCl, 10 mM $MgCl_2$, 10 mM $MgSO_4$ (≥99.5%, Sigma-Aldrich, Missouri, USA) and 20 mM glucose.

Size exclusion chromatography column: Superdex 75 10/300 GL column, separation range of 3 – 70 kDa, bed volume 24 mL, void volume 7.2 mL and sample volume 25-500 µL.

B. Glassware

All glassware was washed with 10% (v/v) Contrad (Thermo Scientific, Waltham, Massachusetts, USA), rinsed with $dddH_2O$ and acetone (≥99.5%) (Sigma-Aldrich, Missouri, USA), autoclaved at 121ºC for 60 minutes (Hiclave HVE-50 Hirayama autoclave) and dried in an oven at 110ºC (Ecotherm Labotech oven).

C. Equipment

Table 2-1: Table of equipment.

Machinery	Model, company and country
Laminar flow	Fibatron Laminar flow cabinet Johannesburg, South Africa
Centrifuge	Beckman Avanti J-25, California, USA
Spectrophotometers	UV-1600PC UV-VIS, VWR, Pennsylvania, USA Molecular devices SpectraMax Paradigm Microplate Reader Multimode Detection Platform San Jose, California, USA
Water bath	FMH 110 electronics, Labotec, Midrand, South Africa
Incubator	Labcon shaking incubator, 1081K, CA, USA
Electroporation machine	Bio-Rad Gene pulser II Apparatus, CA, USA
pH meter	Metrohm Swiss Mode 827 Lab, Herisau, Switzerland
Heat block	Reacti-Therm Thermo Scientific Pierce III, USA
Vortex	Velp Scientifica Wizard Advanced IR Vortex Mixer, Italy
Analytical balance	Labotech, USA
Table top centrifuge	Eppendorf Centrifuge 5451R, Hamburg, Germany
ELISA plate washer	Wellwash 4MK2, Thermo electron corporation, Shanghai, China
ELISA plate reader	Multiskan EX type 335 Thermo electron corporation, Shanghai, China
Superdex 75 10/300 GL	Amersham Pharmacia, Uppsala, Sweden
Electrophoresis machine	Bio Rad miniprotean tetra system, CA, USA
UV transluminator	White/UV transluminator UVP, USA
Polymerase chain reaction (PCR) machine	Eppendorf EP gradient S, Hamburg, Germany

2.2.2 Methods

A. Expression of the 15 amino acid linker anti-mycolic acids scFv's (anti-MA scFv's)

Overnight growth of anti-MA scFv's from clones 12, 16 and 18

The anti-mycolic acids (anti-MA) scFv genes were cloned into pHEN1 vector as shown in Figure 2-2. Small amounts of frozen anti-MA bacterial culture glycerol stocks from phage clones 12, 16 and 18 - the size of 0.5 mm beads - were inoculated into 10 mL of 2XTY culture medium and resuspended at room temperature. The clones in the growth medium were incubated at 37ºC overnight (16 h) with shaking at 220 revolutions per minute (rpm) for bacterial cell growth. After 16 h, a 1:100 dilution of the bacterial overnight culture was prepared by adding 500 µL of the bacterial overnight culture to 50 mL of 2XTY dilution medium and grown at 37ºC with shaking at 220 rpm, until the optical density ($OD_{600\ nm}$) was between 0.6 - 0.9. Once the cultures reached the target $OD600_{nm}$, the cultures were pelleted at 2000 x g for 10 minutes at 4ºC and the supernatants were discarded. The pellets were resuspended in 10 mL IPTG medium, and the cells were grown at 30ºC with shaking at 220 rpm for 16 h to induce the expression of anti-MA scFv's.

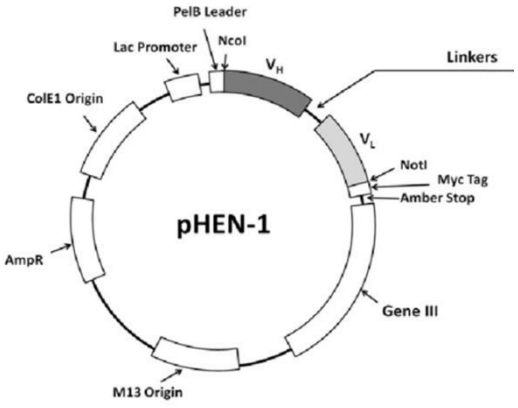

Figure 2-2: pHEN1 phagemid construct. The V_H and V_L chains are cloned in pHEN1 phagemid vector downstream of Lac promoter and PelB leader sequence (Li *et al*., 2015).

Obtaining supernatant (SN) and periplasmic (PP) anti-MA scFv's

To obtain secreted anti-MA scFv's in the supernatant, the IPTG cultures were pelleted at 2000 x g for 15 minutes at 4ºC. The yellow-gold supernatant (SN) contained the secreted anti-MA scFv's. To obtain periplasmic (PP) anti-MA scFv's, the pellets were resuspended in ice cold lysis solution that was 1/10 of the volume of the bacterial overnight culture, and the resuspended cells were left on ice for 30 minutes to facilitate the lysis reaction. The resuspended cells were centrifuged in a table top centrifuge at 4ºC at 7500 x g for 10 minutes to obtain the supernatants. The supernatants were then re-centrifuged at 16 000 x g for 10 minutes at 4ºC to remove insoluble debris, thus obtaining PP scFv's. The SN and PP anti-MA scFv's were stored at -20ºC.

Indirect enzyme-linked immunosorbent assay (ELISA) to determine the activity of SN and PP anti-MA scFv's on mycolic acids (MAs)

Half of the wells of a Nunc Maxisorp 96 well immunoplate (Sigma-Aldrich, Missouri, USA) were coated with 50 µL of freshly distilled hexane per well using a Hamilton syringe (Sigma-Aldrich, Missouri, USA). Hexane was used as a negative antigen control. The other half of the wells were coated with 0.25 mg/mL mycolic acids (MAs) dissolved in hexane. The well contents were left to evaporate at room temperature before wrapping the plate in foil and storing overnight at 4ºC to ensure successful coating. The following day, blocking of non-specific binding was carried out by pipetting 300 µL of ELISA block buffer per well. The plate was incubated in a container overlaid with a damp paper towel for 1 h at 37ºC. The plate was washed three times with ELISA wash buffer using ELISA plate washer. The anti-MA scFv's were diluted with the ELISA dilution buffer at a 1:1 volume ratio by mixing 25 µL of the scFv's with 25 µL of the ELISA dilution buffer per well and incubating for 1 h at 37ºC to allow binding of anti-MA scFv's to the MAs. For the scFv negative control, ELISA dilution buffer (50 µL) without scFv's was pipetted in designated wells. The plate was washed again three times with ELISA wash buffer to remove unbound scFv's. A volume of 50 µL per well of secondary antibody (mouse monoclonal anti-c-MYC antibody (clone 9E10) conjugated to peroxidase) diluted to 1:000 with ELISA dilution buffer was pipetted per well and incubated for 1 h at 37ºC to allow for binding to the anti-MA scFv's. The plate was then washed three times to remove unbound secondary antibody, before 50 µL of substrate TMB Single solution was added to each well and incubated for 2-5 minutes at room temperature for colour development. TMB is

oxidized faster than other HRP substrates, therefore the 2-5 minutes incubation time allows for reading the plate at major absorbance maxima at 370 nm, with 652 nm as the reference wavelength to compensate for individual well surface irregularities. ELISA stop solution was used to stop the reaction by pipetting 50 µL per well. The absorbance was read at 450 nm using SpectraMax paradigm plate reader. The binding signals were then corrected by subtracting the background signal obtained from the relevant antigen negative control wells. Statistical analysis (standard deviation from the mean, the reproducibility of signals by biological repeats and student t-test) was carried out on the obtained data.

Affinity column purification of anti-MA scFv's from phage clones 12, 16 and 18

Anti-c-MYC conjugated Pierce agarose (Thermo Scientific, Waltham, Massachusetts, USA) was used to capture the anti-MA scFv's as these scFv's have a c-MYC tag. The columns were first equilibrated with five bed volumes of 1X Tris Buffered Saline (TBS), pH 7.2. The SN and PP anti-MA scFv's from one clone were pooled together and passed through the column three times, and the flow through was collected. This was done with the anti-MA scFv's from each of the three clones 12, 16 and 18. The columns were washed twice with ten bed volumes of 1X TBS/0.05% (v/v) Tween20 and the washes were collected. The anti-MA scFv's were eluted with 1 mL of 0.1 M glycine/HCl pH 2.7 and collected in tubes containing 500 µL of 1 M Tris buffer pH 9.1 for neutralization. Four separate elutions were carried out for each of the scFv's from the three clones. The columns were then regenerated with five bed volumes of 3 M sodium thiocyanide (NaSCN). The columns were washed again with ten bed volumes of 1X TBS then stored in 1X TBS/0.05% (v/v) sodium azide. The eluted anti-MA scFv's were concentrated in conjunction with a buffer change in PBS pH 7.4 using Vivaspin PES protein concentrator columns that possess a membrane with a cutoff retention of everything larger than 10 000 Daltons (VivaScience, Sartorius Group, United Kingdom). All fractions were stored at -20ºC to track the purification.

Determination of anti-MA scFv's concentrations using Bradford assay

Bovine serum albumin (BSA) was used to make a protein standard curve for the determination of the anti-MA scFv concentrations. BSA dilutions - 0 mg/mL, 0.06 mg/mL 0.125 mg/mL, 0.25 mg/mL, 0.5 mg/mL and 1 mg/mL - were prepared in PBS pH 7.4. To 10 µL of each BSA dilution and concentrated anti-MA scFv sample, 250 µL of a 1:4 diluted Bradford reagent in PBS was added and the reaction was incubated at room temperature for 5 minutes before reading the absorbance at 595 nm using SpectraMax spectrophotometer.

Sodium dodecyl sulphate polyacrylamide gel electrophoresis (SDS-PAGE) and Western blot to track the purification of the scFv's

β-mercaptoethanol was added to the fractions from the affinity column purification (section 2.2.2 A). Volumes of 15 µL of the β-mercaptoethanol were added to the purified anti-MA scFv's, the flowthrough and the wash fractions at a 1:1 volume ratio and heated for 5 minutes at 100ºC. The reactions were further vortexed after heating and were allowed to reach room temperature. Pre-made Bio-Rad protean TGX gels (Thermo Scientific, Waltham, Massachusetts, USA) with a 4-15% gel concentration gradient were used for the separation of the denatured proteins. The TGX gels were assembled in Miniprotean Tetra System tanks as per manufacturer's instruction. Briefly, the green strips at the bottom of each pre-made gel were removed to allow the current to pass through the gels, then the gels were assembled onto the cassette, ensuring that the short side of each gel comb was facing the inside of the cassette. The arms of the cassette were clamped on the gels to secure the gels. The cassette holding the gels was then placed into the tank such that the anode of the cassette corresponded with the anode of the tank. The 1X TGS running buffer was then used to fill the inside of the cassettes to the brim before filling the tank to the specified marks. The combs of the gels were gently removed, and the wells were each washed with TGS buffer by pipetting, so as to remove the bubbles in the wells. The samples were then loaded in each well to the maximum capacity, being 30 µL per well. A Precision Plus protein (Bio-Rad, USA) molecular mass marker of 250 kDa was used (10 µL). The electrophoretic reaction was carried out for 1 h at 100 V. A modified SDS-PAGE analysis was then carried out under denaturing and non-denaturing conditions by adding 2X β-mercaptoethanol (denaturing sample buffer) to one anti-MA scFv sample and non-denaturing protein sample buffer to the other anti-MA scFv sample from the same clone.

After SDS-PAGE, Western blot analysis was carried out to detect the anti-MA scFv's. The gels were disassembled from the cassettes and equilibrated in 1X towbin buffer. The Western blot sandwich for each gel was then assembled by first placing a sponge soaked in towbin buffer on the bottom support grid. A Western blotting filter membrane (Thermo Scientific, Waltham, Massachusetts, USA) pre-soaked in towbin buffer was then overlaid on the sponge followed by the gel. An Invitrolon PVDF 0.45 µm pore size membrane (Thermo Scientific, Waltham, Massachusetts, USA) was then recharged with absolute methanol by soaking, followed by equilibration in towbin buffer before overlaying on the gel without trapping bubbles. Another towbin buffer pre-soaked filter paper was placed on the membrane before completing the sandwich with a towbin buffer pre-soaked sponge and another support grid. The sandwich was then placed in the electrophoretic tank such that the gel was facing the anode. The tank was then filled with towbin buffer to the specified marks. The electrophoretic reaction was carried out for 1 h at 100 V. After 1 h, the sandwich was disassembled, and the membrane was immersed and incubated in Western blot block buffer for 1 h at room temperature on a rocker at 10 rpm. After incubation, the membrane was incubated in Western blot anti-c-MYC HRP conjugate for 1 h at room temperature on a rocker (10 rpm). The membrane was then washed three times with 10 mL of Western blot wash buffer after incubation to remove unbound conjugate before developing with TMB blot solution for 2-5 minutes. Because TMB oxidation is fast, colour development must be recorded before 5 minutes, after which precipitation of the product colour stain occurs which yields inaccurate results. The reaction was stopped by washing with dddH_2O and the membrane was left to dry overnight.

B. Increasing avidities of anti-MA scFv's through multimer formation

Linker shortening of anti-MA scFv's

Deoxyribonucleic acid (DNA) templates for each anti-MA scFv from the three phage clones 12, 16 and 18 were obtained by growing bacterial overnight cultures from glycerol stocks in 10 mL of 2XTY medium and incubating at 37ºC overnight (16 h) with shaking at 220 rpm. Plasmid extraction was carried out from the bacterial overnight cultures by pelleting the bacterial cells at 4000 x g for 10 minutes. A QIAquick miniprep kit (QIAGEN, Germany) was used to obtain the

pHEN1 vector DNA from the cells according to the manufacturer's instructions. Briefly, a lysis buffer was used to resuspend and break open the cells, a neutralization buffer was added to the reaction to renature circular DNA and encourage its dissolution while the linear DNA remained denatured and out of solution. The reactions were centrifuged at 16 000 x g for 10 minutes to obtain supernatants, the supernatants with DNA were bound to QIAprep spin columns with silica gel membranes composed of sodium silicate. The columns were washed with a wash buffer containing ethanol to remove trace nuclease activity, salts and other impurities. The DNA was eluted with a low-ionic elution buffer that weakens the hydrogen bonds.

The variable light chain (V_L) and variable heavy chain (V_H) genes of anti-MA scFv's from each of the three phage clones were amplified from the pHEN1 DNA using the primers from Table 2-2 excluding HendG1 and LstartG1. Only the sequences of the V_L and V_H would be amplified from the template anti-MA scFv DNA; therefore, excluding the translation codons for the normal 15 amino acid polypeptide linker of chicken anti-MA scFv's consisting of four glycine residues and one serine residue $(Gly_4Ser)_3$. The polymerase chain reaction (PCR) was carried out as indicated in Table 2-3.

Table 2-2: Primer sequences for shortening the anti-MA scFv linker.

Name	Sequence
Hend1	5' CCG GAG GAG ACG ATG ACT TCG G 3'
Lstart1	5' GCG CTG ACT CAG CCG TCC TCG G 3'
HendG1	5' CGG CTG AGT CAG CGC TCC GGA GGA GAC GA 3'
LstartG1	5' TCG TCT CCT CCG GAG CGC TGA CTC AGC CG 3'
Sfi1L	5' GTC CTC GCA ACT GCG GCC CAG CCG GCC CTG ATG GCG GCC GTG ACG 3'
LCNot1	5' TGA TGG TGG CGG CCG CAT TGG GCT G 3'

Table 2-3: Polymerase chain reaction (PCR) to amplify V_H and V_L chains of anti-MA scFv's.

REAGENT	V_H	V_L
10X Ex Taq Buffer (TaKaRa)	1/10 of final volume	1/10 of final volume
dNTPs (TaKaRa)	2.5 mM	2.5 mM
Sfi1L (forward primer) (Inqaba Biotech Industries)	0.2 µM -1 µM	-
Hend1 (reverse primer) (Inqaba Biotech Industries)	0.2 µM -1 µM	-
LStart1 (forward primer) (Inqaba Biotech Industries)	-	0.2 µM -1 µM
LCNot1 (reverse primer) (Inqaba Biotech Industries)	-	0.2 µM -1 µM
Plasmid DNA	< 1 µg	< 1µg
Ex Taq polymerase (TaKaRa)	5 U/µL	5 U/µL
Nuclease free water	Make up the volume	Make up the volume
TOTAL	50 µL	50 µL

The PCR conditions were 1 cycle of initial denaturation at 96ºC for 15 sec, followed by 30 cycles of denaturation at 94ºC for 15 sec, annealing at 55ºC for 15 sec and extension at 72ºC for 30 sec, finishing with a final extension at 72ºC for 1 minute.

A 1% (m/v) agarose/1X TAE gel with 1% (v/v) ethidium bromide was prepared for the electrophoretic analysis of the PCR products. The gel was immersed in an electrophoretic tank filled with 1X TAE buffer pH 8.3, such that the wells faced the negative (anode) side of the tank. Hyperladder 1 kbp (Bioline, London, UK) was used as reference for the band sizes. Each PCR sample was mixed with 6X loading dye (Promega, USA) at a 5:1 ratio before being loaded in the gel wells. The electrophoresis was carried out at 100 V for 40 minutes.

The V_H and V_L chain bands were analysed using a UV transilluminator. The bands were extracted from the gel using QIAquick gel extraction kit (QIAGEN, Hilden, Germany) according to the manufacturer's instructions. Briefly, the DNA was excised from the gel and the extracted gel containing DNA was dissolved in 3 volumes of a pH indicator containing dissolution buffer and heated to 50ºC to encourage dissolution. The pH indicator ensures that the buffer maintains its acidic pH important for DNA adsorption to the silica gel membrane. A single volume of isopropanol was added to increase DNA yield. The DNA was then bound to the column with silica gel membrane through hydrogen bonding. A wash buffer containing ethanol was used to

remove impurities, salts and unbound DNA. A low-ionic elution buffer was then used to elute the DNA by weakening the DNA-silica gel membrane hydrogen bonds.

A second PCR to add a single glycine codon that would serve as a linker was then carried out using the primers from Table 2-2, however, the primers HendG1 and LStartG1 replaced Hend1 and LStart1 respectively, as these primers are responsible for the addition of the glycine codon on the chains. The PCR was carried out as indicated in Table 2-4.

Table 2-4: PCR to add glycine codon as a linker to the V_H and V_L chains of the anti-MA scFv's.

REAGENT	V_H	V_L
10X Ex Taq Buffer (TaKaRa)	1/10 of final volume	1/10 of final volume
dNTPs (TaKaRa)	2.5 mM	2.5 mM
Sfi1L (forward primer) (Inqaba Biotech Industries)	0.2 µM -1 µM	-
HendG1 (reverse primer) (Inqaba Biotech Industries)	0.2 µM -1 µM	-
LStartG1 (forward primer) (Inqaba Biotech Industries)	-	0.2 µM -1 µM
LCNot1 (reverse primer) (Inqaba Biotech Industries)	-	0.2 µM -1 µM
Plasmid DNA	< 1 µg	< 1µg
Ex Taq polymerase (TaKaRa)	5 U/µL	5 U/µL
Nuclease free water	Make up the volume	Make up the volume
TOTAL	50 µL	50 µL

The PCR conditions remained the same as for the first PCR. Electrophoretic analysis of the PCR products was carried out as was done previously to investigate successful amplification.

The PCR products were then purified using QIAquick PCR purification kit (QIAGEN, Germany) according to the manufacturer's instructions. The kit functions the same way as the gel extraction kit through binding of DNA to silica gel membrane, washing off impurities and eluting the DNA with a low-ionic solution.

The V_H and V_L chains were then joined to form a complete anti-MA scFv through splicing by overlap extension (SOE). It is important to mention that the V_H-V_L orientation of the anti-MA

scFv's was maintained. In the SOE PCR reaction the V_H and V_L chains prime each other. The SOE was carried out as indicated in Table 2-5.

Table 2-5: SOE PCR to join the V_H and V_L chains of the anti-MA scFv's.

REAGENT	$V_H + V_L$
Ex Taq Buffer (TaKaRa)	1/10 of final volume
dNTPs (TaKaRa)	2.5 mM
Ex Taq polymerase (TaKaRa)	5 U/µL
DNA	100 ng each
pfu enzyme (Promega)	5 U/µL
Nuclease free water	Make up volume
TOTAL	50 µL

The SOE PCR conditions were 1 cycle of initial denaturation at 95ºC for 15 sec, followed by 15 cycles of denaturation at 95ºC for 30 sec, annealing at 47ºC for 30 sec (T_m for the overlap) and extension at 72ºC for 30 sec, finishing with a final extension at 72ºC for 1 minute.

Another PCR to add *Sfi1* and *LCNot1* restriction enzyme (RE) sites to the SOE PCR products was carried out as indicated in Table 2-6.

Table 2-6: PCR to add *Sfi1* and *LCNot1* RE sites to SOE PCR products.

REAGENT	$V_H + V_L$
Ex Taq Buffer (TaKaRa)	1/10 of final volume
dNTPs (TaKaRa)	2.5 mM
Ex Taq polymerase (TaKaRa)	5 U/µL
pfu enzyme (Promega)	5 U/µL
Sfi1 enzyme (Inqaba Biotech Industries)	5 U/µL
LCNot1 enzyme (Inqaba Biotech Industries)	5 U/µL
Nuclease free water	Make up volume
TOTAL	50 µL

To each of the SOE PCR products, 50 µL of the RE extension mixture was added. The PCR conditions were 1 cycle of initial denaturation at 95ºC for 15 sec, followed by 25 cycles of denaturation at 95ºC for 30 sec, annealing at 60ºC for 30 sec (T_m for *Sfi1* and *LCNot1* enzymes) and extension at 72ºC for 60 sec, finishing with a final extension at 72ºC for 1 minute.

Electrophoretic analysis of the PCR products was carried out as was done previously to investigate successful joining of the V_H and V_L chains after addition of the glycine codon. Gel extraction was also carried out to purify the DNA fragments.

Sfi1 and *LCNot1* double RE digestion of the pHEN1 vector and SOE anti-MA scFv DNAs was carried out for ligation. The pHEN1 vector DNA was obtained by growing bacterial overnight culture from the pHEN1 bacterial glycerol stock in 2XTY medium at 37ºC with shaking at 220 rpm and extracting the vector DNA using QIAprep kit. *Sfi1* reaction was carried out first and the *LCNot1* reaction second as indicated in Tables 2-7 and 2-8 respectively.

Table 2-7: *Sfi1* digestion of SOE anti-MA scFv DNAs and pHEN1 vector DNA.

REAGENT	SOE anti-MA scFv	pHEN1
10X Buffer M (Roche)	1/10 of final volume	1/10 of final volume
Sfi1L enzyme (Inqaba Biotech Industries)	0.2 µM -1 µM	0.2 µM – 1 µM
DNA	100 ng	100 ng
Nuclease free water	Make up the volume	Make up the volume
TOTAL	50 µL	50 µL

The *Sfi1* digestion was carried out at 50ºC for 2 h.

Table 2-8: *LCNot1* digestion of SOE anti-MA scFv DNAs and pHEN1 vector DNA.

REAGENT	SOE scFv DNAs	pHEN1
NaCl	0.15 M	0.15 M
LCNot1 enzyme (Inqaba Biotech Industries)	10 U/µL	10 U/µL
Tris, pH 8	0.012 M	0.012 M
Xho1 enzyme (Promega)	-	5 U/µL
Nuclease free water	Make up the volume	Make up volume
TOTAL	50 µL	50 µL

Half of the *LCNot1* reaction was then added to 1 volume of *Sfi1* digestion reaction products. The *Xho1* enzyme was added to discourage religation of the vector. The *LCNot1* digestion was carried out at 37ºC for 2 h.

The PCR products were purified using QIAquick PCR purification kit and an electrophoretic analysis of the PCR products was carried out as was done previously to ensure that the DNA fragments were not completely digested. The DNA fragments were extracted from the gel using QIAquick gel extraction kit.

Ligation of SOE anti-MA scFv DNAs and pHEN1 vector DNA was then carried out as indicated in Table 2-9. The molar ratio of ligation of vector DNA to scFv DNA was 100 ng to 40 ng respectively.

Table 2-9: Ligation of the SOE anti-MA scFv DNAs to pHEN1 DNA.

REAGENT	Final concentrations
pHEN1 DNA	100 ng
SOE scFv DNA	40 ng
10X T4 Ligase Buffer (Promega)	1/10 of final volume
T4 DNA ligase (Promega)	0.2 µM -1 µM
Nuclease free water	Make up the volume
TOTAL	10 µL

The ligation reaction was carried out at 15ºC overnight and purified using QIAquick PCR purification kit. The ligated DNAs were eluted using water to avoid sparks during electroporation of the ligated DNAs into *E. coli* TG1 competent cells (Inqaba Biotech Industries).

The clone 12, 16 and 18 ligation reaction products were electroporated into the TG1 cells at a 1:9 volume ratio respectively such that the ligation reaction products were 5 µL and the TG1 cells were 40 µL each. The DNA and cell mixtures were mixed by tapping the tube before subjecting to 1700 V in electroporation cuvettes and transferring to super optimal broth with catabolite repression (SOC) medium pre-warmed at 37ºC. The SOC medium was 955 µL, such that the whole reaction mixture amounted to 1 mL. The electroporated TG1 cells were incubated at 37ºC

with shaking at 220 rpm for 1 h. After incubation, 100 µL of the cultures were plated on fresh agar plates. The remaining 900 µL of the cultures were pelleted at 4000 x g for 10 minutes, and the supernatants discarded, leaving only a little supernatant to resuspend the pellets and plate them. The plates were then lidded and incubated upside down on a damp paper towel at 37ºC overnight to allow for bacterial colony growth.

Colony PCR was carried out using the primers indicated in Table 2-10 to investigate which of the overnight colonies had the desired inserts. Agar reference plates were gridded for each anti-MA scFv from each phage clone, such that each agar plate had 10 blocks, one block per colony. For each phage clone, 10 colonies were picked using sterile tips. A colony was picked up and transferred to a block on the reference plate by gently swabbing before resuspending the remaining cells on the tip in 25 µL of water. The resuspended colony cells were then heated at 100ºC for 5 minutes to break the cells open and were immediately cooled on ice. This was done for 10 colonies per clone. The reference plates were then incubated upside down on a damp paper towel at 37ºC overnight to allow for growth. Colony PCR was carried out as indicated in Table 2-11.

Table 2-10: Primer sequences for colony PCR and Sanger sequencing.

Name	Sequence
OP52	5’ CCC TCA TAG TTA CGC TAA CG 3’
M13 reverse	5’ CAG GAA ACA GCT ATG AC 3’

Table 2-11: Colony PCR to investigate anti-MA scFv SL inserts.

REAGENT	Final concentrations
Go Taq Green (Promega)	12.5 µL
DNA	10 µL
OP52 primer (Inqaba Biotech Industries)	0.2 µM -1 µM
M13 reverse primer (Inqaba Biotech Industries)	0.2 µM -1 µM
Nuclease free water	Make up the volume
TOTAL	25 µL

The PCR conditions were 1 cycle of initial denaturation at 96ºC for 15 sec, followed by 25 cycles of denaturation at 96ºC for 1 minute, annealing at 50ºC for 30 sec, extension at 72ºC for 1 minute, finishing with a final extension at 72ºC for 1 minutes. Electrophoretic analysis was carried out on the PCR products. However, loading dye was not used as *Go Taq Green* acts as a loading dye. The PCR products were then purified using QIAquick PCR purification before sequencing by the Sanger method (Inqaba Biotech Industries). These engineered scFv's were now dubbed anti-MA scFv short-linkers (anti-MA scFv SLs). Sequence alignment was carried out using Bioedit (Hall, 1999). From phage clone 12, three anti-MA scFv SLs with correct sequences were picked being scFv SLs 12-1, 12-2 and 12-3. From phage clone 16, two anti-MA scFv SLs with correct sequences were scFv SLs 16-4 and 16-7 and from phage clone 18, two anti-MA scFv SLs with correct sequences were scFv SLs 18-11 and 18-13. Bacterial overnight cultures of the colonies carrying correct sequence anti-MA scFv SLs were grown in 2XTY medium at 37ºC with shaking at 220 rpm. Bacterial glycerol stocks of the anti-MA scFv SLs were then made from the bacterial overnight cultures by adding 60% (m/v) glucose to the cultures to a final glucose concentration of 15% (v/v). The stocks were stored at -80ºC. An ELISA was carried out as described in section 2.2.2 A to investigate active anti-MA scFv SLs after obtaining SN and PP anti-MA scFv SLs as described in section 2.2.2 A.

Affinity column purification of anti-MA scFv SLs

The same method as described in section 2.2.2 A was followed with a few optimizations. To the unpurified samples, 0.1% (v/v) SDS was added and the reactions were incubated at room temperature for 15 minutes to slightly denature the oligomeric scFv's and allow for binding on the anti-c-MYC agarose column. 1X TGS buffer was then added to the samples at a 1:1 volume ratio before passing through the column. The TGS dilution was to prevent the SDS from damaging the column. The oligomeric scFv's were eluted using 3 M NaSCN to encourage maximal elution. The scFv's were concentrated in conjunction with a buffer change into PBS pH 7.4 as described in section 2.2.2 A. To determine protein concentration, the Bradford assay was carried out as described in section 2.2.2 A. Afterwards, SDS-PAGE and Western blot analysis on anti-MA scFv SLs were carried to track the purification of the multimeric scFv's as described in section 2.2.1 A.

Size exclusion chromatography (SEC) on anti-MA scFv SLs

A Superdex 75 10/300 GL column, with a separation range of 3 – 70 kDa and a void volume of 24 mL was used for size exclusion chromatography (SEC). Two proteins of known molecular weight, casein (24 kDa) and BSA (67 kDa) were used to calibrate the column. The purified samples of anti-MA scFv SLs were then passed through the column to obtain their profiles according to the manufacturer's instructions. A minimum concentration of 0.5 mg/mL for each sample was used.

2.3 RESULTS

2.3.1 Activity of the 15 amino acid liner anti-mycolic acid scFv's (anti-MA scFv's)

After the expression of supernatant (SN) or periplasmic space (PP) anti-MA scFv's, the scFv's were used to probe MAs in an indirect ELISA assay, therefore depicting the scFv's activity and avidity towards the antigenic MAs as shown in Figure 2-3.

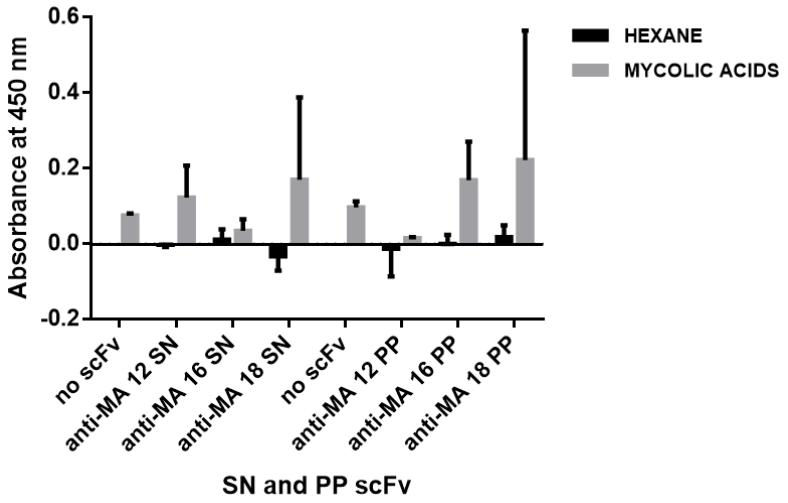

Figure 2-3: Indirect ELISA assay to determine the MA binding activity of the anti-MA scFv's. The scFv's were obtained from phage clones 12, 16 and 18 in either the supernatant (SN) or periplasmic space (PP). ELISA plates were coated with either MA antigen or hexane as antigen control. The binding activity of ELISA dilution buffer (with no antibody) and anti-MA scFv's from either the culture SN or PP space diluted with ELISA dilution buffer on a 1:1 volume ratio were tested on MAs and hexane (antigen control) and measured using anti-c-MYC mouse monoclonal antibody-HRP conjugate. The anti-MA scFv's binding signals were then corrected by subtracting the background signal generated by the binding of the ELISA dilution buffer (without antibody) on the hexane (antigen control). Data represents two biological repeats performed in triplicate. The error bars indicate standard deviation.

The results from Figure 2-3 show that anti-MA scFv's from phage clone 12 are better expressed in the soluble form in the SN fraction compared to the insoluble form in the PP fraction. Anti-MA scFv's from phage clone 16 are better expressed in the insoluble form in the PP fraction and anti-MA scFv's from phage clone 18 are expressed equally well in the soluble SN and insoluble PP fractions. After 2-5 minutes of adding TMB, there was no further significant change in colour, thus, giving the expected low absorbance values that reflect the low binding avidity of

the anti-MA scFv's to the MAs. The large standard deviation indicates high instability of the binding of the anti-MA scFv's to MAs.

2.3.2 Cloning of anti-mycolic acid scFv short-linkers (anti-MA scFv SLs)

The cloning of anti-MA scFv SLs was carried out in five steps as shown by the flow diagram in Figure 2-4.

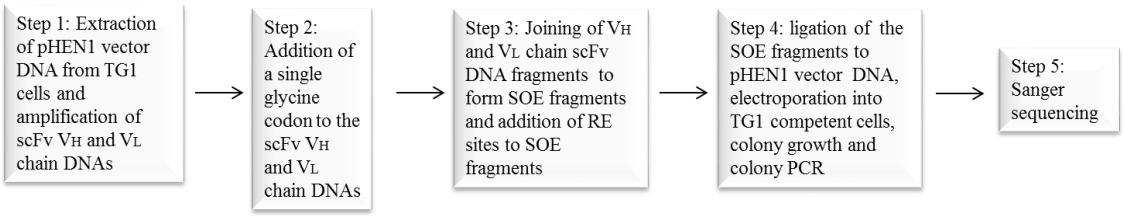

Figure 2-4: The five cloning steps of anti-MA scFv SLs.

To carry out step 1 in Figure 2-4, anti-MA scFv bacterial cultures were grown overnight to obtain anti-MA scFv DNA that would serve as template DNA for the cloning and expression of anti-MA scFv SL scFv's. To determine whether the first PCR to obtain the anti-MA scFv genes from the pHEN1 vector was successful, electrophoretic analysis of anti-MA scFv DNA fragments was carried out using a 1% (m/v) agarose gel with ethidium bromide as shown in Figure 2-5.

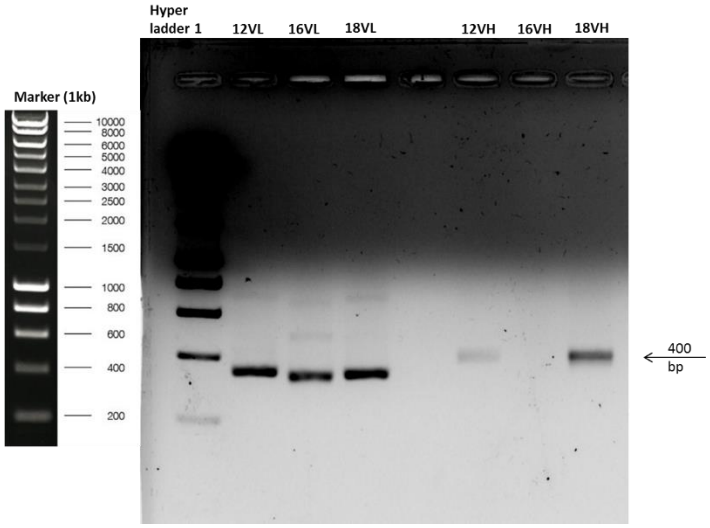

Figure 2-5: Gel electrophoresis for anti-MA scFv DNA amplification analysis. $12V_L$, $16V_L$ and $18V_L$ are the variable light chain DNAs of anti-MA scFv's from phage clones 12, 16 and 18 respectively. $12V_H$, $16V_H$ and $18V_H$ are the variable heavy chain DNAs of anti-MA scFv's from phage clones 12, 16 and 18 respectively.

The results from Figure 2-5 show that the 400 bp V_H and V_L chains anti-MA scFv DNAs from the three phage clones 12, 16 and 18 were successfully amplified. The amplification of V_H chain DNA from phage clone 16 was successfully repeated.

Step 2 in Figure 2-4 then followed to add a glycine codon (that would serve as a linker) to the V_H and V_L chain DNA fragments by means of PCR. Agarose gel electrophoresis of the anti-MA scFv V_H and V_L chain DNA fragments with the added glycine codon was carried out to determine successful amplification of the fragments using 1% (m/v) agarose gel with ethidium bromide. The results of the analysis are shown in Figure 2-6.

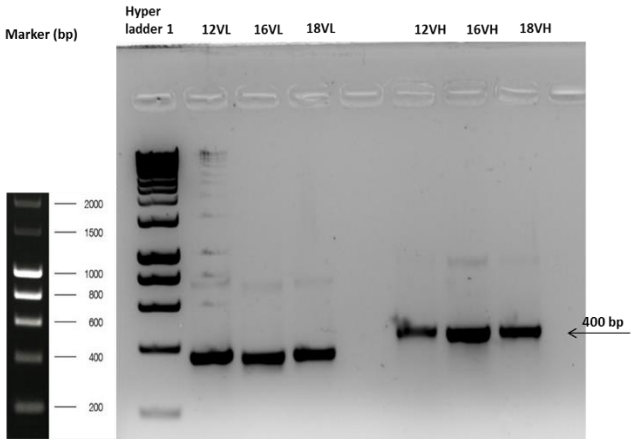

<u>Figure 2-6</u>: Gel electrophoresis for anti-MA scFv DNA analysis after glycine codon addition. $12V_L$, $16V_L$ and $18V_L$ are the variable light chain DNAs of anti-MA scFv's from phage clones 12, 16 and 18 respectively. $12V_H$, $16V_H$ and $18V_H$ are the variable heavy chain DNAs of anti-MA scFv's from phage clones 12, 16 and 18 respectively.

The results from Figure 2-6 show successful amplification of the V_H and V_L chain DNA fragments, however, because the bands are approximately the same in size as the bands in Figure 2-5, sequencing was the only method to confirm successful addition of the glycine codon to the V_H and V_L chain DNA fragments.

Step 3 in Figure 2-4 to join the V_H and V_L genes by means of SOE PCR then followed. A subsequent PCR was carried out to amplify the SOE fragments and another to add RE digestion sites *Sfi1* and *LCNot1* to the SOE fragments. Electrophoretic analysis was carried out on the PCR products to analyse successful joining of the V_H and V_L genes and amplification of the SOE fragments using 1% (m/v) agarose with ethidium bromide as shown in Figure 2-7.

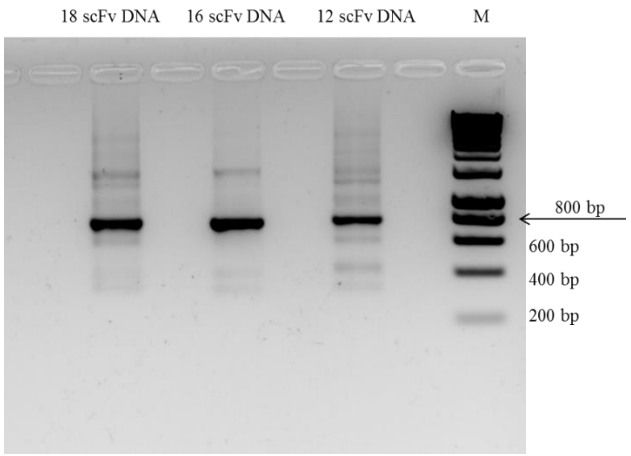

Figure 2-7: Gel electrophoresis for joint (SOE) anti-MA scFv DNA analysis. 12 scFv DNA, 16 scFv DNA and 18 scFv DNA are SOE DNA fragments of anti-MA scFv's from clones 12, 16 and 18 respectively.

The SOE fragments in Figure 2-7 are about 800 bp, i.e. approximately 400 bp of both V_H and V_L chains. This confirms successful joining and amplification of the V_H and V_L chain DNA fragments.

Step 4 in Figure 2-4 which is the ligation of the SOE fragments into pHEN1 vector and electroporation of the vector DNA into TG1 competent cells followed. The cells were plated and incubated at 37ºC overnight for colony growth. Colony PCR was carried out on 10 colonies per phage clone to investigate which of the colonies had the anti-MA scFv SL DNA insert. Electrophoresis was carried out to investigate the DNA inserts as shown in Figure 2-8.

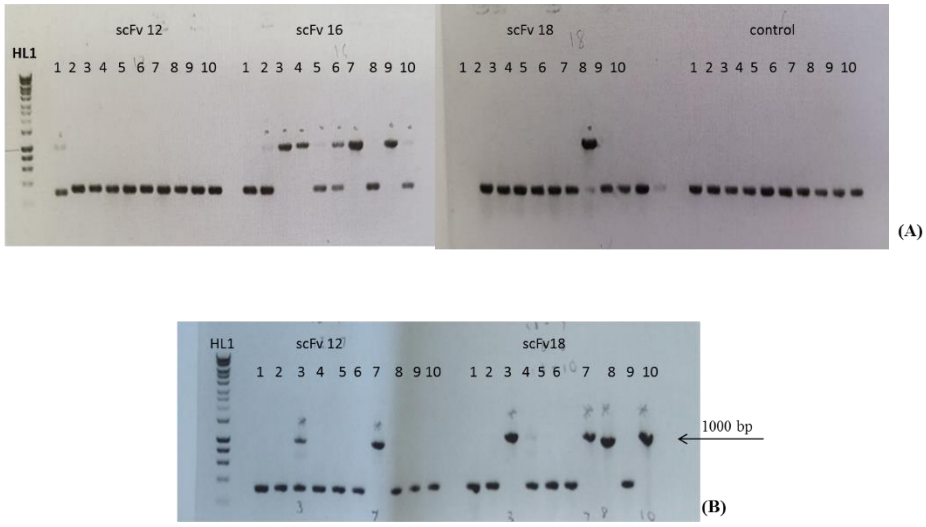

Figure 2-8: Gel electrophoresis successful anti-MA scFv SOE DNA inserts (1000 bp) analysis. (A) SOE DNA inserts from all phage clones including a control (no DNA). (B) Repeated electrophoretic analysis of SOE DNA inserts from phage clones 12 and 18.

The expected band was 800 bp (Figure 2-7). The 200 added base pairs that resulted in 1000 bp inserts were due to the OP52 and M13 reverse primers that each add 100 bp to the expected 800 bp SOE DNA fragments indicated in Figure 2-7. From Figure 2-8 therefore, two colonies successfully carried anti-MA scFv SL DNA inserts from phage clone 12, five colonies successfully carried anti-MA scFv SL DNA inserts from phage clone 16 and five colonies successfully carried anti-MA scFv SL DNA inserts from phage clone 18. The control had no inserts as expected. Figure 2-8 confirms successful ligation of anti-MA scFv SL DNA to pHEN1 vector DNA and successful transformation of vector DNA into TG1 competent cells.

The 5th and final step in Figure 2-4 being Sanger sequencing was then carried out on pHEN1 vector DNAs successfully carrying anti-MA scFv SL inserts (from Figure 2-8) to investigate whether the base sequences of the anti-MA scFv SLs were in the right frame and had no deleterious mutations as shown in Figure 2-9.

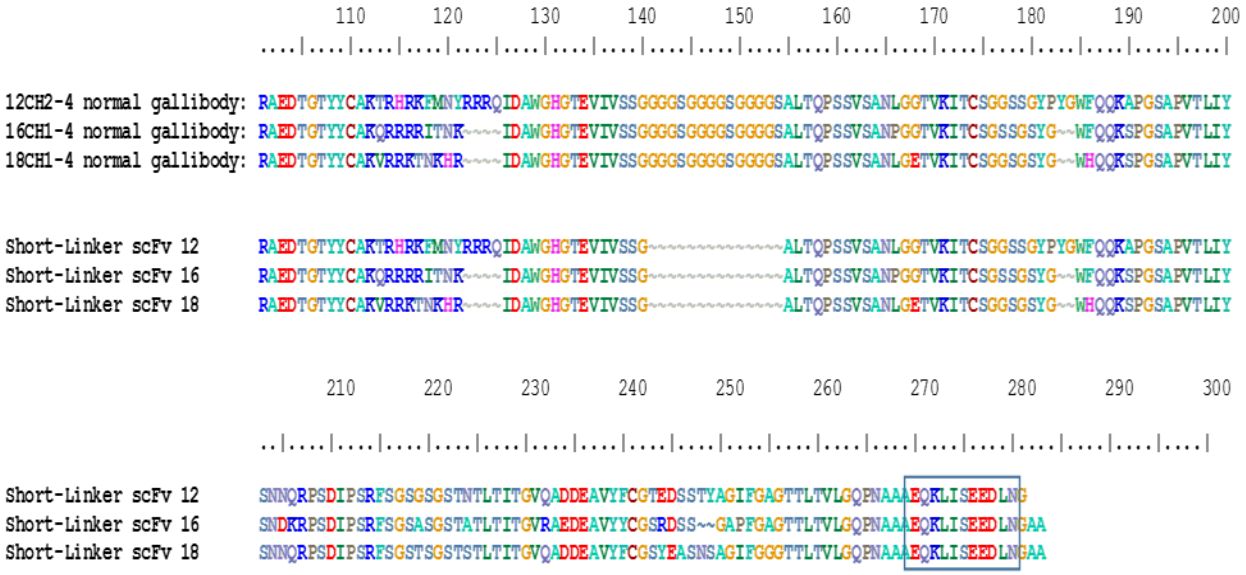

<u>Figure 2-9</u>: Sanger sequencing of normal chicken antibody amino acid sequences and anti-MA scFv SLs amino acid sequences to confirm successful cloning of the glycine codon, correct order and frame of the codons. The base sequences were translated to amino acids that are depicted in one letter code and are colour coded. Alanine (A) is shown in powder blue, arginine (R) in dark blue, asparagine (N) in lilac, aspartic acid (D) in red, cystine (C) in maroon, glutamic acid (E) in red, glutamine (Q) in lilac, glycine (G) in yellow, histidine (H) in magenta, isoleucine (I) in green, leucine (L) in green, lysine (K) in dark blue, methionine (M) in green, phenylalanine (F) in light blue, proline (P) in brown, serine (S) in lilac, threonine (T) in lilac, tryptophan (W) in light green, tyrosine (Y) in light blue and valine (V) in green. The box indicates the c-MYC amino-acid sequence 5' EQKLISEEDLN 3'.

Figure 2-9 shows amino acid sequences translated from normal chicken antibody DNA base sequences (gallibody) and anti-MA scFv SLs DNA sequences using BioEdit. The gallibody amino acid sequences all have the linker sequence of $(Gly_4Ser)_3$ at position 139-154. The anti-MA scFv SLs have the same amino acid sequence as the gallibody, however, the linker at position 140 is a single glycine. Figure 2-9 confirms that the objective to shorten the linker to a single glycine residue was achieved. The anti-MA scFv SL DNAs from phage clone 12, 16 and 18 in Figure 2-8 that had the correct sequences as shown in Figure 2-9 were from colonies 1, 2 and 3 (phage clone 12); colonies 4 and 7 (phage clone 16), and colonies 11 and 13 (phage clone 18).

Amino acid sequences of the complementarity determining regions (CDRs) of the anti-MA scFv SLs were also examined to ensure that there were no residue changes and mutations as shown in Figure 2-10 as these regions are imperative for antigen binding.

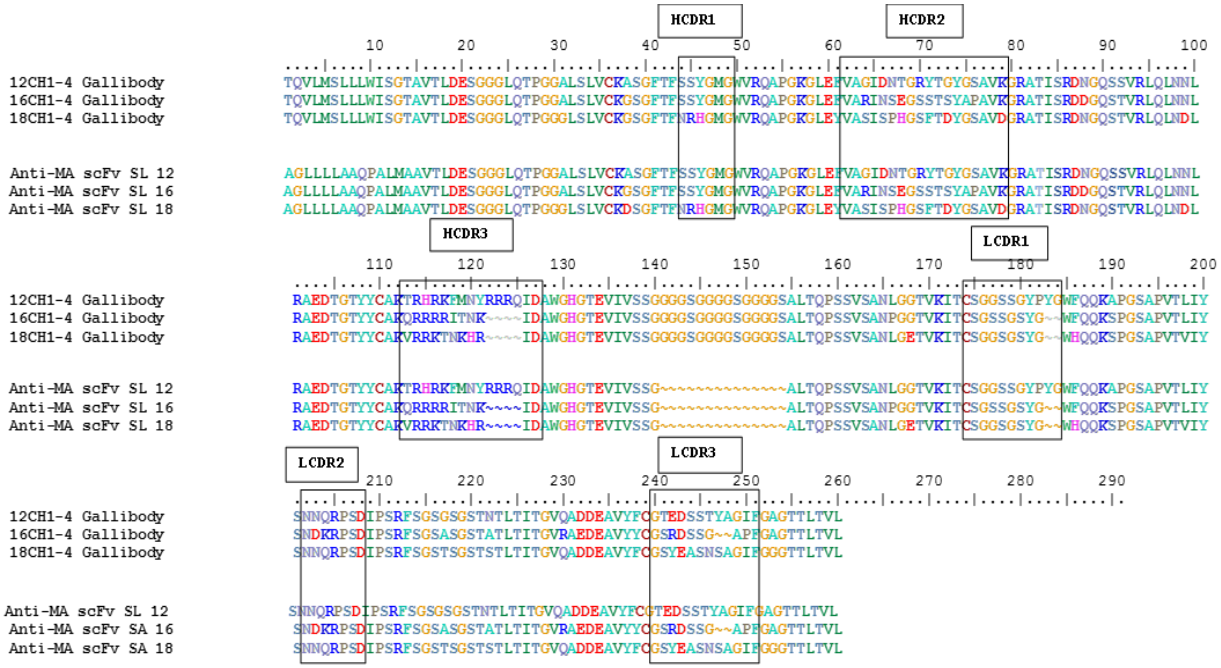

<u>Figure 2-10</u>: Amino acid sequences of the CDRs of the anti-MA scFv SLs. HCDR1, HCDR2 and HCDR3 are the heavy chain CDR 1, 2 and 3 respectively, and LCDR1, LCDR2 and LCDR3 are light chain CDR 1, 2 and 3 respectively.

Figure 2-10 confirms that the amino acid CDR sequences of the V_H chain and V_L chains have all been conserved, therefore, any hindrance of anti-MA scFv SLs from binding to MAs is not expected.

2.3.3 Binding activity of anti-MA scFv SLs on MAs

Following sequencing, an indirect ELISA assay was carried out to investigate which of the anti-MA scFv SLs with the correct sequences as shown in Figure 2-9 were active and could recognize antigenic MAs as shown in Figure 2-11.

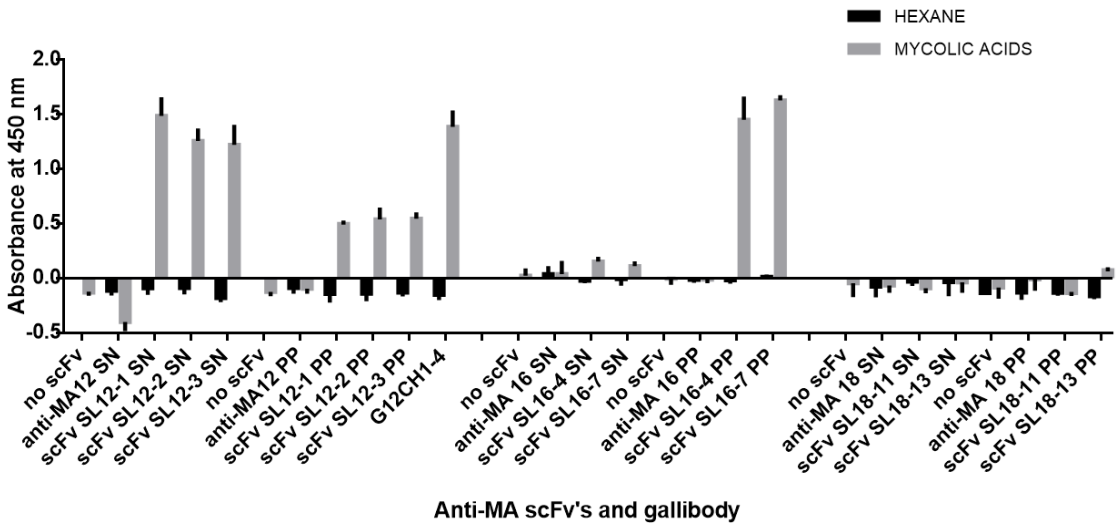

Figure 2-11: Indirect ELISA assay for the MA binding activity of the anti-MA scFv SLs. ELISA plates were coated with either MA antigen or hexane as antigen control. Anti-MA scFv SLs from either the culture SN or PP space and diluted with ELISA dilution buffer on 1:1 volume ratio were tested, and the binding activity was measured using anti-c-MYC mouse monoclonal antibody-HRP conjugate. The anti-MA scFv SLs' binding signals were then corrected by subtracting the background signal generated by the binding of ELISA dilution buffer to hexane (antigen control). Anti-MA 12, 16 and 18 are anti-MA scFv's from phage clones 12, 16 and 18. ScFv SLs are anti-MA scFv SLs from colonies 1, 2 and 3 (phage clone 12), colonies 4 and 7 (phage clone 16) and colonies 11 and 13 (phage clone 18). The data represents two biological repeats performed in triplicate. The error bars represent standard deviation. G12CH1-4 is gallibody 12CH1-4 (positive control).

Figure 2-11 depicts that the SN fractions of all anti-MA scFv SLs from phage clone 12 generated higher binding signals to MAs than the PP fractions. The PP fractions of all anti-MA scFv SLs from phage clone 16 generated higher binding signals to the MAs than the SN fractions. None of the anti-MA scFv SLs from phage clone 18 from either the SN or PP generated binding signals to the MAs. Although the binding signal of the gallibody 12CH1-4 (positive control) seems similar to the binding signals of anti-MA scFv SLs from phage clones 12 and 16, the anti-MA scFv SLs and gallibody binding avidities cannot be compared as the molar concentrations were

not determined. Moreover, the conclusion whether the binding avidity of anti-MA scFv's was increased through the shortening of the linker cannot be deduced from the ELISA as the molar concentrations were not controlled. Nonetheless, the ELISA indicates the anti-MA scFv SLs from phage clones 12 and 16 that are active and can therefore be purified for further characterization.

2.3.4 Affinity column purification

Affinity column purification was carried out on the anti-MA scFv SLs that generated the highest binding signals in the ELISA in Figure 2-11 (anti-MA scFv SL 12-1 and 16-7). Agarose column conjugated with anti-c-MYC was used to capture the anti-MA scFv SLs. SDS-PAGE and Western blot analyses were carried out to track the purification of the anti-MA scFv SLs as shown in Figure 2-12.

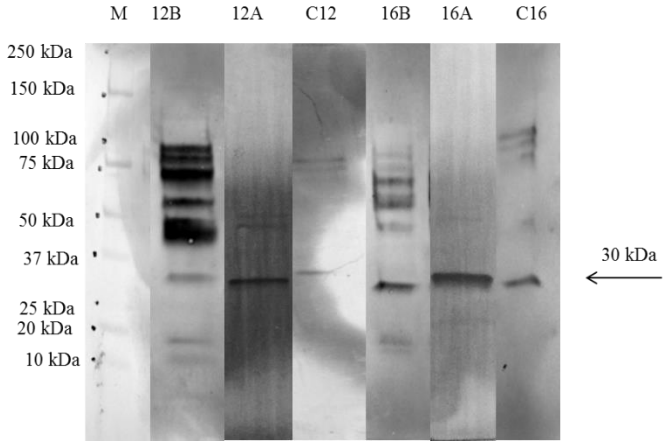

Figure 2-12: Western blot analysis of unpurified and purified anti-MA scFv SLs from phage clones 12 and 16. Samples 12B and 16B depict samples of anti-MA scFv SLs from phage clones 12 and 16 before purification, 12A and 16A after purification, and C12 and C16 the control anti-MA scFv's 12 and 16 respectively.

The Western blot in Figure 2-12 depicts complex profiles with higher molecular weight bands for the unpurified fractions of the anti-MA scFv SLs from phage clones 12 and 16. After purification, uncomplicated profiles are achieved with a definite band at 30 kDa, corresponding

to monomeric anti-MA scFv SLs from phages clone 12 and 16. The profiles of the purified control anti-MA scFv's also show high molecular weight bands corresponding to oligomers. The objective to purify the anti-MA scFv SLs was achieved.

The affinity purification of the multimers as compared to the purification of anti-MA scFv's proved to be a challenge. Although the scFv SL sequences in Figure 2-9 confirmed that the multimers have a c-MYC tag 5' EQKLISEEDLN 3', the multimers were not binding to the anti-c-MYC conjugated agarose column. Adding SDS to the samples before purification resulted in successful binding of the multimers to the anti-c-MYC agarose column. The addition of SDS resulted in the unfolding of the multimers that most likely caused increased accessibility of the c-MYC tag to the agarose column. Buffer changing to PBS resulted in the renaturation of the multimers with retained functional activity. Interestingly, the anti-MA scFv SLs were successfully probed in the ELISA assays using anti-c-MYC mouse monoclonal antibody conjugated to HRP suggesting that the binding of anti-MA scFv SLs to MAs exposes the c-MYC tag, whereas the tag is inaccessible when the anti-MA scFv SLs are in a globular conformation.

2.3.5 Binding avidities of anti-MA scFv's and anti-MA scFv SLs

Indirect ELISA assay was carried out to detect MAs using affinity purified anti-MA scFv's from phage clones 12 and 16, affinity purified anti-MA scFv SLs from phage clones 12 and 16 and purified gallibody 12CH1-4 at concentrations of 0.25 mg/ml in order to compare the binding avidities to MA as shown in Figure 2-13.

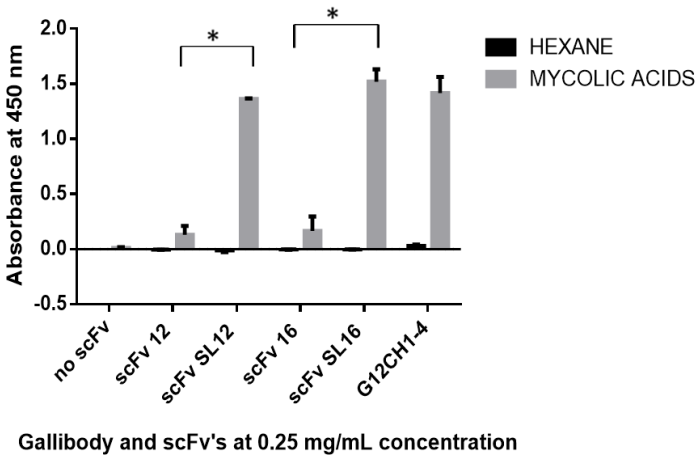

<u>Figure 2-13</u>: Indirect ELISA assay to compare the MA binding avidities of purified anti-MA scFv's and anti-MA scFv SLs. ELISA plates were coated with either MA antigen or hexane as antigen control. ELISA dilution buffer (with no scFv), affinity purified anti-MA scFv's, anti-MA scFv SLs and gallibody 12CH 1-4 (positive control) at 0.25 mg/mL concentration were tested and the binding activity was measured using anti-c-MYC mouse monoclonal antibody-HRP conjugate. The antibodies' binding signals were then corrected by subtracting the background signal generated by the binding of ELISA dilution buffer with no antibody on the hexane (antigen control). ScFv 12 and 16 are anti-MA scFv's from phage clones 12 and 16 and scFv SLs are anti-MA scFv SLs from phage clones 12 and 16. The data represents two biological repeats performed in triplicate. The error bars represent standard deviation and the asterisks (*) indicates the p-value where *$p<0.05$.

Figure 2-13 depicts that at the same concentration, anti-MA scFv SLs have enhanced functional binding avidities to MAs when compared to anti-MA scFv's, with relevant *p* values of 0.003652 and 0.004153 for phage clones 12 and 16 respectively, indicating significance of binding avidity differences. The hypothesis that the oligomeric scFv's from the scFv phage clones 12, 16 and 18 can be obtained by either shortening of the linker peptide between the V_H and V_L domains is therefore supported for anti-MA scFv SLs from phage clones 12 and 16. The binding signals to MAs generated by anti-MA scFv SLs are similar to the signals generated by the gallibody 12CH1-4 at the same mass per millilitre concentration. Absolute comparisons of binding avidity between different anti-MA scFv SLs and gallibodies require dilution titrations, which is done in Chapter 4.

2.3.6 Size characterization of anti-MA scFv SLs

To investigate the types of multimers formed, size exclusion chromatography (SEC) was carried out on anti-MA scFv SLs from phage clones 12 and 16 as shown in Figures 2-14 and 2-15.

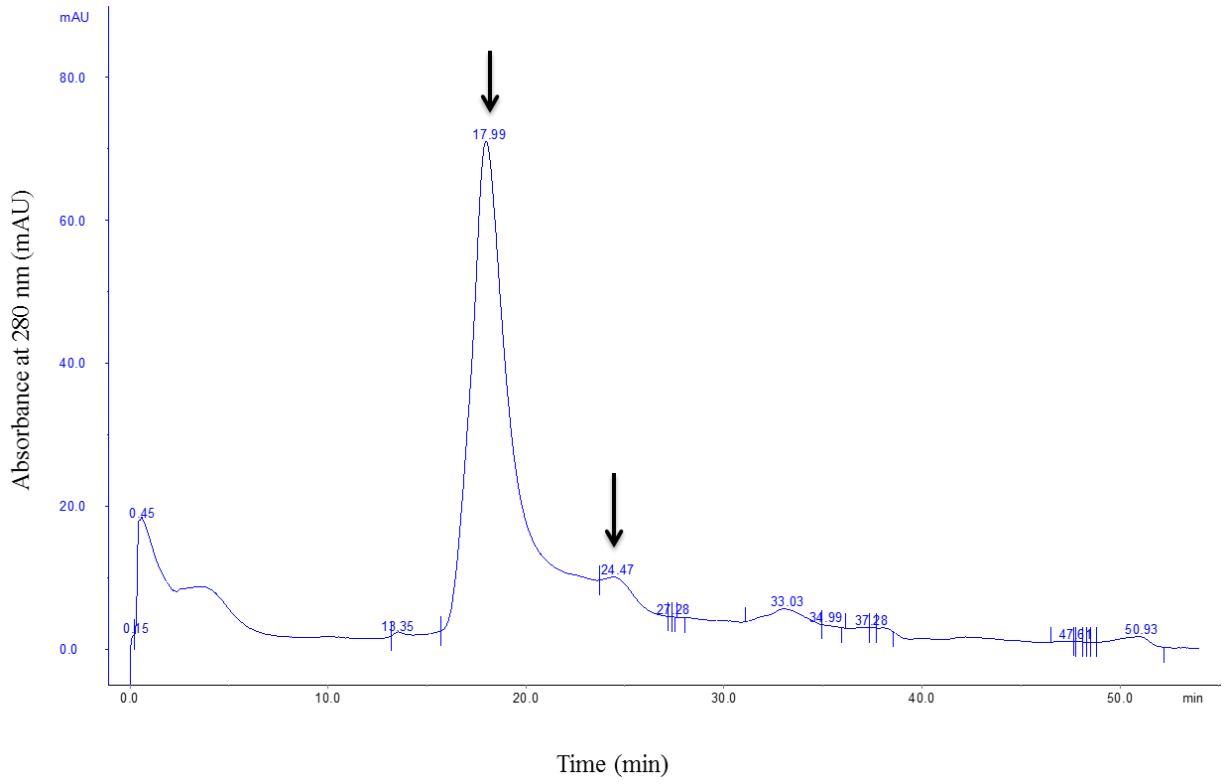

<u>Figure 2-14</u>: SEC on anti-MA scFv SL from phage clone 12 to determine the type of multimer generated after shortening the polypeptide linker. A volume of 25 µL of 0.5 mg/mL concentrated sample was loaded on the column, the flow rate of the column was 0.5 mL/min and the SEC was carried out until all fractions were eluted. Arrows represent eluted anti-MA scFv SLs at different time points.

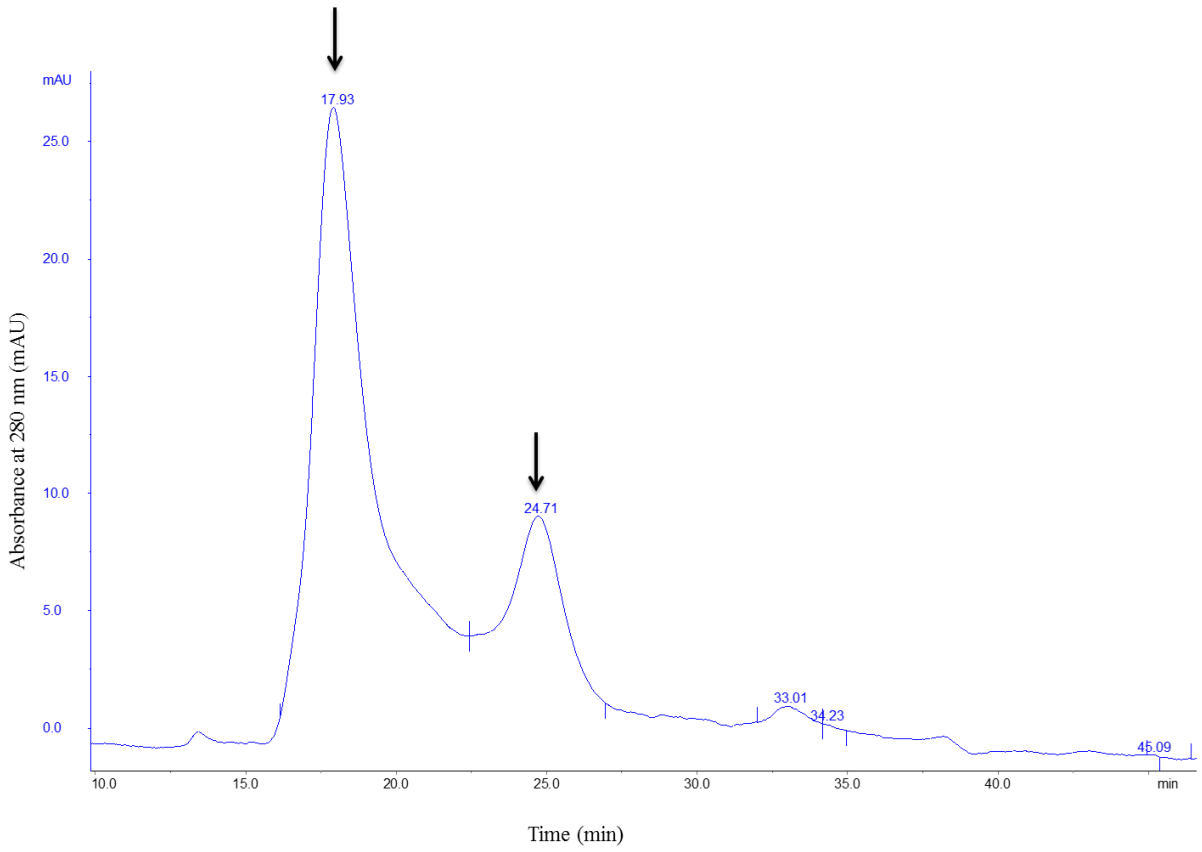

<u>Figure 2-15</u>: SEC on anti-MA scFv SL from phage clone 16 to determine the type of multimer generated after shortening the polypeptide linker. A volume of 25 µL of 0.6 mg/ml concentrated sample was loaded on the column, the flow rate of the column was 0.5 mL/min and the SEC was carried out until all fractions were eluted. Arrows represent eluted anti-MA scFv SLs at different time points.

Figures 2-14 and 2-15 depict that the monomeric scFv's eluted at 24.47 minutes and 24.71 minutes for anti-MA scFv SLs from phage clones 12 and 16 respectively. The elution times correspond to the second peaks on the SEC profiles. These monomers did not elute in the void volume. The anti-MA scFv SLs from phage clones 12 and 16 eluted at 17.99 minutes and 17.93 minutes respectively. The elution times correspond to the first peaks on the SEC profiles. These multimers eluted in the void volume. The monomers eluted correspond to 30 kDa as expected (determined from a standard curve of the log of molecular weight against elution volume). However, the expected sizes of a dimer (60 kDa), trimer (60 kDa) and tetramer (120 kDa) are at the edge of or in the void volume (7.2 mL) as the separation range of the sephadex 75 10/300 GL column is 3 - 70 kDa. For this reason, the multimers display peaks

earlier than the monomeric peaks however, the degree of oligomerization cannot be deduced. Figures 2-14 and 2-15, nevertheless, confirm that the objectives to produce and express multimers through shortening of the polypeptide linker were achieved.

In an attempt to determine the degree of multimerization of anti-MA scFv SLs, an SDS-PAGE analysis was carried out on the anti-MA scFv SLs in denatured (using β-mercaptoethanol) and non-denatured (using non-denaturing protein sample loading buffer) states. A Western blot was then carried out to investigate the difference in sizes of the denatured and non-denatured anti-MA scFv SLs to reveal the degree of multimerization as shown in Figure 2-16.

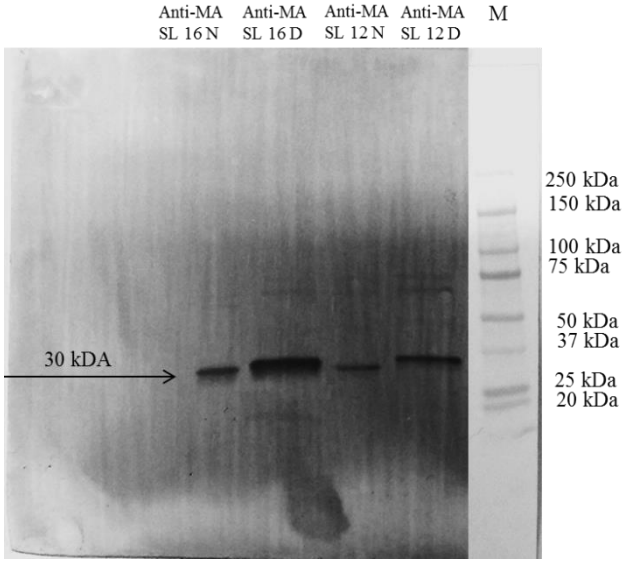

Figure 2-16: Western blot analysis of anti-MA scFv SLs under denaturing and non-denaturing conditions. Anti-MA SL 12 indicates anti-MA scFv SLs from phage clone 12 in non-denatured (N) or denatured (D) state. Anti-MA SL 16 indicates anti-MA scFv SLs from phage clone 16 in non-denatured (N) and denatured (D) state. The arrow represents the bands of interest at 30 kDA.

Figure 2-16 shows only one monomeric band of interest at 30 kDa for anti-MA scFv SLs from both clones in the denatured and non-denatured states. In the non-denatured state, the band sizes expected were either 60 kDa, 90 kDa or 120 kDa representing formation of dimers, trimers or tetramers respectively from the monomeric 30 kDa anti-MA scFv's. The absence of these bands therefore suggests that the anti-MA scFv SLs are dynamic multimers that are destabilized by harsh conditions. The slightly larger band positions obtained in denaturing conditions may be

because of shape change from a compact conformation to a more linear random shape when denatured. In conclusion, the aim to increase functional binding avidity of anti-MA scFv's by multimerization was achieved, however, the degree and stability of non-covalent multimerization could not be determined.

2.4 DISCUSSION

In the history of recombinant antibody engineering, biologically functional scFv molecules have been expressed in the periplasmic space and/or extracellular medium using prokaryotic expression systems such as *E. coli* (Horwitz *et al*., 1988, Better *et al*., 1988, Huston *et al*., 1988, Bird *et al*., 1988). The expression of scFv's is plausible in *E. coli* as glycosylation that is necessary for whole antibody expression is not required in the case of scFv's (Kipriyanov *et al*., 1997). Expression of scFv's into the periplasm of *E. coli* is preferred as compared to expression in the cytoplasm. The periplasmic space is oxidative, as compared to the reducing cytoplasmic environment. Thus, the correct V-domain folding and disulphide bond formation may be better achieved in the periplasmic space, resulting in an active protein (Verma *et al*., 1998). Moreover, the purification of the recombinant protein from the periplasmic space is simpler, as there are fewer contaminating proteins (Makrides, 1996). Lastly, the periplasmic space contains less proteases that target the protein of interest in comparison to the cytoplasm (Makrides, 1996). The expression of scFv's in the periplasmic space can be directed using signal sequences. The synthesis of scFv's occurs in the cytoplasm, these premature scFv's contain a 15-30 amino acid specific sequence called leader sequence that allows transportation into the periplasmic space (Pugsley, 1993, Choi and Lee, 2004, Skerra and Pluckthun, 1988). Several leader sequences - PelB, OmpA, PhoA, endoxylanase, and StII - have been utilized for periplasmic directed scFv expression. In this study, the PelB leader sequence was used as shown by the pHEN1 gene map in Figure 2-2.

The three anti-MA scFv's from phage clones 12, 16 and 18 from the *Nkuku* library were selected due to their stability, specificity and retained functionality after long term storage (Ndlandla *et al*., 2016). These recombinant monoclonal scFv's generally have low binding signals in the ELISA as shown in Figures 2-3 and 2-13 reflecting low functional binding avidity to MAs. Since the anti-MA scFv's are monovalent, most anti-MA scFv's are easily washed off during the washing steps in ELISA, leaving few scFv's bound to the MAs to generate the signal. The anti-MA scFv's also have different expression and solubility properties. Greater expression of anti-MA scFv's from phage clone 12 was observed in the supernatant, indicating that they are soluble. On the other hand, anti-MA scFv's from phage clone 16 were mostly expressed in the periplasm, depicting less solubility. Anti-MA scFv's from phage clone 18 expressed equally well

in the supernatant and periplasmic as shown in Figure 2-3. As expected, the anti-MA scFv SLs retained the solubility properties of their parent scFv's as shown by the ELISA assays in Figures 2-11 and 2-13. Although directed for expression in the periplasmic space, some scFv's can be found in the extracellular medium. Extracellular secretion of scFv's occurs during periplasmic leakage under certain conditions. The accumulation of the recombinant scFv's in the periplasmic space can lead to osmotic imbalance that drives the extracellular secretion of the proteins (Hasenwinkle *et al*., 1997). Also, the scFv's can cause membrane perturbations that allow for selective periplasmic space protein leakage (Pugsley *et al*., 1997). Conversely, the sequences of the scFv's can target the scFv's for SecB dependent transport from the periplasmic space to the extracellular space (Pugsley *et al*., 1997).

The *Nkuku* chicken scFv's were found to occur mostly as monomers. The anti-MA scFv's were found to be monomeric in nature as depicted by the SDS-PAGE analysis in Figure 2-12 that shows molecular weight of 30 kDa for the anti-MA scFv's. These purified anti-MA scFv's, however, also portray high molecular weight band scFv's that indicate the presence of a population of oligomers in unmodified scFv's. A study that investigated a 16 kDa mycobacterial antigen by the use of scFv's from the *Nkuku* library also verified that the scFv's occurred as a mixture of monomers with trace amounts of multimers (Sixholo, 2008, Sixholo *et al*., 2011). scFv's are predominantly monomeric when the variable domains are joined by polypeptide linkers of at least 12 residues, however, these monomeric scFv's can also exist in equilibrium with dimers, trimers and tetramers (Kortt *et al*., 2001). The flexible 15 residue linker $(Gly_4Ser)_3$ allows the V_H and V_L chains to associate into a single scFv molecule. The component residues of the linker play a crucial role in the functionality of the antibody. The glycine residues of the linker afford flexibility to the polypeptide linker, allowing the linker to assume a range of conformations, and the serine residues allow for hydrophilic interactions through hydrogen bonding (Argos, 1990).

Shortening the linker of the weak antigen binding anti-MA scFv's significantly improved the binding signals to the MAs in the ELISA. Shortening of the linker resulted in the non-covalent association of complementary V_H and V_L chains from two adjacent scFv's to form high molecular oligomers as shown by the model in Figure 2-17 (Kortt *et al*., 2001, Todorovska *et al*., 2001). The non-covalent association of the V_H and V_L chains is demonstrated by the Western

blot in Figure 2-12 where the multimeric scFv's are monomerized by β-mercaptoethanol. Generally, when the linker is shortened to 3-10 residues, bivalent dimers of 60 kDa size result. Further reducing the linker length below three residues results in the formation of trimers of 90 kDa, or tetramers of 120 kDa depending on the length of the linker and the orientation of the V-domain (Kortt et al., 2001, Hudson and Kortt, 1999). The increased signals in the ELISA assays in Figures 2-11 and 2-13 are therefore a result of increased valency of the scFv's, as demonstrated graphically in Figure 2-17. Increased valency allows for concurrent binding of one scFv to two or more adjacent antigen molecules on the same surface, resulting in increased avidity (Hudson and Kortt, 1999, Kortt *et al.*, 2001). However, if steric requirements are not met, multiple binding is not possible, more especially for surface-bound antigens, regardless of correct CDR sequences that enable antigen binding. As such, increased functional avidity expected for the multimer is abnegated, and this could be the possible reason behind the apparent inactivity of anti-MA scFv SLs from phage clone 18 (Kortt *et al*., 2001). While the SEC analysis in Figures 2-14 and 2-15 could not quantify the degree of oligomerization of the anti-MA scFv SLs, the peaks prove formation of scFv SL oligomers. Moreover, the SDS-PAGE and Western blot analysis in Figure 2-16, as well as the SEC results in Figures 2-14 and 2-15 suggest that the anti-MA scFv SLs are probably non-covalent dynamic multimers. Electrophoretically, only the 30 kDa (monomer) band was visible in the non-denatured state, and the expected higher molecular weight bands of 60 kDa (dimer), 90 kDa (trimer) and 120 kDa (tetramer) were not seen, but higher oligomerisation was detectable in combination with monomeric peaks with SEC.

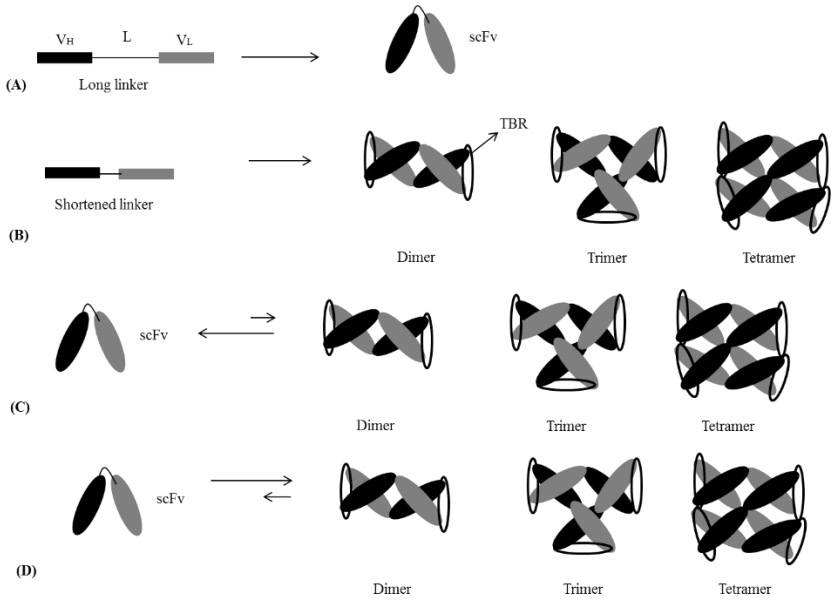

Figure 2-17: Schematic model of oligomers formed from shortening the length of the polypeptide linker. The black oval represents the variable heavy chain (V_H) and the grey oval represents the variable light chain (V_L). (A) ScFv formed from long polypeptide linker. (B) Oligomers formed from shortening the polypeptide linker. (C) Dynamic nature of multimers under harsh conditions. (D) Dynamic nature of multimers under mild conditions (Kortt *et al*., 1997).

To the best of our knowledge, multimeric scFv's against antigenic MAs have not been reported, making this study the first to engineer multimeric scFv's against MAs. It is also important, however, to establish the anti-MA scFv SLs' cholesterol cross-reactivity in order to establish the anti-MA scFv SLs that would be suitable specifically for use in a POC devise for diagnostic purposes (Ranchod *et al.*, 2018). The cholesterol cross-reactivity of the anti-MA scFv SLs is investigated in chapter 4.

2.5 CONCLUSION

In conclusion, the aim to increase MAs binding avidity of anti-MA scFv's was achieved through the shortening of the flexible polypeptide linker from 15 amino acid residues to one glycine residue. Anti-MA scFv's from phage clones 12 and 16 were successfully engineered into anti-MA scFv SLs that exhibited dynamic reversible oligomerisation, with increased net binding avidity to the antigenic MAs due to multivalency. The hypothesis that oligomeric scFv's from the scFv phage clones 12, 16 and 18 can be obtained by shortening of the linker peptide between the V_H and V_L domains supported for oligomers from clones 12 and 16.

CHAPTER 3: Towards streptavidin tetramers of anti-mycolic acids scFv's (Anti-MA scFv SAs)

3.1 INTRODUCTION

Another method to increase affinity and avidity of short chain variable fragments (scFv's) to the antigen is by the production of recombinant fusion proteins. One of the most promising strategies exploits the use of streptavidin, a non-glycosylated 60 kDa homotetrameric protein from the bacterium *Streptomyces avidinii*. Streptavidin protein consists of four identical 15 kDa subunits. The natural ligand of streptavidin is biotin, and the binding of streptavidin to biotin is a very strong non-covalent interaction with a dissociation constant (K_d) of 10^{-14} M (Cloutier *et al*., 2000). The N- and C-termini of the 159 amino acids full-length protein can be processed to give a truncated 'core' streptavidin, consisting of 125-139 residues (Sano *et al*., 1995). Truncation of the protein has been shown to not affect the binding of biotin to streptavidin (Hendrickson *et al*., 1989, Pähler *et al*., 1987). The advantage of truncated streptavidin over full length streptavidin is the decreased likelihood to form aggregates (Sano and Cantor, 1990). The fusion of scFv's to streptavidin has been shown in various studies to result in homotetramers, which are protein complexes made up of four identical units that spontaneously interact non-covalently (Schultz *et al*., 2000).

Some research studies have also utilized core streptavidin to increase the functional binding affinity and avidity of scFv's. Some studies have produced streptavidin fused scFv's that target diseases like Avian influenza virus and Venezuelan equine encephalitis virus, and scFv's that have been used for neurotherapeutic drug delivery (Pearce *et al*., 1997, Li *et al*., 1999, Hu *et al*., 2002). However, the focal point in most of the studies to increase the avidity of scFv's to their target by means of streptavidin fusion was cancer diagnosis (Dübel *et al*., 1995, Won *et al*., 2009, Cheung *et al*., 2004, Förster *et al*., 2006). In one study, the biodistribution and tumour-targeting ability of an anti-mesothelin tetravalent scFv-streptavidin fusion protein (SS1scFvSA) was evaluated in mice. The SS1scFvSA demonstrated good tumour pre-targeting ability (Sato *et al*., 2005).

The homotetrameric streptavidin fused scFv protein is such that with the core streptavidin forms the core of the protein, and the scFv's the termini for antigen binding. The schematic diagram of

the fusion protein is shown in Figure 3-1. The advantage of this strategy over the shortening of the linker of the scFv's is the predictability of the type of oligomers formed. Moreover, this strategy provides an opportunity to express an active oligomer from phage clone 18 as the shortening of the linker of the scFv's strategy yielded inactive multimers from phage clone 18. On the other hand, the potential disadvantage of this strategy is the expression of potentially indisplaceable tetrameric scFv's in Mycolic acid lateral flow immunoassay (MALIA) due to high binding avidity to mycolic acids (MAs). In this chapter, the *Nkuku* library anti-mycolic acids (anti-MA) scFv genes will be fused to the core streptavidin gene with the aim to form tetrameric anti-MA scFv's with increased binding avidity to the antigenic MAs.

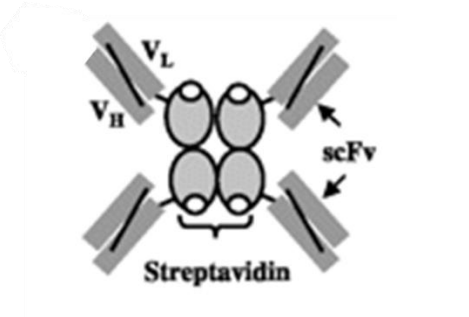

Figure 3-1: Schematic diagram of core streptavidin-scFv fusion protein. Streptavidin forms the core of the fusion protein and the scFv's the termini (Schultz *et al*., 2000).

3.1.1 Hypothesis

Oligomeric scFv's from the scFv phage clones 12, 16 and 18 can be obtained by creating scFv-streptavidin fusion proteins.

3.2 MATERIALS AND METHODS

3.2.1 Materials

Phosphate buffered saline (PBS) 1X, pH 7.4: Sodium chloride (NaCl, 0.137 M), 0.0027 M potassium chloride (KCl), 0.01 M disodium hydrogen phosphate (Na_2HPO_4), 0.0018 M monopotassium phosphate (KH_2PO_4). All reagents obtained from Sigma-Aldrich, Missouri, USA. All reagents have quality of ≥99.0%. The PBS was autoclaved at 121ºC before use.

Histidine columns: HisPur Ni-NTA resin (Thermo Scientific, Waltham, Massachusetts, USA). The resin was packed in empty 15 mL disposable plastic drip columns with polyethylene frits (Thermo Scientific, Waltham, Massachusetts, USA). The bed volume used was 2 mL.

Lysis Buffer pH 8.0: NaCl (0.3 M), 0.05 M disodium phosphate (Na_2SO_4) (≥99.0%), Sigma-Aldrich, Missouri, USA), 0.01 M imidazole (≥99.0%, Sigma-Aldrich, Missouri, USA).

Wash Buffer pH 8.0: NaCl (0.3 M) and 0.05 M Na_2SO_4.

Elution Buffer pH 8.0: NaCl (0.3 M), 0.05 M Na_2SO_4 and 0.25 M imidazole.

Mycolic acid from *Mycobacterium tuberculosis* (bovine strain): MAs (0.25 mg) dissolved in 1 mL hexane (≥99%) (Sigma-Aldrich, Missouri, USA).

ELISA block buffer pH 7.4: Casein hydrolysate (4% (m/v), Oxoid, United Kingdom) in PBS pH 7.4

ELISA dilution buffer pH 7.4: Casein hydrolysate (4% (m/v)) dissolved in PBS pH 7.4 and 0.05% (v/v) Tween20 (Sigma-Aldrich, Missouri, USA).

ELISA wash buffer pH 7.4: PBS 1X, pH 7.4 and 0.1% (v/v) Tween20.

Anti-c-MYC Horseradish perodixase (HRP): Mouse monoclonal anti-c-MYC antibody (clone 9E10) conjugated to peroxidase, (Roche Diagnostics GmbH, Germany).

Gallibody HRP: Goat anti-chicken Fc: HRP (AbD Serotic, Kidlington, UK).

ELISA Tetramethyl Benzidine (TMB) HRP substrate solution: TMB Single solution (Life Technologies, California, USA).

Blot test Tetramethyl Benzidine (TMB) HRP substrate solution: TMB for blot tests (Life Technologies, California, USA).

Tryptone-yeast (2XTY) media: Tryptone (1.6% (m/v)) (Sigma-Aldrich, Missouri, USA), 1% (m/v) yeast extract (Sigma-Aldrich, Missouri, USA) and 0.5% (m/v) NaCl in 1L $dddH_2O$. Media was autoclaved at 121°C for 20 minutes.

Glucose (20% (m/v)): Glucose (20 g) (≥99.5%, Sigma-Aldrich, Missouri, USA), dissolved in 100 mL $dddH_2O$ and autoclaved at 121ºC for 20 minutes.

Culture media (2XTY): 2XTY media (9 mL), 1 mL 20% (m/v) glucose and 10 µL ampicillin (Sigma-Aldrich, Missouri, USA).

Isopropyl β-D-1 thiogalactopyranoside (IPTG) media: 2XTY media (10 mL), 1 mM IPTG (≥99%) (Sigma-Aldrich, Missouri, USA) and 10 µM ampicillin (Sigma-Aldrich, Missouri, USA).

Dilution media (2XTY): 2XTY (45 mL), 5 mL 20% (m/v) glucose and 50 µL ampicillin.

Cell lysis solution: PBS (1X) pH 7.4, 1 M NaCl and 1mM Ethylenediaminetetraacetic acid (EDTA) (Sigma-Aldrich, Missouri, USA).

Tris-buffered saline (TBS) 1X, pH 7.2: Tris (0.0025 M) (≥99.9%) (Sigma-Aldrich, Missouri, USA) and 0.15 M NaCl.

Tris-acetate_EDTA (TAE) buffer 50X, pH 8.3: EDTA (50 mM), 2 M Tris, 1 M glacial acetic acid (≥99.9%) (Sigma-Aldrich, Missouri, USA).

2XTY dilution media: 45 ml 2XTY, 5 mL 20% (m/v) glucose, 50 µL ampicillin.

Cell lysis solution: 1X PBS pH 7.4, 1 M NaCl and 1mM Ethylenediaminetetraacetic acid (EDTA) (Sigma-Aldrich, Missouri, USA).

Agarose gel: Agarose1% (m/v) dissolved in 1X TAE with 1% (v/v) ethidium bromide (Sigma-Aldrich, Missouri, USA).

Agar plates: Tryptone (1% (m/v)), 0.5% (m/v) yeast extract, 0.8% (m/v) NaCl and 1.5% (m/v) agar in 1 L dddH_2O and autoclaved at 121°C for 20 minutes.

Column storage buffer: Ethanol (30% (v/v)) (≥99.8%, Sigma-Aldrich, Missouri, USA).

ELISA Stop solution: Sulphuric acid (H_2SO_4) (2 N) (99.999%), Sigma-Aldrich, Missouri, USA).

Super optimal broth with catabolite repression (SOC) medium: Tryptone (2% (m/v)), 0.5% (m/v) yeast extract, 10 mM NaCl, 2.5 mM KCl, 10 mM magnesium chloride ($MgCl_2$) (≥98%) (Sigma-Aldrich, Missouri, USA), 10 mM magnesium sulphate ($MgSO_4$) (≥95%, Sigma-Aldrich, Missouri, USA) and 20 mM glucose.

TGS buffer 1X, pH 8.3: Tris (0.025 M), 0.192 M glycine and 0.1% (w/v) Sodium dodecyl sulphate (SDS) (Sigma-Aldrich, Missouri, USA).

Towbin buffer 1X, pH 8.3: Tris (25 mM) and 192 mM glycine.

Western blot block buffer: Bovine serum albumin (BSA) (2% (m/v)) (≥98.0%, Sigma-Aldrich, Missouri, USA) dissolved in 1X PBS pH 7.4.

Western blot anti-c-MYC HRP conjugate: BSA (2% (m/v)) dissolved in PBS pH 7.4, 0.05% (v/v) Tween20, 1:1000 Mouse monoclonal anti-c-MYC antibody (clone 9E10) HRP conjugated to peroxidase.

Western blot wash buffer: PBS 1X, pH 7.4 and 0.05% (v/v) Tween20.

Anti-MA scFv glycerol stocks: Anti-MA scFv phage clones 12, 16 and 18 bacterial cultures diluted with 60% (m/v) glucose to a 15% (v/v) final glucose concentration, stored at -80ºC. The stocks were obtained from Onderstepoort Veterinary Institute and were prepared according to Ranchod *et al*. (2018).

Core streptavidin lyophilized plasmid DNA: Synthesized by GenScript (Piscataway, New Jersey, USA).

β-mercaptoethanol: ≥99.0% (Sigma-Aldrich, Missouri, USA).

SDS-PAGE gels: Pre-made Bio-Rad protean TGX gels (Thermo Scientific, Waltham, Massachusetts, USA) with a 4-15% gel concentration gradient.

Protein marker: Precision Plus protein marker (Bio-Rad, USA).

Western blotting filter papers: Western blotting cotton sheet filter papers (Thermo Scientific, Waltham, Massachusetts, USA).

Western blotting membrane: Invitrolon PVDF 0.45 µm pore size membrane (Thermo Scientific, Waltham, Massachusetts, USA).

Deoxyribonucleic acid (DNA) extraction kit: QIAquick miniprep kit (QIAGEN, Hilden, Germany).

Gel extraction kit: QIAquick gel extraction kit (QIAGEN, Hilden, Germany).

Polymerase chain reaction PCR clean up purification kit: QIAquick PCR purification kit (QIAGEN, Hilden, Germany).

DNA marker: Hyperladder 1 kbp (Bioline, London, UK).

Mix & Go TG1 competent *E. coli* cells: Inqaba Biotech Industries, Pretoria, South Africa.

BugBuster Master Mix: Thermo Scientific, Waltham, Massachusetts, USA.

3.2.2 Methods

A. Increasing antigen binding avidity of anti-MA scFv's through fusion of anti-MA scFv and streptavidin genes, and expression of oligomeric scFv's

Gene construct and primer design

Core streptavidin consists of about 139 amino acid residues (equivalent to 415 bp of DNA). The construct was planned such that the anti-MA scFv gene (800 bp) would be at the 5' end. The 15 amino acid residue polypeptide linker of the anti-MA scFv's was retained, but the *NotI* RE site and c-MYC tag sequences were removed from the 3' end of the anti-MA scFv gene. The core streptavidin gene was placed at the 3' end with a hexa-histidine tag for purification. The gene construct was cloned between *Sfi1* and *Not1* restriction enzyme (RE) sites as shown in Figure 3-2.

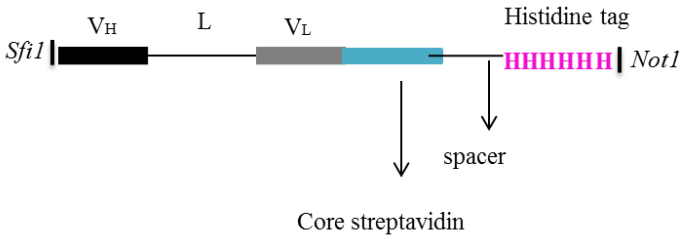

Figure 3-2: Schematic diagram of the gene construct for the fusion of anti-MA scFv's and streptavidin genes. The black block represents variable heavy (V_H) chain of the anti-MA scFv, (L) represents the 15 amino acid polypeptide linker and grey block represents the variable light (V_L) chain of the anti-MA scFv. The blue bock represents the core streptavidin gene and the six pink (H) represent the hexa-histidine tag.

The overlap of the anti-MA scFv genes and streptavidin gene was determined for primer design. Long 33-mer primers were designed that comprised the overlap sequence (15 amino acids) of the streptavidin and anti-MA scFv genes, as well as the overhangs (15-18 amino acids) of each gene. According to the construct in Figure 3-2, the primer for the streptavidin gene extension (SOE strep for) would be in the forward direction and the primer for the anti-MA scFv genes in the reverse direction (SOE scFv reverse). The primers were designed to be long in order to increase specificity of ligation. To decrease promiscuity, the primers did not end with a thymine residue. The melting temperatures of the overlaps were also determined for each primer in order to utilize optimal temperatures that allow for template-primer hybridization.

Streptavidin bacterial glycerol stocks preparation

The core streptavidin gene (415 bp) was cloned into a pUC57 vector (2710 bp) between *XbaI* and *BamHI* RE sites (Genscript, Nanjing, China) as shown in Figure 3-3. The pUC57 vector DNA (obtained as lyophilized DNA) was transformed into JM109 competent bacterial cells according to the manufacturer's instructions. Briefly, 1 µL of the pUC57 vector DNA was added to 50 µL of the JM109 cells and mixed by tapping the tube. The DNA-cell mixture was incubated on ice for 15 minutes before heat shocking at 42ºC for 20 sec for transformation of the DNA into the competent cells. The cells containing DNA were immediately placed back on ice for 2 minutes before transferring them to 950 µL of SOC medium preheated to 37ºC and incubating for 1 h at 37ºC for cell growth. After incubation, a 1/10 serial dilution of the cells was carried out from 10^{-1} to 10^{-3} and 100 µL of each serial dilution was plated on agar plates. The rest of the undiluted cells (990 µL) were pelleted at 3000 x g for 10 minutes. Most of the supernatant was then discarded leaving enough supernatant to resuspend and plate the cells on an agar plate. The agar plates were lidded and incubated upside down on a wet paper towel at 37ºC overnight for colony growth. From the resulting colonies, five colonies were picked using sterile tips. The colonies were resuspended in 10 mL 2XTY medium and were grown overnight at 37ºC with shaking at 220 revolutions per minute (rpm). From the bacterial overnight culture, 1 mL of streptavidin gene glycerol stocks were made by adding 60% (m/v) glucose to the cultures to a final glucose concentration of 15% (v/v). The stocks were stored at -80ºC.

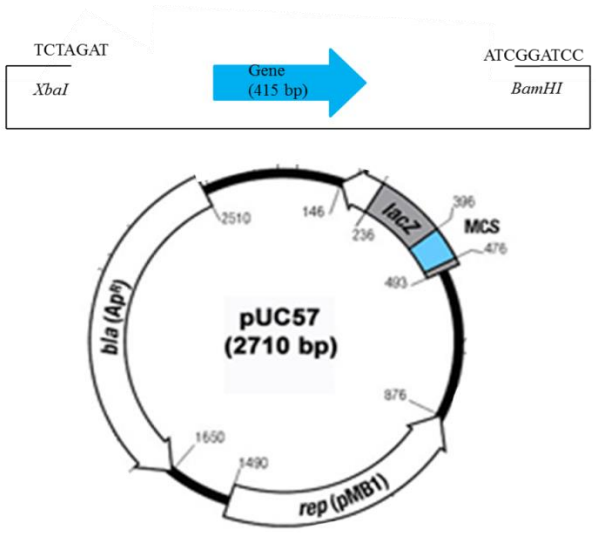

Figure 3-3: pUC57 gene map. The streptavidin gene of 415 bp is cloned in the multiple cloning site (MCS) (light blue) between the *Xba1* and *BamH1* restriction enzyme sites downstream of the lacZ gene (Genscript.com, 2019).

RE digestion of the pUC57 vector DNA was then carried out to determine whether the five picked colonies had the streptavidin gene. Overnight cultures of JM109 bacterial cells containing pUC57 vector were grown for vector DNA extraction. To do this, small amounts of pUC57 bacterial culture glycerol stocks - the size of 0.5 mm beads - were inoculated into 10 mL of 20% (m/v) glucose depleted 2XTY culture medium and resuspended at room temperature. Glucose was not added to the medium to prevent plasmid instability and therefore loss. The cells in the growth medium were incubated at 37ºC overnight (16 h) with shaking at 220 rpm for bacterial cell growth. The pUC57 vector DNA was obtained using a QIAquick miniprep kit (QIAGEN, Hilden, Germany) as described in chapter 2, section 2.2.2 B. Briefly, a lysis buffer was used to resuspend and break open the cells, a neutralization buffer was added to the reaction to renature circular DNA and encourage its dissolution while the linear DNA remained denatured and out of solution. The reactions were centrifuged at 16 000 x g for 10 minutes to obtain supernatants, the supernatants with DNA were bound to QIAprep spin columns with silica gel membranes made up of sodium silicate. The columns were washed with a wash buffer containing ethanol to remove trace nuclease activity, salts and other impurities. The DNAs were eluted with a low-ionic elution buffer that weakens the hydrogen bonds. Since the streptavidin gene was cloned

between *XbaI* and *BamHI* RE sites of the pUC57 vector, these enzymes were used for RE digestion as indicated in Table 3-1.

Table 3-1: Restriction enzyme digestion of pUC57 DNA.

REAGENT	Final concentrations
pUC57 vector DNA	1 µg
BamHI (Roche)	1 U/µL
XbaI (Roche)	1 U/µL
10X buffer M (Roche)	1/10 of final volume
Nuclease free water	Make up the volume
TOTAL	50 µL

The digestion was carried out at 37ºC for 90 minutes. An electrophoretic analysis was carried out on the RE digestion products to investigate which of the five picked colonies carried the streptavidin gene. A 1% (m/v) agarose/1X TAE gel with 1% (v/v) ethidium bromide was prepared for the electrophoretic analysis of the RE digestion products. The gel was immersed in an electrophoretic tank filled with 1X TAE buffer pH 8.3, such that the wells faced the negative (anode) side of the tank. Hyperladder 1 kbp (Bioline, London, UK) was used as reference marker for the band sizes. Each sample was mixed with 6X loading dye (Promega, USA) at a 5:1 volume ratio before being loaded in the gel wells. The electrophoresis was carried out at 100 V for 40 minutes. The streptavidin bands (415 bp) were analysed using a UV transilluminator and all the 5 colonies were found to carry the streptavidin gene.

Streptavidin gene and anti-MA scFv gene fusion

Anti-MA scFv template DNAs from phage clones 12, 16 and 18, and streptavidin template DNA were then obtained for fusion of the genes. Anti-MA scFv genes were cloned in pHEN1 vector shown in Figure 2-2 in Chapter 2, section 2.2.2 A, while the streptavidin gene was cloned in pUC57 vector (Figure 3-3). Bacterial overnight cultures of anti-MA scFv's from phage clones 12, 16 and 18, and streptavidin were first grown from bacterial glycerol stocks in 2XTY medium at 37ºC with shaking at 220 rpm as described in section 2.2.2 A. Plasmid DNA extraction from

the cultures was then carried out using QIAquick miniprep kit as described in chapter 2, section 2.2.2 B. Polymerase chain reaction (PCR) then followed to amplify the anti-MA scFv and streptavidin genes from their vectors pHEN1 and pUC57 respectively using the primers indicated in Table 3-2. The PCR was carried out as indicated in Table 3-3.

Table 3-2: Primer sequences for streptavidin-scFv DNA fusion.

Name	Sequence
SOE strep forward	5' GTC CTA GGC CAG CCC AAT GCG GAG GCG GGC ATC 3'
Strep reverse	5' GAT GGT GGC GGC CGC ATG 3'
Sfi1L	5' GTC CTC GCA ACT GCG GCC CAG CCG GCC CTG ATG GCG GCC GTG ACG 3'
SOE scFv reverse	5' GCC CGC CTC CGC ATT GGG CTG GCC TAG GAC 3'

Table 3-3: PCR for amplification of streptavidin gene from pUC57 DNA and scFv genes from pHEN1 DNA.

REAGENT	Streptavidin gene	scFv gene
10X Ex Taq buffer	1/10 of total volume	1/10 of final volume
Ex Taq polymerase (TaKaRa)	5 U/µL	5 U/µL
dNTPs	2.5 mM	2.5 mM
Streptavidin DNA	200 ng	200 ng
SOE Strep forward primer (10 pmol/µL) (Inqaba Biotech Industries)	0.1 µM	-
STREP reverse primer (Inqaba Biotech Industries)	0.1 µM	-
Sfi1L forward primer	-	0.1 µM
SOE scFv reverse	-	0.1 µM
Nuclease free water	Make up the volume	Make up volume
TOTAL	50 µL	50 µL

The PCR conditions were 1 cycle of initial denaturation at 95ºC for 60 sec, followed by 25 cycles of denaturation at 95ºC for 30 sec, annealing for 30 sec, extension at 72ºC for 1 minute, finishing with final extension at 72ºC for 5 minutes. The T_m's for SOE strep forward primer and strep reverse primer are 59ºC and 62ºC respectively, making 59ºC the T_m for streptavidin gene

amplification. The T_m's for SOE scFv reverse primer and Sfi1L primer are 56ºC and 60ºC respectively, making 56ºC the T_m for anti-MA scFv genes amplification.

Electrophoretic analysis of the PCR products was carried out to investigate successful gene amplification using 1% agarose/1X TAE with 1% (v/v) SYBR green safe to avoid damaging the DNA. Gel extraction was carried out to obtain the anti-MA scFv and streptavidin DNA fragments using a QIAquick gel extraction kit (QIAGEN, Hilden, Germany) as described in chapter 2, section 2.2.2 B. A splicing by overlap extension (SOE) PCR was then carried out to fuse the anti-MA scFv's and streptavidin genes as indicated in Table 3-4.

Table 3-4: SOE PCR to fuse anti-MA scFv and streptavidin DNAs.

REAGENT	Final concentrations
Ex Taq polymerase (TaKaRa)	5 U/µL
10X TaKaRa PCR buffer	1/10 of total volume
dNTPs TaKaRa	2.5 mM
Streptavidin DNA	100 ng
Anti-MA scFv DNA	100 ng
pfu polymerase (Promega)	0.2 µM -1 µM
Nuclease free water	Make up the volume
TOTAL	50 µL

The PCR conditions were 1 cycle of initial denaturation at 94ºC for 2 minutes, followed by 15 cycles of denaturation at 94ºC for 30 sec, annealing at 72ºC for 30 sec, and extension at 72ºC for 1 minute, finishing with a final extension at 72ºC for 5 minutes. Immediately after the SOE PCR, a PCR to amplify with end specific primers was carried out as indicated in Table 3-5.

Table 3-5: PCR to amplify scFv-streptavidin fused genes with end specific primers.

REAGENT	Final concentrations
10X TaKaRa PCR buffer	1/10 of total volume
Ex Taq polymerase (TaKaRa)	5 U/µL
dNTPs TaKaRa	2.5 mM
SOE PCR products	50 µL
Strep reverse primer (Inqaba Biotech Industries)	0.1 µM
Sfi1L forward primer (Inqaba Biotech Industries)	0.1 µM
Nuclease free water	Make up the volume
TOTAL	50 µL

A touchdown PCR reaction was done with 1 cycle of initial denaturation at 94ºC for 2 minutes, followed by 30 cycles of initial denaturation at 94ºC for 30 sec, annealing at 56ºC (T_m-0.5ºC) for 30 sec, and extension at 72ºC for 1 minute, finishing with a final extension at 72ºC for 5 minutes. An electrophoretic gel analysis was carried out on the PCR products to investigate successful fusion of the anti-MA scFv and streptavidin genes using SYBR green safe.

Since the pHEN1 vector has the c-MYC sequence, the fused anti-MA scFv-streptavidin DNAs were ligated into the pHEN1 vector, as the vector would allow for the fusion protein to have both histidine and c-MYC tags. Double RE digestion of the fused anti-MA scFv-streptavidin DNAs and pHEN1 vector DNA was carried out as indicated in Tables 3-6 (*Sfi1* digestion) and 3-7 (*Not1* digestion). *Sfi1* digestion was carried out at 50ºC for 2 h and *Not1* digestion at 37ºC for 2 h.

Table 3-6: *Sfi1* digestion of anti-MA scFv-streptavidin DNA and pHEN1 vector DNA.

REAGENT	Anti-MA scFv-streptavidin	pHEN1
10X Buffer M (Roche)	1/10 of final volume	1/10 of final volume
Sfi1L enzyme (Inqaba Biotech Industries)	0.2 µM -1 µM	0.2 µM – 1 µM
DNA	100 ng	100 ng
Nuclease free water	Make up the volume	Make up the volume
TOTAL	50 µL	50 µL

Table 3-7: *LCNot1* digestion of anti-MA scFv-streptavidin DNA and pHEN1 DNA.

REAGENT	Anti-MA scFv-streptavidin	pHEN1
NaCl	0.15 M	0.15 M
LCNot1 enzyme (Inqaba Biotech Industries)	10 U/µL	10 U/µL
Tris, pH 8	0.012 M	0.012 M
Xho1 enzyme (Promega)	-	5 U/µL
Nuclease free water	Make up the volume	Make up volume
TOTAL	50 µL	50 µL

Half of the volume of the *Not1* digestion reaction products was added to 1 volume of *Sfi1* digestion. The *Xho1* enzyme was added to discourage religation of the vector.

A ligation reaction of anti-MA scFv-streptavidin DNAs from phage clones 12, 16 and 18 with pHEN1 vector DNA was carried out as indicated in Table 3-8 at 15ºC overnight after the RE digestion. Transformation of the ligated DNAs into Mix & Go TG1 competent *E. coli* cells (Inqaba Biotech Industries) was carried out according to the manufacturer's instructions. Briefly, thawed competent cells were mixed with the ligated DNAs such that the DNA was less than 5% (v/v) of the total volume. The DNA-cell mixtures were immediately placed on ice for 30 minutes before plating on 37ºC pre-warmed agar plates. The plates were lidded and incubated facing upside down on a dampened paper towel at 37ºC overnight for colony growth.

Table 3-8: Ligation of the anti-MA scFv-streptavidn DNAs to pHEN1 DNA.

REAGENT	Final concentrations
pHEN1 DNA	100 ng
SOE scFv DNA	40 ng
10X T4 Ligase Buffer (Promega)	1/10 of final volume
T4 DNA ligase (Promega)	0.2 µM -1 µM
Nuclease free water	Make up the volume
TOTAL	10 µL

Colony PCR was then carried out to investigate which of the colonies had inserts as indicated in Table 3-9, after bursting the cells open at 100ºC as in chapter 2, section 2.2.2 B. The DNAs were

then sequenced by the Sanger method (Inqaba Biotech Industries). The engineered scFv's were then named anti-MA scFv streptavidin (anti-MA scFv SAs). Six colonies carried correct sequence anti-MA scFv SAs, with two colonies each from phage clones 12, 16 and 18.

Table 3-9: Colony PCR to investigate anti-MA scFv SA DNA inserts.

REAGENT	Final concentrations
Go Taq Green (Promega)	12.5 µL
DNA	10 µL
OP52 primer (Inqaba Biotech Industries)	0.2 µM -1 µM
M13 reverse primer (Inqaba Biotech Industries)	0.2 µM -1 µM
Nuclease free water	Make up the volume
TOTAL	25 µL

Bacterial overnight cultures of the colonies carrying correct sequence anti-MA scFv SAs were grown in 2XTY medium and 20% (m/v) glucose at 37ºC with shaking at 220 rpm. Bacterial glycerol stocks of the anti-MA scFv SAs were then made from the bacterial overnight cultures by adding 60% (m/v) glucose to the cultures to a final glucose concentration of 15% (v/v). The glycerol stocks were stored at -80ºC. The supernatant (SN) and periplasmic (PP) anti-MA scFv SAs were expressed and obtained as described in chapter 2, section 2.2.2 A.

ELISA to determine activity of anti-MA scFv SAs on MAs

Activity of the anti-MA scFv SAs was investigated using indirect ELISA assay as described in chapter 2, section 2.2.2 A, after obtaining SN and PP anti-MA scFv SAs as described in chapter 2, section 2.2.2 A. Induction temperatures of the anti-MA scFv SAs from phage clones 16 and 18 that were previously at 30ºC were reduced to 18ºC and 25ºC respectively, while the induction temperature of anti-MA scFv SA from phage clone 12 remained 30ºC.

Spot blot assay to investigate expression of the anti-MA scFv SAs

Confirmation of the production of the anti-MA scFv SAs (previously all induced at 30ºC) was done by means of a spot blot assay to investigate whether the inactivity of the anti-MA scFv SAs in indirect ELISA assay was due to the absence of the proteins or the detrimental effect of the fusion with streptavidin. To perform the assay, a PVDF membrane and filter paper were cut to fit the 96-well filter plate of a filter pump. The filter paper was soaked in 1X TBS pH 7.2 and overlaid on the filter plate. The PVDF membrane was charged with cold absolute methanol to activate the chemical groups on the membrane for the binding of the anti-MA scFv SAs by hydrogen bonding. Methanol was drained and the membrane was soaked in 1X TBS pH 7.2 and was overlaid on the filter paper. The filter plate lid was attached and screwed to the plate. To each designated well, 20 µL of anti-MA scFv SAs from each of the three clones was pipetted. A non-related scFv with a c-MYC tag was used as a positive control. The pump was then switched on to suck the scFv's onto the PVDF membrane for 1 minute. The pump was disassembled and the PVDF membrane was air dried for 30 minutes. After drying, the PVDF membrane was recharged with methanol, the methanol was drained, and the membrane was soaked in 1X TBS pH 7.2 before blocking in Western blot block buffer for 1 h with shaking at 10 rpm. The membrane was then soaked in Western blot anti-c-MYC HRP secondary antibody (mouse monoclonal anti-c-MYC antibody (clone 9E10) conjugated to peroxidase) for 1 h with shaking at 10 rpm to bind the anti-MA scFv SAs. The membrane washed three times by soaking in Western blot wash buffer to remove unbound secondary antibody before adding TMB for blot tests for colour development. Colour development was allowed for 2-5 minutes before stopping the reaction by soaking the membrane in dddH_2O. Allowing colour development beyond 5 minutes results in precipitation of the product colour stain which yields inaccurate results

Extraction of anti-MA scFv SAs from the inclusion bodies (IBs)

After overnight anti-MA scFv SAs induction with IPTG (previously all induced at 30ºC), the cultures were pelleted at 3000 x g and the cells were burst open by four cycles of repeated freezing and thawing at -70ºC for 10 minutes and room temperature for 10 minutes. The cells were vortexed after each thawing step to facilitate cell bursting. The cells were then resuspended in 100 µL PBS pH 7.4 and incubated at room temperature for 10 minutes at 700 rpm to ensure dissolution of soluble proteins. The reaction was then centrifuged at 3000 x g to obtain the PP

fraction. To extract the IB fraction, the pellets were resuspended in a volume of BugBuster Master Mix (Thermo Scientific, Waltham, Massachusetts, USA) that was 1/5 of the bacterial culture volume. The resuspension was centrifuged at 13 000 x g for 15 minutes to obtain the supernatant which was the IB fraction.

Affinity column purification of anti-MA scFv SAs

Because the anti-MA scFv SAs have a hexa-histidine tag, these oligomeric scFv's were purified using nickel-liganded affinity columns, HisPur Ni-NTA resin (Thermo Fischer Scientific, SA). The columns were equilibrated with two bed volumes of lysis buffer before use. The anti-MA scFv SAs samples were diluted to a 1:1 volume ratio with lysis buffer before passing twice through the column and collecting the flow through. The columns were then washed twice with two bed volumes of wash buffer and the washes were collected. The anti-MA scFv SAs were eluted six times with a quarter bed volume (500 µL) of elution buffer. The eluted anti-MA scFv SAs were concentrated in conjunction with a buffer change into PBS pH 7.4 as described in chapter 2, section 2.2.2 A. To determine protein concentration, the Bradford assay was carried out as described in chapter 2, section 2.2.2 A. Afterwards, SDS-PAGE and Western blot analysis were carried out as described in chapter 2, section 2.2.2 A to track the purification of the anti-MA scFv SAs. The columns were stored in 30% (v/v) ethanol and the scFv's were stored at -20ºC.

SDS-PAGE and Western blot analysis of anti-MA scFv SAs

SDS-PAGE and Western blot analysis of anti-MA scFv SAs were carried out as described in chapter 2, section 2.2.2 A. Analysis was carried out under denaturing and non-denaturing conditions by adding 2X β-mercaptoethanol (denaturing sample buffer) to one anti-MA scFv SA and non-denaturing protein sample buffer to the other anti-MA scFv SA from the same clone.

3.3 RESULTS

3.3.1 Cloning of anti-mycolic acid scFv's streptavidin (anti-MA scFv SAs)

The cloning of anti-MA scFv SAs was carried out in five steps as depicted in Figure 3-4.

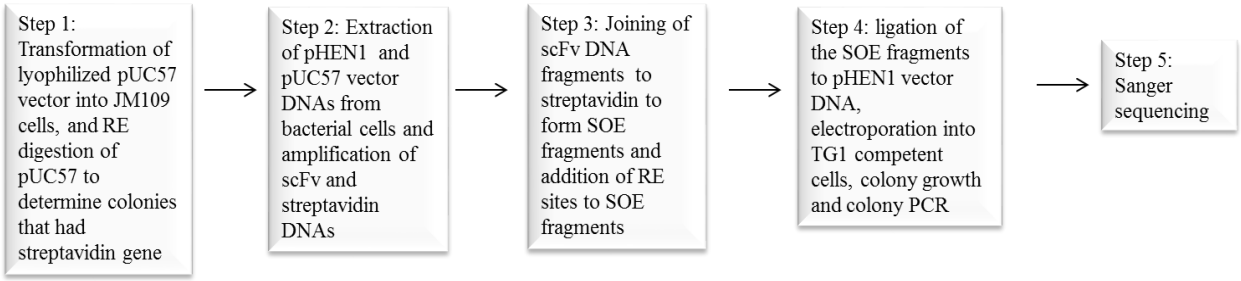

Figure 3-4: The five cloning steps of anti-MA scFv SAs.

Step 1 of the cloning steps in Figure 3-4 was carried out to begin the cloning process. Because the pUC57 vector carrying the streptavidin gene was obtained as lyophilized DNA, the pUC57 vector had to be transformed into JM109 bacterial cells for colony growth. RE digestion of the pUC57 vector DNA and electrophoretic analysis of the digested pUC57 vector DNA was carried out to determine which of the five picked colonies had the streptavidin gene as shown in Figure 3-5.

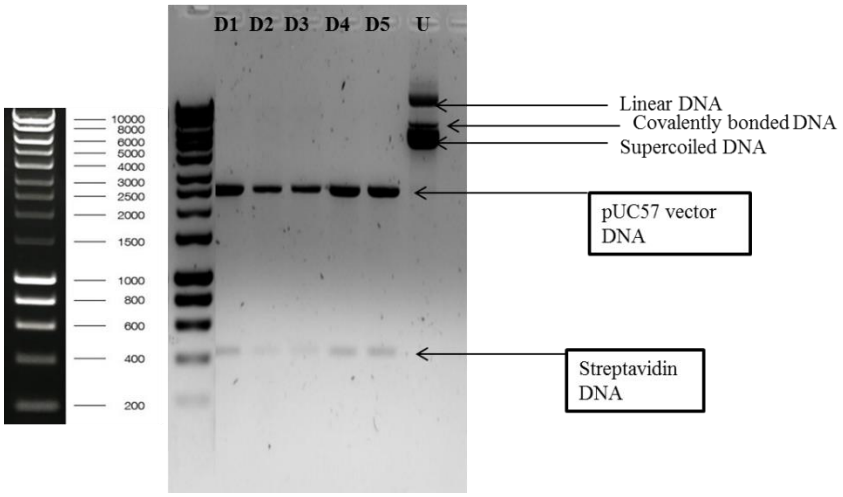

Figure 3-5: Gel electrophoresis for RE digested pUC57 DNA analysis. D1 – D5 are the digested pUC57 DNA samples and U is the undigested pUC57 vector DNA sample.

Figure 3-5 shows that all the five picked colonies carried the pUC57 vector with the streptavidin gene (415 bp). The undigested pUC57 vector DNA depicts three bands that represent supercoiled, covalently bonded and linear DNA. Any of the picked colonies were viable to be used in the cloning of the streptavidin oligomeric scFv's.

Step 2 of the cloning process in Figure 3-4 then followed. The anti-MA scFv DNAs and streptavidin DNA were obtained and amplified from their vectors, pHEN1 and pUC57 respectively, and electrophoretic analysis was carried out on the DNA fragments to analyse the successful amplification of the DNAs as shown in Figure 3-6.

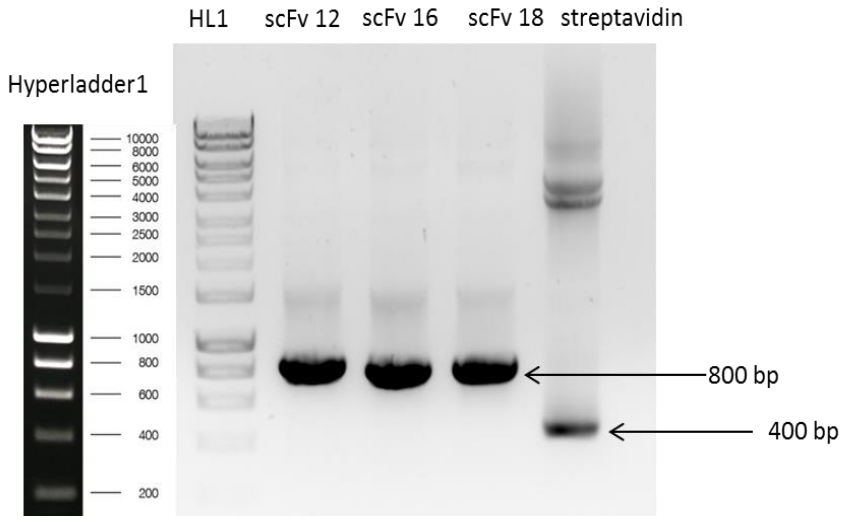

Figure 3-6: Gel electrophoresis for analysis of amplified anti-MA scFv and core streptavidin DNA. ScFv 12, 16 and 18 are DNAs of anti-MA scFv's from phage clones 12, 16 and 18 respectively.

The results from Figure 3-6 show that the anti-MA scFv DNAs of 800 bp length and the streptavidin DNA of about 415 bp length were successfully amplified. The higher bands seen in the streptavidin lane represent the supercoiled DNA.

Splicing by overlap extension (SOE) PCR, which is step 3 of the cloning steps was then carried out to join the streptavidin DNA to each of the anti-MA scFv DNAs from the three phage clones 12, 16 and 18. Electrophoretic analysis of the SOE fragments was carried out to investigate successful joining of the SOE DNA fragments as shown in Figure 3-7.

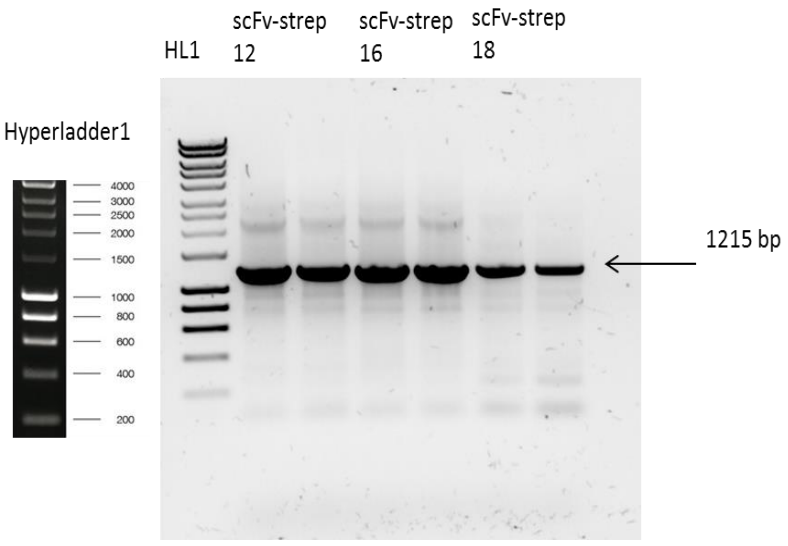

Figure 3-7: Gel electrophoresis for analysis of joint (SOE) DNAs of core streptavidin and anti-MA scFv's. ScFv-strep 12, 16 and 18 are the joint DNA samples of streptavidin and anti-MA scFv's from phage clones 12, 16 and 18 respectively.

Figure 3-7 shows that the SOE DNA fragments (anti-MA scFv SA DNAs) of 1215 bp length were successfully joint and amplified.

Step 4 of the cloning steps in Figure 3-4 was then executed. Following successful ligation of the SOE DNA fragments of the anti-MA scFv SAs to pHEN1 vector DNA, the DNAs were transformed into TG1 competent bacterial cells, and the cells were allowed to grow into colonies overnight at 37ºC. Colony PCR was carried out on 10 colonies per phage clone to investigate which of the colonies had the anti-MA scFv SA DNA inserts. Electrophoresis of the DNAs was carried out to investigate the DNA inserts as shown in Figure 3-8.

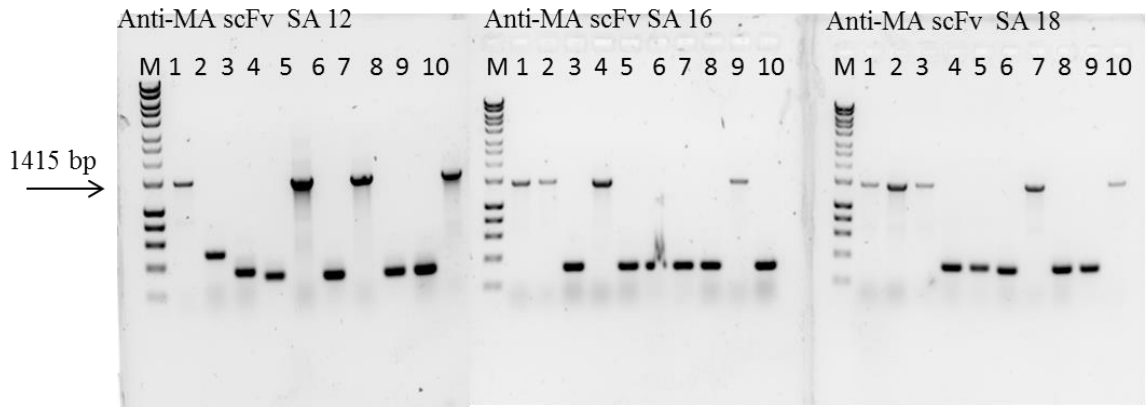

Figure 3-8: Gel electrophoresis for analysis of successful anti-MA scFv SA DNA inserts (1415 bp). (M) 1 kbp Hypper ladder DNA marker. Lanes numbered 1-10 represent the colony numbers. Anti-MA scFv SA 12, 16 and 18 are the anti-MA scFv SAs from phage clones 12, 16 and 18.

The expected band was 1215 bp as shown in Figure 3-7. The 200 added base pairs that yielded 1415 bp inserts (Figure 3-8) were due to the OP52 and M13 reverse primers that each added 100 bp to the expected 1215 bp SOE DNA fragments. From Figure 3-8 therefore, four colonies successfully carried anti-MA scFv SA DNA inserts from phage clone 12, four colonies successfully carried DNA inserts from phage clone 16 and five colonies successfully carried DNA inserts from phage clone 18.

Step 5 of the cloning steps from Figure 3-4 followed. Sanger sequencing method was carried out on the anti-MA scFv SA DNA inserts from Figure 3-8 (colony PCR) to determine which of the DNAs were in the right frame with no deleterious mutations to the proteins. Figure 3-9 depicts the amino acid sequences of the inserts.

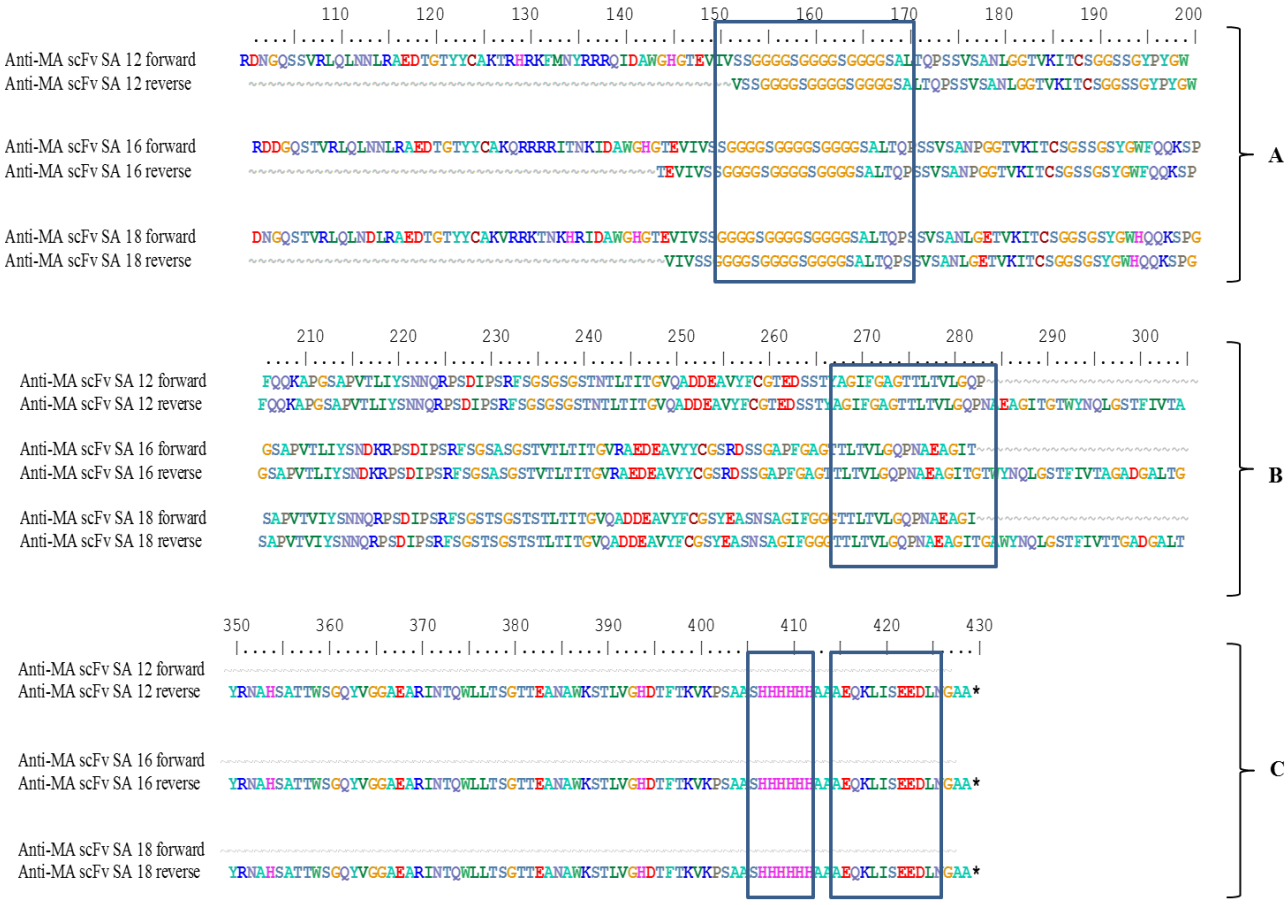

<u>Figure 3-9</u>: Amino acid sequences of anti-MA scFv SAs translated from Sanger base sequences to confirm the successful fusion of anti-MA scFv DNAs to core streptavidin DNA, correct order and frame of the codons. The base sequences were translated to amino acids that are depicted in one letter code and are colour coded. Alanine (A) is shown in powder blue, arginine (R) in dark blue, asparagine (N) in lilac, aspartic acid (D) in red, cystine (C) in maroon, glutamic acid (E) in red, glutamine (Q) in lilac, glycine (G) in yellow, histidine (H) in magenta, isoleucine (I) in green, leucine (L) in green, lysine (K) in dark blue, methionine (M) in green, phenylalanine (F) in light blue, proline (P) in brown, serine (S) in lilac, threonine (T) in lilac, tryptophan (W) in light green, tyrosine (Y) in light blue and valine (V) in green. The boxes in three brackets indicate (A) the full-length linker sequence $(Gly_4Ser)_3$; (B) scFv-streptavidin alignment sequence 5'-LTVLGQPNAEAG-3' and (C) hexa histidine tag (left box) and c-MYC tag (right box).

The sequences in Figure 3-9 are amino acid sequences that were translated from base sequences obtained from Sanger sequencing using BioEdit. Figure 3-9 (A) shows that full length linkers were successfully retained. Figure 3-9 (B) depicts correct alignment of anti-MA scFv and core streptavidin genes, therefore, the aim to fuse the genes was successful. Figure 3-9 (C) depicts the two affinity tags of the oligomers. The anti-MA scFv SA DNAs from phage clone 12, 16 and 18

in Figure 3-8 (colony PCR) that had the correct sequences as shown in Figure 3-9 were from colonies 1 and 5 (phage clone 12); colonies 1 and 9 (phage clone 16), and colonies 1 and 7 (phage clone 18).

The amino acid sequences of the anti-MA scFv SAs were also examined to ensure there were no sequence changes in the complementarity determining regions (CDRs) as depicted in Figure 3-10.

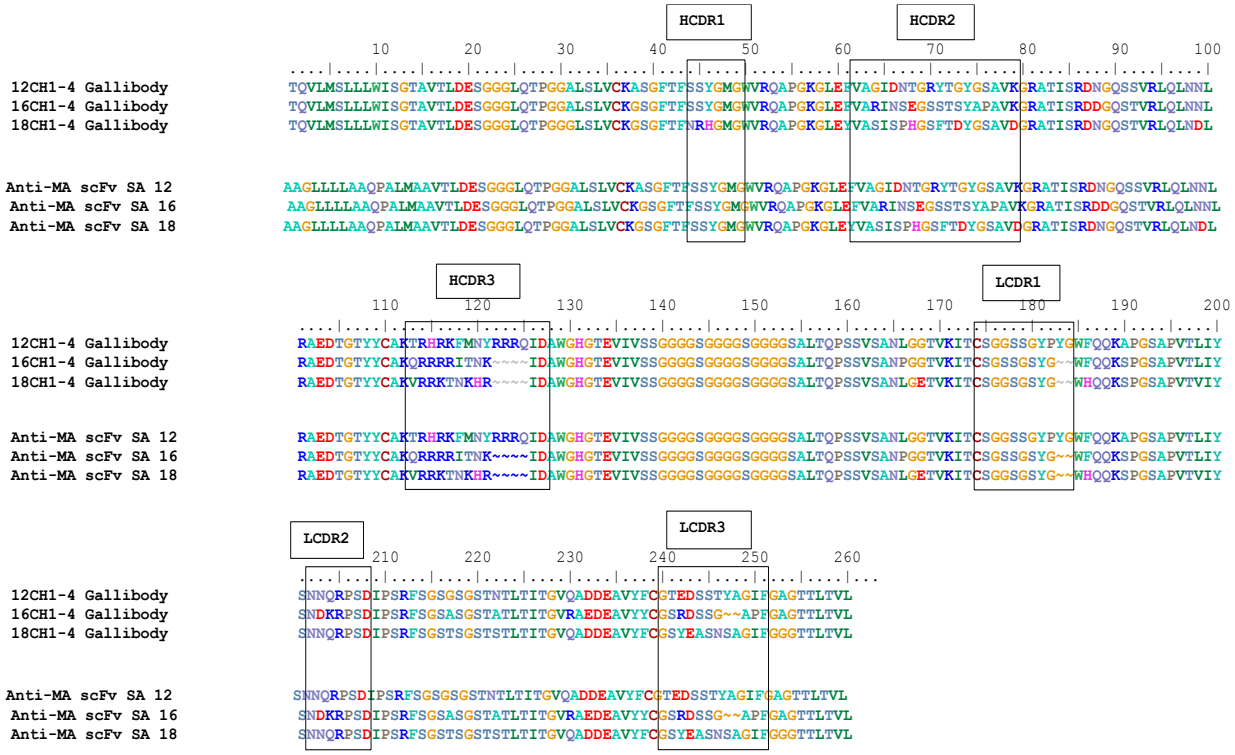

<u>Figure 3-10</u>: Complementarity determining regions (CDRs) sequences of anti-MA scFv SAs. HCDR1, HCDR2 and HCDR3 are the heavy chain CDR 1, 2 and 3 respectively, and LCDR1, LCDR2 and LCDR3 are light chain CDR 1, 2 and 3 respectively.

Figure 3-10 shows that there are no sequence changes in the CDRs that would hamper the anti-MA scFv SAs from binding to the antigen.

3.3.2 Binding activity of anti-MA scFv SAs on MAs

The activity of the anti-MA scFv SAs with the right sequences (Figure 3-8) was carried out in an indirect ELISA assay as shown in Figure 3-11.

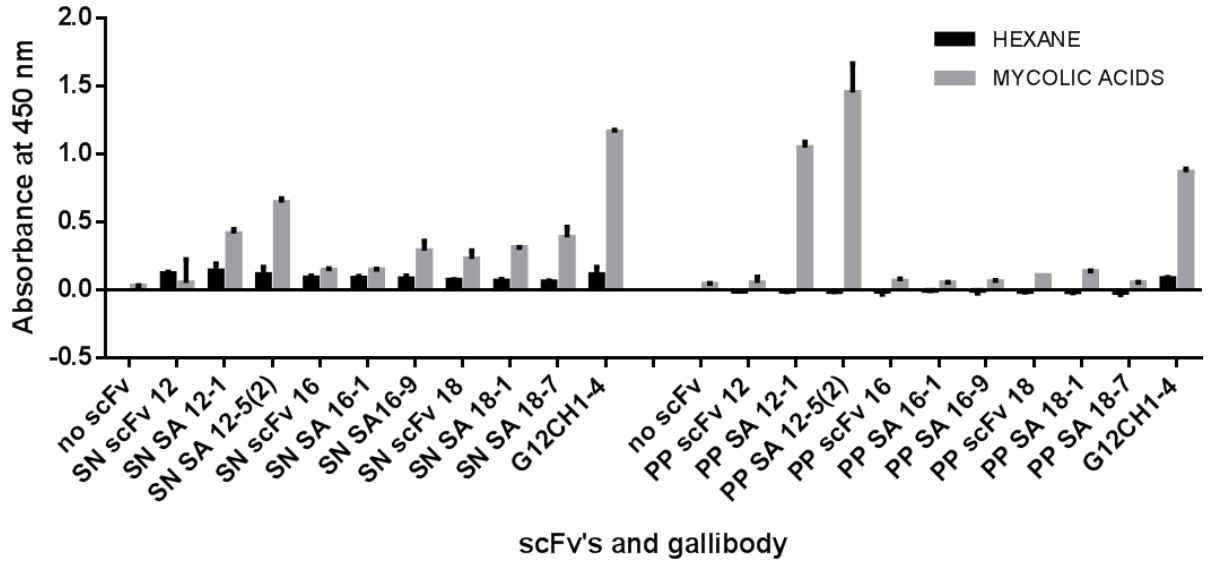

Figure 3-11: Indirect ELISA assay to determine the MA binding activity of the anti-MA scFv SAs. ELISA plates were coated with either MA antigen or hexane as antigen control. Anti-MA scFv SAs from either the culture SN or PP space and diluted with ELISA dilution buffer on 1:1 volume ratio were tested, and the binding activity was measured using anti-c-MYC mouse monoclonal antibody-HRP conjugate. The anti-MA scFv SAs' binding signals were then corrected by subtracting the background signal generated by the binding of ELISA dilution buffer to hexane (antigen control). ScFv 12, 16 and 18 are anti-MA scFv's from phage clones 12, 16 and 18. SAs are anti-MA scFv SAs from colonies 1and 5(2) (phage clone 12), colonies 1 and 9 (phage clone 16), and colonies 1 and 7 (phage clone 18). G12CH1-4 is gallibody 12CH1-4 (positive control). The data represents two biological repeats performed in triplicate. The error bars represent standard deviation.

Figure 3-11 depicts poor binding signals generated by the SN and PP anti-MA scFv SAs from phage clones 16 and 18. Only PP anti-MA scFv SAs from phage clone 12 generated high binding signals to MAs. Although the signals generated by the anti-MA scFv SAs from phage clone 12 seem to compare with the signal generated by the gallibody 12CH1-4, the binding avidities cannot be compared as the concentrations were not controlled. The aim therefore to increase the

binding avidities of anti-MA scFv's by fusion with streptavidin cannot be deduced from Figure 3-11. However, the indirect ELISA assay depicts good activity of anti-MA scFv SAs from phage clone 12 and poor activities of anti-MA scFv SAs from phage clones 16 and 18.

Because the results from Figure 3-11 showed that only the PP anti-MA scFv SAs from phage clone 12 generated high signals, a spot blot assay was carried out to investigate whether the anti-MA scFv SAs from phage clones 16 and 18 were being expressed at all in the SN and PP as shown in Figure 3-12 (A). A second spot blot assay was carried out to investigate whether the anti-MA scFv SAs were expressing in the inclusion bodies, as shown in Figure 3-12 (B).

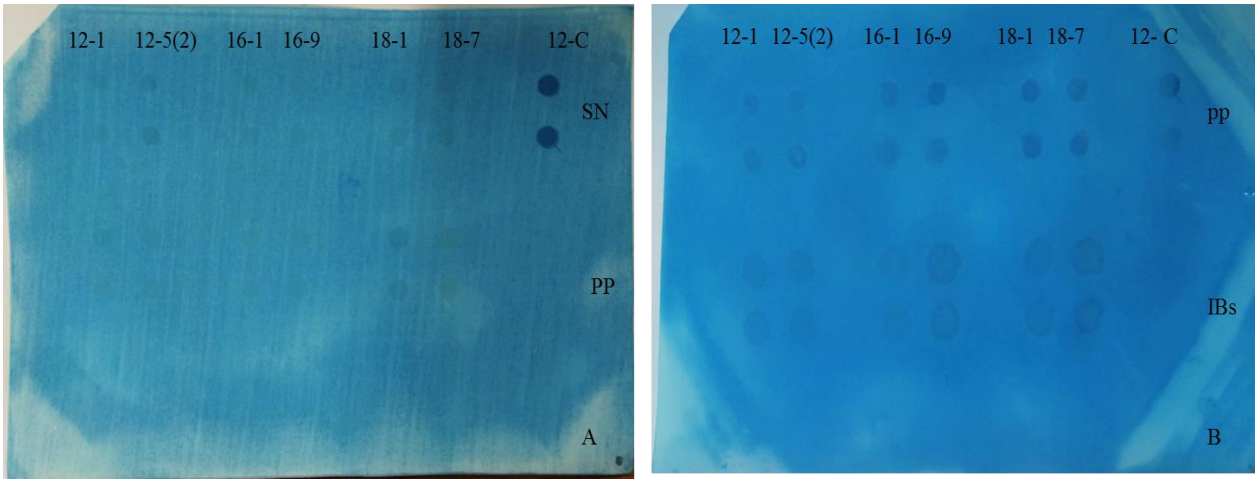

Figure 3-12: Spot blot assays on anti-MA scFv SAs to determine their expression in the supernatant (SN), periplasmic (PP) and inclusion body (IB) fractions. The anti-MA scFv SAs were directly spotted on the PVDF membrane and the scFv's were probed with anti-c-MYC mouse monoclonal HRP conjugate. (A) Spot blot assay of SN and PP fractions of anti-MA scFv SAs from colonies 1 and 5(2) (phage clone 12), colonies 1 and 9 (phage clone 16) and colonies 1 and 7 (phage clone 18). 12-C is the control anti-MA scFv from phage clone 12. (B) Spot blot assay of PP and IB fractions of anti-MA scFv SAs from colonies 1 and 5(2) (phage clone 12), colonies 1 and 9 (phage clone 16) and colonies 1 and 7 (phage clone 18). The PP fractions in (A) were obtained by mechanical cell bursting while the PP fractions in (B) were obtained by resuspending the cells in EDTA.

Figure 3-12 (A) shows that all the anti-MA scFv SAs produced very faint spots both in the SN and PP, demonstrating that the anti-MA scFv SAs from phage clones 16 and 18 were being expressed in like manner with the anti-MA scFv SAs from phage clone 12. Figure 3-12 (B) demonstrates that the anti-MA scFv SAs from all clones obtained from the PP fraction -

extracted by mechanical cell bursting - showed better expression than the PP anti MA scFv SAs from Figure 3-12 (A) that were extracted by resuspending and incubating the cells in a solution with EDTA. Generally, the anti-MA scFv SAs have poorer expression in the IB fraction than in the PP fraction. Figure 3-12 depicts that the anti-MA scFv SAs were all being expressed in a similar fashion. Therefore, expression did not seem to be a restraining factor to the activity of the anti-MA scFv SAs from phage clones 16 and 18.

An indirect ELISA assay was then carried out using the PP and IB fractions from Figure 3-12 (B) to determine whether the anti-MA scFv SAs from these fractions generated better binding signals to MAs than the fractions used in the indirect ELISA assay in Figure 3-11. The results are shown in Figure 3-13.

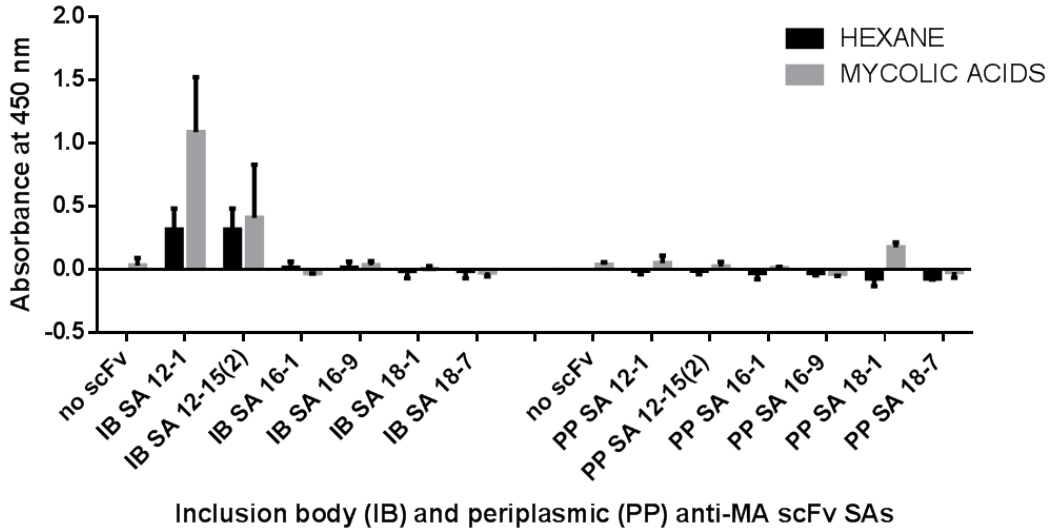

Figure 3-13: Indirect ELISA assay to determine the MA binding activity of the anti-MA scFv SAs obtained in either the inclusion bodies (IB) or periplasmic space (PP). ELISA plates were coated with either MA antigen or hexane as antigen control. Anti-MA scFv SAs from either the PP space or IB and diluted with ELISA dilution buffer on 1:1 volume ratio were tested, and the binding activity was measured using anti-c-MYC mouse monoclonal antibody-HRP conjugate. The anti-MA scFv SAs' binding signals were then corrected by subtracting the background signal generated by the binding of ELISA dilution buffer to hexane (antigen control). IB SAs and PP SAs are anti-MA scFv SAs obtained from inclusion bodies and periplasmic space respectively, from colonies 1 and 5(2) (phage clone 12), colonies 1 and 9 (phage clone 16), and colonies 1 and 7 (phage clone 18). The data represents two biological repeats performed in triplicate. The error bars represent standard deviation.

Figure 3-13 represents the data obtained using the PP and IB fractions from Figure 3-12 (B). Only the anti-MA scFv SAs from phage clone 12 obtained from the IB fraction produced high signals, and all the PP fractions extracted by mechanical disruption of the cell wall did not generate satisfactory binding signals to MAs. The poor binding signals of the anti-MA scFv SAs led to the decrease of the induction temperatures of the anti-MA scFv SAs as the spot blot assay and indirect ELISA assay depicted in Figures 3-12 and 3-13 respectively showed that expression was not a preventative aspect to the activity of the anti-MA scFv SAs.

The anti-MA scFv SAs from phage clones 16 and 18 were re-induced at lower temperatures of 18ºC and 25ºC respectively to encourage better folding of the scFv's. An indirect ELISA assay was carried out using the low temperature induced anti-MA scFv SAs to investigate the activity of the anti-MA scFv SAs on MAs as shown in Figure 3-14.

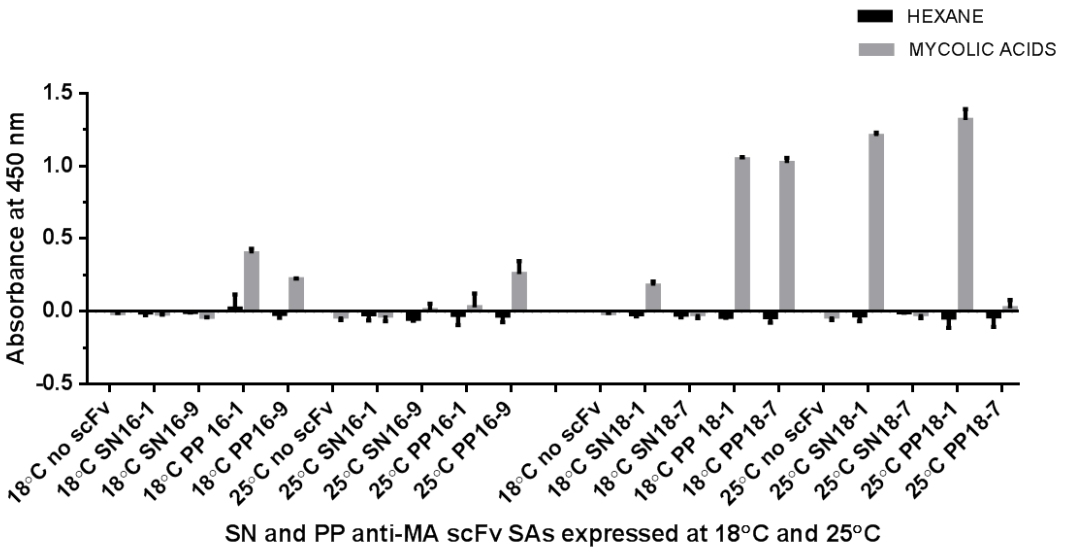

Figure 3-14: Indirect ELISA assay to determine the MA binding activity of the low temperature-induced (18ºC and 25ºC) anti-MA scFv SAs obtained in either the culture supernatant (SN) or periplasmic space (PP). ELISA plates were coated with either MA antigen or hexane as antigen control. Anti-MA scFv SAs from either the PP space or SN and diluted with ELISA dilution buffer on 1:1 volume ratio were tested, and the binding activity was measured using anti-c-MYC mouse monoclonal antibody-HRP conjugate. The anti-MA scFv SAs' binding signals were then corrected by subtracting the background signal generated by the binding of ELISA dilution buffer to hexane (antigen control). SN and PP are anti-MA scFv SAs obtained from supernatant and periplasmic space respectively, from colonies 1and 5(2) (phage clone 12), colonies 1 and 9 (phage clone 16), and colonies 1 and 7 (phage clone 18). The data represents two biological repeats performed in triplicate. The error bars represent standard deviation.

Figure 3-14 shows that anti-MA scFv SAs 16-1 and 16-9 from the PP space generated improved binding signals when induced at 18ºC. Only anti-MA scFv SA 16-9 from the PP space generated a signal when induced at 25ºC. SN fractions of anti-MA scFv SAs 16-1 and 16-9 did not generate any binding signal when induced at both temperatures. Anti-MA scFv SA 18-1 from both SN and PP fractions generated high signals when induced at 25ºC, and anti-MA scFv SA 18-7 from the PP space only generated a high signal when induced at 18ºC. While the signals generated by the anti-MA scFv SAs showed improvement, the aim to increase avidity of the anti-MA scFv's by fusion with streptavidin cannot be deduced from Figure 3-14 as the molar concentrations were not determined. Figure 3-14 therefore indicates successful activity of anti-MA scFv SAs from phage clones 16 and 18. These were purified further for characterization.

3.3.3 Affinity column purification and size characterization of anti-MA scFv SAs

The anti-MA scFv SAs that generated the highest signals in the indirect ELISA assays in Figures 3-11 and 3-14 (anti-MA scFv SA 12-5(2) from PP space (induced at 30ºC), anti-MA scFv SA 16-1 from the PP space (induced at 18ºC) and anti-MA scFv SA 18-1 from both the PP and SN (induced at 25ºC)) were affinity purified using nickel liganded columns and characterized by size using SDS-PAGE and Western blot as shown in Figure 3-15.

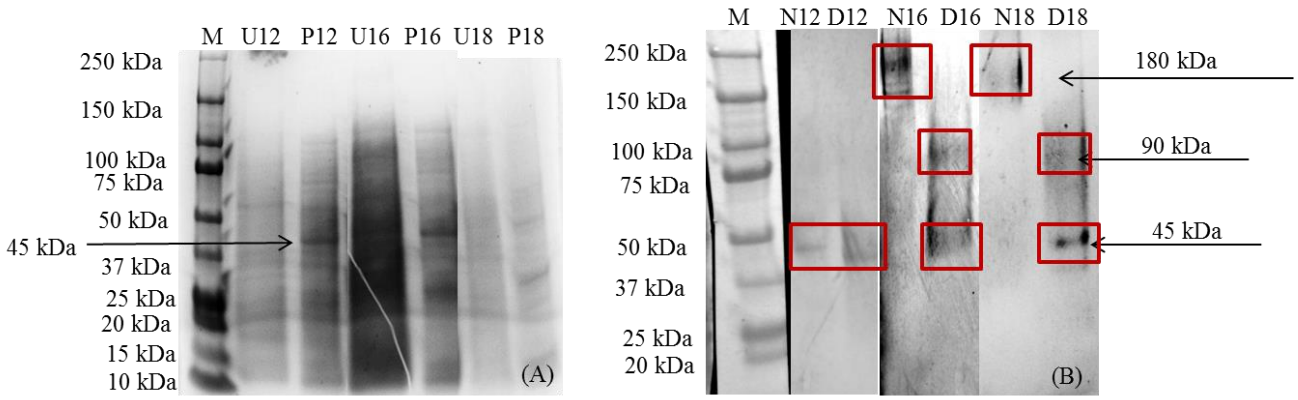

<u>Figure 3-15</u>: SDS-PAGE and Western blot analysis of anti-MA scFv SAs to track purification and define the anti-MA scFv SA sizes. (A) SDS-PAGE gel where (U) and (P) represent the unpurified and purified anti-MA scFv SAs from phage clones 12, 16 and 18 respectively. (B) Western blot where (N) represents the anti-MA scFv SAs from phage clones 12, 16 and 18 under non-denaturing conditions and (D) represents anti-MA scFv SAs from phage clones 12, 16 and 18 under denaturing conditions.

Figure 3-15 (A) shows more concentrated bands at 45 kDa after purification which corresponds to the monomeric anti-MA scFv SAs. Figure 3-15 (B) shows no differences in size between anti-MA scFv SAs from phage clone 12 under non-denaturing and denaturing conditions. For anti-MA scFv SAs from phage clones 16 and 18, there are smudges at 180 kDa obtained under non-denaturing conditions which correspond to the tetrameric anti-MA scFv SAs. Under denaturing conditions, there are bands at 90 kDa which correspond to dimeric anti-MA scFv SAs, and bands at 45 kDa which correspond to monomeric anti-MA scFv SAs. Figure 3-15 (A) depicts successful purification of anti-MA scFv SAs and Figure 3-15 (B) depicts successful formation of tetramers from the fusion of anti-MA scFv's to streptavidin.

3.3.4 Binding avidities of anti-MA scFv's and anti-MA scFv SAs

An indirect ELISA assay was carried out using anti-MA scFv SAs from phage clones 12, 16 and 18 at concentrations of 0.25 mg/mL in order to compare the binding avidities to MA as shown in Figure 3-16.

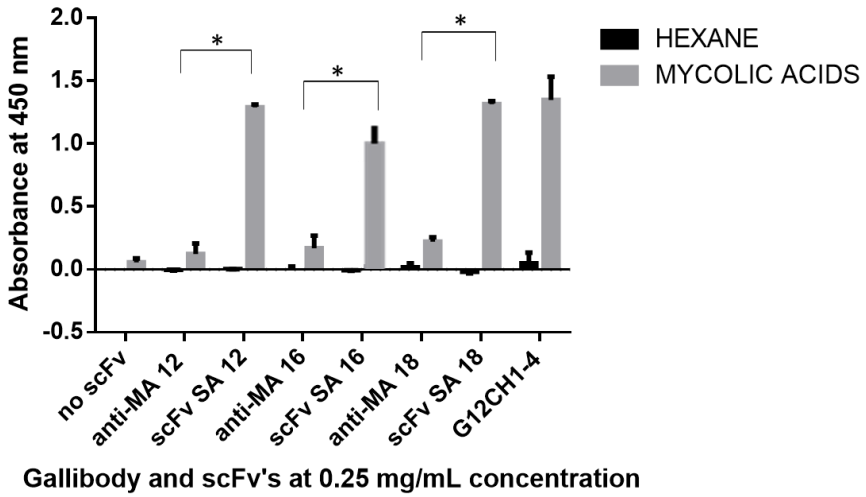

Figure 3-16: Indirect ELISA assay to compare the MA binding avidities of purified anti-MA scFv's and anti-MA scFv SAs. ELISA plates were coated with either MA antigen or hexane as antigen control. ELISA dilution buffer with no scFv, affinity purified anti-MA scFv's, anti-MA scFv SAs and gallibody 12CH 1-4 (positive control) at 0.25 mg/ml concentration were tested and the binding activity was measured using anti-c-MYC mouse monoclonal antibody-HRP conjugate. The antibodies' binding signals were then corrected by subtracting the background signal generated by the binding of ELISA dilution buffer with no antibody on the hexane (antigen control). Anti-MA 12, 16 and 18 are anti-MA scFv's from phage clones 12 and 16, and scFv SAs are anti-MA scFv SAs from phage clones 12 and 16. The data represents two biological repeats in performed triplicate. The error bars represent standard deviation and the asterisks (*) indicates the p-value where *$p<0.05$.

Figure 3-16 depicts that at the same concentration, anti-MA scFv SAs have enhanced functional binding avidities to MAs when compared to anti-MA scFv's with relevant *p* values of 0.00712, 0.0046325 and 0.00348 for clones 12, 16 and 18 respectively indicating significance of binding avidity differences. The hypothesis that oligomeric scFv's from the scFv phage clones 12, 16 and 18 can be obtained by creating scFv-streptavidin fusion proteins. tetramers will gain a greater binding avidity to the MAs is therefore supported. The aim to increase the functional binding

avidities of anti-MA scFv's through fusion with streptavidin was therefore achieved. Absolute comparisons of binding avidity between different anti-MA scFv SAs and gallibodies require dilution titrations, which is done in Chapter 4.

3.4 DISCUSSION

E. coli was successfully used as an expression system for oligomeric anti-MA scFv SAs derived from scFv phage clones 12, 16 and 18 (Ranchod *et al*., 2018). The successful expression of anti-MA scFv SAs in a prokaryotic system such as *E. coli* demonstrates affordable means for the expression of stable and active antibodies, eliminating the need for expensive and tedious eukaryotic expression systems for antibodies. The anti-MA scFv SAs were designed for expression in the *E. coli* periplasm - as were the anti-MA scFv SLs described in chapter 2 - where the oxidizing environment enables disulphide bond formation and proper folding of the protein domains (Schultz *et al*., 2000). Although the anti-MA scFv SAs were directed for expression in the *E. coli* periplasm due to the pelB leader sequence of the pHEN1 vector (chapter 2, Figure 2-2), anti-MA scFv SAs from phage clones 16 and 18 generated low absorbance signals in the indirect ELISA assay in Figure 3-11. The low absorbance signals reflect poor binding to MAs, which led to the belief that the anti-MA scFv SAs from phage clones 16 and 18 were being expressed as insoluble proteins in inclusion bodies (IBs).

Because most fusion proteins have been known to express as insoluble proteins in the IBs, investigation of the IB fraction was imperative (Schultz *et al*., 2000, Won *et al*., 2009, Dübel *et al*., 1995). Overexpression of recombinant proteins can lead to expression of misfolded inactive recombinant proteins in the IBs (Kane and Hartley, 1988, Castellanos-Mendoza *et al*., 2014). Nonetheless, the investigation of the IBs demonstrated that the anti-MA scFv SAs did not generate expected binding signals to MAs as shown by the indirect ELISA in Figure 3-13, indicating that the anti-MA scFv SAs were not expressed in desired amounts in the IBs. It was to our advantage that the anti-MA scFv SAs did not express in the IBs as the refolding, solubilisation and purification of recombinant antibodies from the IBs requires elaborate techniques that will yield biologically active proteins in preferred amounts (Rudolph and Lilie, 1996). Recovery of anti-MA scFv SAs from the IBs would therefore be cumbersome and undesirable.

The decrease in induction temperatures of the anti-MA scFv SAs from phage clones 16 and 18 resulted in better expression of active tetrameric scFv's. The indirect ELISA assays in Figure 3-14 shows that the anti-MA scFv SAs from phage clones 16 and 18 induced at lower temperatures of 18ºC and 25ºC respectively, generated expected binding signals to MAs. Most studies have

induced scFv-streptavidin fusion proteins at 30ºC successfully, and other studies have performed induction as high as 37ºC (Lin *et al.*, 2006, Cloutier *et al.*, 2000, Koo *et al.*, 1998, Dübel *et al.*, 1995). However, at high temperatures, anti-MA scFv SAs from phage clones 16 and 18 have higher free energies in the denatured state than the native state, resulting in the unfolding of the proteins. The decreased temperatures therefore allow for decreased protein self-association and kinetics that support proper folding of the anti-MA scFv SAs as well as the correct association of the subunits, thus yielding active proteins (Jaenicke, 1990, Georgiou and Valax, 1996). Figure 3-16 shows that at the same concentration, the anti-MA scFv SAs generated higher binding signals to the MAs when compared to anti-MA scFv's, verifying that the activity of the anti-MA scFv SAs was enhanced by proper folding of the scFv's prompted by the lowering of the induction temperatures. The decreased induction temperature therefore resulted in successful pelB leader sequence directed expression of the anti-MA scFv SAs in the periplasm and supernatant, yielding active oligomers in desired amounts. The functional binding avidities of the anti-MA scFv's was therefore increased by the fusion of streptavidin as shown by high absorbance signals in ELISA in Figure 3-16 due to increased valency that resulted in multiple binding of more than one surface bound antigenic MAs by a single oligomeric scFv (Hudson and Kortt, 1999, Kortt et al., 2001).

The folding of the fusion protein is such that the streptavidin forms the core and the anti-MA scFv's form the terminal ends as shown by the model in Figure 3-17 (Wang *et al.*, 2007). A monomer of the anti-MA scFv SA is a 45 kDa subunit that consists of 30 kDa anti-MA scFv's covalently bonded to the 15 kDa core streptavidin as depicted by the Western blot in Figure 3-15. These monomers spontaneously and non-covalently associate such that the core streptavidin forms the core of the protein and the anti-MA scFv's form the terminal ends for the binding of MAs (Kipriyanov *et al.*, 1996, Lin *et al.*, 2006). Interestingly, the profile of anti-MA scFv SAs from phage clone 12 on the Western blot analysis in Figure 3-15 shows monomeric 45 kDa bands under both denaturing and non-denaturing conditions, suggesting that anti-MA scFv SAs from phage clone 12 do not form stable oligomers. Although the ELISA in Figure 3-16 evidences high binding signals of anti-MA scFv SAs from phage clone 12, suggesting oligomerisation of the scFv's, the non-denaturing electrophoresis in Figure 3-15 depicts that anti-MA scFv SAs from phage clone 12 may exist as a dynamic (reversible), metastable, non-covalent oligomer. It is possible that the subunit interactions of the anti-MA scFv SAs from

phage clone 12 give rise to the metastable oligomer (Wörn and Plückthun, 1999). The stability of the anti-MA scFv SAs from phage clone 12 is further discussed in chapter 4.

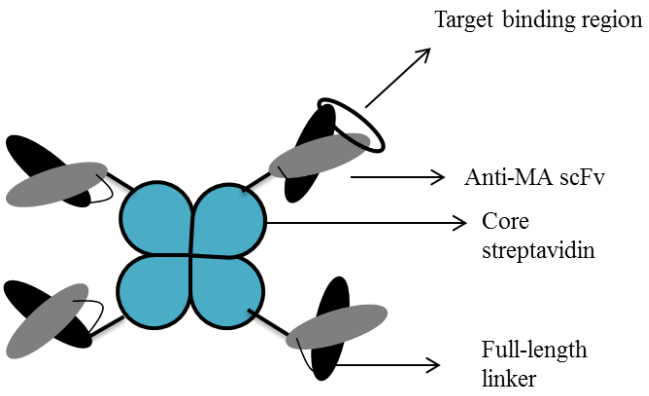

Figure 3-17: Schematic model of the anti-Ma scFv SAs. The black block represents the variable heavy chain (V_H) and the grey block represents the variable light chain (V_L). The blue spheres represent the streptavidin (Lin *et al*., 2006, Won *et al*., 2009).

The pHEN1 vector can benefit the anti-MA scFv SAs with more than one purification and immuno-detection method. The gene map of the scFv-streptavidin construct shown in Figure 3-2 indicates that the construct was designed to incorporate a hexa-histidine tag. Cloning the anti-MA scFv SA genes into the pHEN1 vector instead of the pUC57 vector resulted in expression of anti-MA scFv SAs with a c-MYC tag in addition to a hexa-histidine tag. Protein affinity tags are indispensable not only for detection and high through-put purification, but also for increased protein yield and solubility (Waugh, 2005). Having two affinity tags provides multiple strategies for the method of purification and detection of a protein as no single affinity tag is ideal (Young *et al*., 2012). The comparison of the affinity tags is discussed in chapter 4.

The fusion of the anti-MA scFv's with streptavidin therefore successfully resulted in non-covalent tetrameric anti-MA scFv's from phage clones 16 and 18. To the best of our knowledge, no literature has been found that engineered and expressed scFv-streptavidin fusion proteins against MAs, consequently making this the first study. It is also important to establish the anti-MA scFv SAs' cholesterol cross-reactivity in order to establish the anti-MA scFv SAs that would be suitable candidate oligomers for use in a point of care (POC) devise for TB diagnostic

purposes (Ranchod *et al*., 2018). The cholesterol cross-reactivity of the anti-MA scFv SAs is investigated in chapter 4.

3.5 CONCLUSION

In conclusion, the aim to increase MAs binding avidity of anti-MA scFv's was achieved through the fusion of anti-MA scFv's with a homotetrameric protein, streptavidin. Anti-MA scFv's from phage clones 16 and 18 were successfully engineered into stable anti-MA scFv SAs with increased binding avidity to the antigenic MAs due to multivalency, while anti-MA scFv's from phage clone 12 was engineered into a possibly metastable tetramer. The hypothesis that oligomeric scFv's from the scFv phage clones 12, 16 and 18 can be obtained is supported for phage clones 16 and 18.

CHAPTER 4: Potential application of oligomeric anti-MA scFv's in lateral flow immunoassay for TB diagnosis

4.1 INTRODUCTION

In light of the WHO and FIND call for a non-sputum based triage test with specific target product profiles (TPP) for the eradication of TB by 2035 (WHO, 2014), and the limitations of current TB diagnostic tests, our research group set out to develop a lateral flow blood-based test - Mycolic Acid Lateral flow Immunoassay (MALIA) - for the diagnosis of active TB in less than 1 h as described in chapter 1, section 1.1.7 (Ranchod *et al*., 2018). A first achievement towards that goal was the development of recombinant monoclonal antibodies (gallibodies) to mycolic acids (MAs) (Ranchod *et al*., 2018). Attempts to apply the gallibodies directly in MALIA using standard labelling of the monoclonal antibodies with nanogold particles failed, due to loss of activity of the gallibodies after labelling (Truyts, 2019). One way to potentially solve this problem, was to prepare oligomers of anti-MA scFv's that would potentially increase the avidity of binding to MAs, while simultaneously becoming more tolerant towards labelling. In Chapters 2 and 3 of this dissertation, two different approaches towards oligomerization of anti-MA scFv's were attempted and achieved with selected original clones of scFv's against MA that differed in their specificity of binding to different synthetic MA classes and cholesterol. The shortening of the linkers of the anti-MA scFv's yielded two multimers, anti-mycolic acid scFv short-linkers (anti-MA scFv SLs) from phage clones 12 and 16, and the fusion of streptavidin to the anti-MA scFv's yielded two tetramers, anti-mycolic acid streptavidin scFv's (anti-MA scFv SAs) from phage clones 16 and 18.

Some of the anti-MA scFv's from the *Nkuku* library were found to be cross-reactive with cholesterol (Ranchod *et al*., 2018). Anti-MA scFv's from phage clones 12 and 16 were found to cross-react with cholesterol, while the anti-MA scFv from phage clone 18 was found to be more specific to MAs (Ranchod *et al*., 2018). Studies have proven the indistinctive binding of Amphotericin B (AmB), a cholesterol binding anti-fungal drug to MAs, indicating that the packed structure of MAs is similar to that of cholesterol (Benadie *et al.*, 2008). This explains the recognition of cholesterol by the anti-MA scFv's from phage clones 12 and 16. The possible cross-reactivity of oligomeric scFv's would therefore disqualify the cross-reactive clones for use in MALIA to ensure the specificity of the test.

The plausible application of the anti-MA scFv SLs from phage clones 12 and 16, and anti-MA scFv SAs from phage clones 16 and 18 was investigated in a prototype lateral flow indirect immunoassay (LFIA). For the anti-MA scFv oligomers to be tested, the prerequisites of the LFIA had to be met. Our research group unexpectedly discovered the partial solubility of MAs in acetone during the purification of self-extracted MAs using counter current distribution (CCD) (Ragavaloo, 2019). CCD separates substances according to their partition properties by performing repetitive extractions in multiple tubes using a biphasic tricomponent system (Goodrum *et al*., 2001). Owing to their large lipid wax nature, the purified MAs are extracted from the first tubes of the CCD machine (Goodrum *et al*., 2001). Surprisingly, the expected purified MA yield was short by 30% after acetone precipitation of MAs to extract trace polar impurities that were not removed by CCD. The unexpected yield loss led to the investigation of the acetone waste fraction using a spot blot on aluminium based thin later chromatography (TLC) plates. The acetone soluble fraction was first separated using TLC. On the same plate, TLC unseparated acetone fractions were spotted, and both separated and unseparated acetone soluble fractions were then probed with the gallibodies to investigate the whereabouts of the MA component in the separated acetone soluble fraction after CCD. The extent of solubility of MAs in acetone was then further investigated by Arthessa Ragavaloo, a fellow research student, who found that around 0.25 mg/mL of MAs can be dissolved in acetone by melting, and which remains in a transferable but milky solution up to 4 h at room temperature, after which the MA micelles start coalescing and sedimenting (Ragavaloo, 2019).

This unexpected finding was to our advantage as non-polar solvents such as the hexane solvent used to immobilize MAs on nitrocellulose are not compatible with the bio-printing machinery that is used for upscale test-line antigen printing on LFIA tests, which will be problematic for large-scale manufacture and assembly of MALIA test kits (Okino, 2019). Acetone on the other hand is polar, making it an amenable solvent for automated antigen printing on lateral flow substrates (Okino, 2019). Acetone however dissolves nitrocellulose, making it incompatible for antigen printing on typical nitrocellulose paper substrates. Silica coated TLC plates with an aluminium base were found to be suitable substrate to spot MA antigen on from acetone solution instead. Because the TLC silica plates were used before to detect MA fractions from the CCD train after purification, these plates were considered for the LFIA purpose. Usually TLC silica plates are not compatible with water, which tends to harm the silica layer, howbeit our group

unexpectedly found that the particular plates used could withstand the effect of protein containing water for the few minutes required to perform short distance capillary flow of aqueous antibody solution to approach the MA-coated test spots as shown in Figure 4-1 (Ragavaloo, 2019). Thus, the immobilization of MAs in acetone in an antigenic manner on aluminium based TLC plates and the ability of the TLC plates to withstand aqueous antibody solutions provides an opportunity for the application of the oligomeric scFv's produced in chapters 2 and 3 to be tested in a prototype lateral flow test.

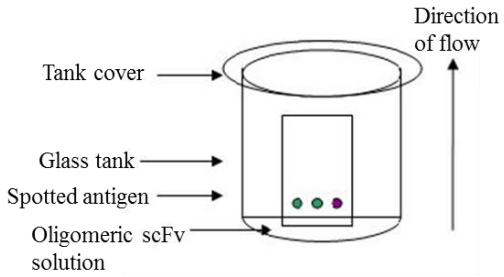

Figure 4-1: Lateral flow indirect immunoassay (LFIA) to investigate the potential application of oligomeric anti-MA scFv's in TB diagnostic tests. MAs or stearic acid (negative antigen control) were dissolved in acetone and spotted on aluminium based TLC plate at increasing concentrations. The bottom edge of the TLC plate was vertically immersed into the oligomeric scFv solution diluted with block buffer. After washing, the bound oligomeric scFv was detected using mouse monoclonal antibody 9E10 conjugated to horse radish peroxidase (HRP) (Ragavaloo, 2019).

In this chapter cholesterol cross-reactivity was tested simultaneously during characterisation of the oligomeric scFv products in terms of their avidity for binding MA. The suitability of the oligomeric scFv's were then tested for their feasibility of use in LFIA as a next step in characterising the products for their utility in MALIA.

4.1.1 Hypothesis

The prokaryotically expressed SL- and SA-oligomers of anti-MA scFv's derived from any of scFv phage clones 12, 16 and 18 can be applied in the prototype lateral flow immunoassay to recognise immobilised MA on the test spot.

4.2 MATERIALS AND METHODS

4.2.1 Materials

Mycolic acid from *Mycobacterium tuberculosis* (bovine strain): Sigma-Aldrich, Missouri, USA.

Cholesterol: (Sigma Grade: ≥99%, Sigma-Aldrich, Missouri, USA).

ELISA block buffer pH 7.4: Casein hydrolysate (4% (m/v), Oxoid, United Kingdom) dissolved in 1X PBS pH 7.4.

ELISA dilution buffer pH 7.4: Casein hydrolysate (4% (m/v)) dissolved in 1X PBS pH 7.4 and Tween20 (0.05% (v/v), Sigma-Aldrich, Missouri, USA).

ELISA wash buffer pH 7.4: PBS 1X pH 7.4 and 0.1% (v/v) Tween20.

Anti-c-MYC Horseradish peroxidase (HRP): Mouse monoclonal anti-c-MYC antibody (clone 9E10) conjugated to peroxidase, (Roche Diagnostics GmbH, Germany).

ELISA Tetramethyl Benzidine (TMB) HRP substrate solution: TMB Single solution (Life Technologies, California, USA).

Blot test Tetramethyl Benzidine (TMB) HRP substrate solution: TMB for blot tests (Life Technologies, California, USA).

ELISA Stop solution: Sulphuric acid (H_2SO_4) (2 N) (99.999%, Sigma-Aldrich, Missouri, USA).

Thin layer chromatography (TLC) plates: TLC silica gel 60 F_{254} 20 x 20 cm, aluminium sheets (Merck, Kenilworth, New Jersey, USA).

Acetone: (99.5%, Sigma-Aldrich, Missouri, USA).

Petri dishes: Polystyrene petri dish, 60 mm by 15 mm (Sigma-Aldrich, Missouri, USA).

Stearic acid: (99%, Sigma-Aldrich, Missouri, USA).

Thin layer chromatography tank: Rectangular TLC developing tank, 100 mm by 100 mm (Sigma-Aldrich, Missouri, USA).

Anti-MA scFv short-linker (SL): from phage clones 12 and 16. (Chapter 2). Stored in PBS pH 7.4 at -20ºC in 20 µL aliquots. Thawed only once.

Anti-MA scFv-streptavidin (SA): from phage clone 12, 16 and 18. (Chapter 3). Stored in PBS pH 7.4 at -20ºC in 20 µL aliquots. Thawed only once.

4.2.2 Methods

A. Avidity determination of MA and cholesterol binding for selected anti-MA scFv SLs and anti-MA scFv SAs

The avidity of binding of the various scFv multimer products listed in 2.1 were determined by limiting dilution of the products in MA or cholesterol coated microplates by indirect ELISA. A third of the wells of Nunc Maxisorp 96 well immunoplate were coated with 50 µL of distilled hexane per well using a Hamilton syringe. This part of the plate was used as negative antigen control. The second third of the wells were coated with 0.25 mg/mL MAs dissolved in hexane, and the last third were coated with 1 mg/mL cholesterol dissolved in hexane. The well contents were left to evaporate at room temperature before wrapping the plate in foil and storing overnight at 4ºC to ensure successful coating. The following day, blocking of non-specific binding was carried out by pipetting 300 µL of ELISA block buffer per well and incubating for 1 h at 37ºC. The plate was washed three times with ELISA wash buffer. ELISA dilution buffer was used to dilute the anti-MA scFv SLs and anti-MA scFv SAs in a 1:2 dilution series ranging from 0.5 mg/mL to 0.0005 mg/mL. A volume of 50 µL of each dilution was pipetted in duplicate in the wells and the plate was incubated for 1 h at 37ºC to allow binding of anti-MA scFv SLs and anti-MA scFv SAs to the MAs. For the scFv negative control, ELISA dilution buffer without scFv's was used. The plate was then washed three times with ELISA wash buffer to remove unbound oligomeric scFv's. A volume of 50 µL per well of secondary antibody (mouse monoclonal antibody 9E10 HRP conjugated to peroxidase) diluted in ELISA dilution buffer at a 1:1000 volume ratio was pipetted per well and incubated for 1 h at 37ºC to allow for binding to the anti-MA scFv SLs and anti-MA scFv SAs. The wells were then washed three times with ELISA wash buffer to remove unbound secondary antibody, and 50 µL of substrate TMB Single solution was added to each well and incubated for 2-5 minutes at room temperature to allow the reaction to reach major absorbance at 370 nm, with 652 nm as the reference wavelength to compensate for individual well surface irregularities. ELISA stop solution was used to stop the reaction by pipetting 50 µL into each well. The absorbance was read at 450 nm using SpectraMax paradigm plate reader. The binding signals were then corrected by subtracting the background signal obtained from the relevant antigen negative control wells. Statistical analysis

(standard deviation from the mean, the reproducibility of signals by biological repeats, and dissociation constants of each oligomer) was carried out on the obtained data.

B. Comparing the performance of anti-MA scFv SL and anti-MA scFv SA in a typical lateral flow indirect immunoassay

The unique lateral flow indirect immunoassay (LFIA) for comparing the performance of anti-MA scFv SL and anti-MA scFv SA for their detection on a test spot of MA was designed by Arthessa Ragavaloo, a fellow MSc student in our research group. MAs and stearic acid (negative control) were dissolved in acetone to concentrations of 0.25 mg/mL by heating to 90ºC for 5 minutes, followed by cooling at room temperature for over 1 h but used within 4 h after heating. Two aluminium foil based thin TLC silica gel plates were cut with scissors to fit into 60 mm by 15 mm petri dishes. At the centre of the plates, four dots were pencilled to designate the MA spots, and two dots were pencilled below the MA dots to designate the stearic acid spots. The anti-MA scFv SLs and anti-MA scFv SAs from phage clone 16 were diluted using ELISA dilution buffer to concentrations of 0.06 mg/mL (anti-MA scFv SL) and 0.03 mg/mL (anti-MA scFv SA). The MAs (0.25 mg/mL in acetone) were spotted repeatedly in volumes of 10 µL per event with drying in between to achieve an increasing MA spot concentration range of 0.25 mg/mL, 0.5 mg/mL, 0.75 mg/mL and 1 mg/mL on the silica gel plate. The stearic acid (0.25 mg/mL in acetone) was spotted likewise at spot concentrations of 0.25 mg/mL and 0.5 mg/mL on the plate, at their designated positions just below the MA spots. The bottom edge of one of the TLC plates were immersed vertically into approximately 1 mL of a solution of anti-MA scFv SL (diluted with 4% casein hydrolysate/PBS to a concentration of 0.06 mg/mL) in the TLC tank. The anti-MA scFv SL solution was allowed to move up the plate until about 1 cm from the top of the plate. The plate was removed from the tank and placed into the petri dish to wash three times by immersing in ELISA wash buffer and tapping the side of the petri dish for 30 sec to facilitate the shaking of the plate and thus, to remove unbound oligomeric scFv's. The ELISA wash buffer was discarded, and the plate was immersed in anti-c-MYC Horseradish perodixase (HRP) diluted in ELISA dilution buffer at a 1:1000 volume ratio with incubation at room temperature for 1 h. The plate was washed three times to remove unbound secondary antibody with ELISA wash buffer before 2-3 mL of TMB for blot tests was added to develop the colour for 2 minutes after which the colour signals on the plate were recorded by camera.

Because TMB oxidation is fast, colour development must be recorded before 5 minutes, after which precipitation of the product colour stain occurs which yields inaccurate results. The same procedure was carried out for anti-MA scFv SA.

4.3 RESULTS

4.3.1 Avidity determination of MA and cholesterol binding for selected anti-MA scFv SLs and scFv SAs

The avidity of binding of the scFv multimer products listed in 2.1 were determined by limiting dilution of the multimer scFv products on MA or cholesterol coated microplates by indirect ELISA. The results are shown in Figures 4-2 to 4-6.

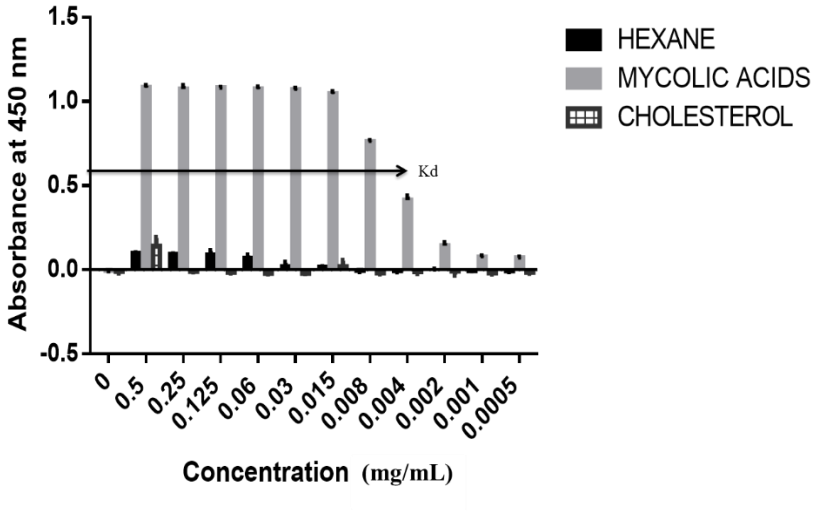

Figure 4-2: Indirect ELISA assay to determine the avidity of the anti-MA scFv SL from phage clone 12 for binding MA and cholesterol. ELISA plates were coated with either MA antigen at a 0.25 mg/mL concentration or cholesterol at a 1 mg/mL concentration. Hexane was used as antigen control. Anti-MA scFv SL from phage clone 12 was applied unlabelled. Binding activity was indirectly measured by using a secondary anti-c-MYC mouse monoclonal antibody-HRP conjugate, of which the bound amount was quantified by the HRP enzyme reaction with colour indicator substrate. The anti-MA scFv SLs' binding signals were then corrected by subtracting the background signal generated by the binding of ELISA dilution buffer (antibody control) to hexane (antigen control). The data represents two biological repeats performed in triplicate. The error bars represent standard deviation and K_d represents the apparent dissociation constant, defined as the highest dilution of scFv multimer (expressed in mg/mL) that still gives a binding signal at or above 50% of the average plateau region achieved at higher scFv SL concentrations.

Figure 4-2 shows a constant binding signal of anti-MA scFv SLs from phage clone 12 to MAs from a scFv SL concentration of 0.5 mg/mL to 0.015 mg/mL referred to as the plateau domain. The scFv SL concentration at half the plateau domain gives the apparent dissociation constant (K_d) of the scFv SL, depicting binding avidity (sensitivity). The calculated apparent K_d for anti-

MA scFv SLs from phage clone 12 is 0.006 mg/mL. The anti-MA scFv SLs from phage 12 recognized cholesterol only at a scFv concentration as high as 0.5 mg/mL, implying that the K_d is even weaker. Figure 4-2 indicates that the aim to increase functional binding avidity of anti-MA scFv's was attained, as the plateau maximum signal was maintained up to a scFv dilution of 0.015 mg/mL giving an apparent K_d at 0.006 mg/mL. Anti-MA scFv SLs from phage clone 12 qualify to become a candidate oligomer for use in a TB serodiagnostic test at concentrations up to 0.25 mg/mL, after which cholesterol cross-reactivity comes into play.

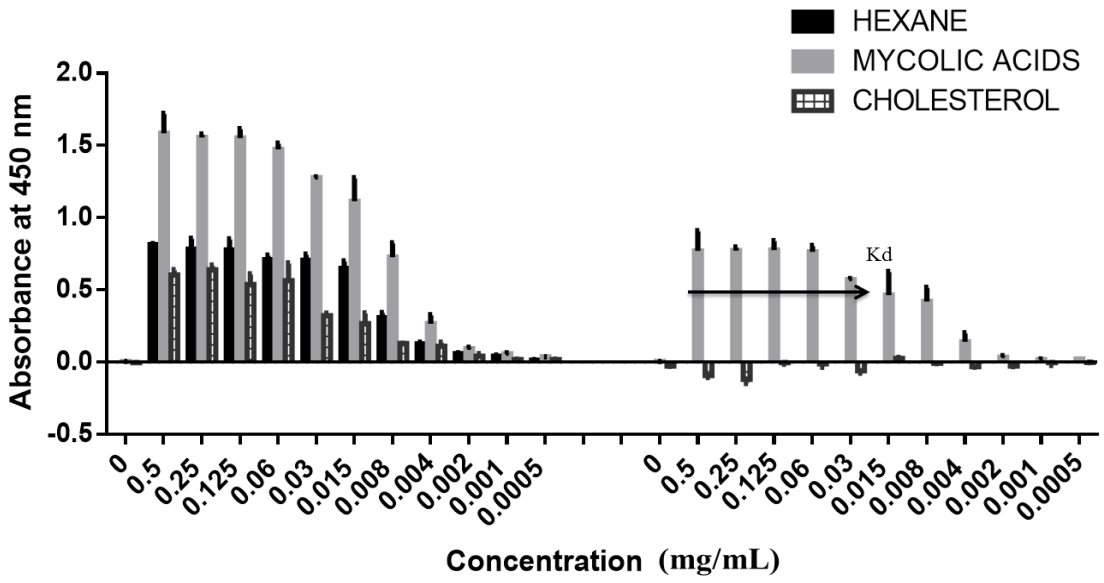

Figure 4-3: Indirect ELISA assay to determine the avidity of the anti-MA scFv SL from phage clone 16 for binding MA and cholesterol. ELISA plates were coated with either MA antigen or cholesterol. Hexane solvent was used as antigen control. Anti-MA scFv SL from phage clone 16 was applied unlabelled. Binding activity was indirectly measured by using a secondary anti-c-MYC mouse monoclonal antibody-HRP conjugate, of which the bound amount was quantified by the HRP enzyme reaction with colour indicator substrate. The anti-MA scFv SLs' binding signals were then corrected by subtracting the background signal generated by the binding of ELISA dilution buffer (antibody control) to hexane (antigen control). The data represents two biological repeats performed in triplicate. The error bars represent standard deviation and K_d represents the apparent dissociation constant, defined as the highest dilution of scFv multimer (expressed in mg/mL) that still gives a binding signal at or above 50% of the average plateau region achieved at higher scFv SL concentration. (Left graph) High background signals generated by anti-MA scFv SL from phage clone 16 (Right graph) Binding signals of anti-MA scFv SL from phage clone 16 after correcting for the high background signal.

Figure 4-3 shows a plateau domain of the binding of anti-MA scFv SL from clone phage 16 to MA from a scFv SL concentration of 0.5 mg/mL to 0.06 mg/mL. A decrease in the binding signal occurs from 0.03 mg/mL implying dissociation from the bound antigen. The calculated apparent K_d of anti-MA scFv SL from phage clone 16 is 0.02 mg/mL, indicating sensitivity. The anti-MA scFv SL from phage clone 16 generates high binding background signal as shown by the high hexane signals (left graph). However, after correcting for the background signals, anti-MA scFv SL 16 does not recognize cholesterol at any concentrations of scFv SL measured (see right graph) signifying specificity to MAs. Figure 4-3 hereby provides evidence that the aim to increase functional binding avidity of anti-MA scFv SL was achieved, as a plateau ELISA binding signal was found to be maintained up to a scFv SL concentration of 0.06 mg/mL, and the apparent K_d registered at 0.02 mg/mL. From this it can be concluded that anti-MA scFv SL from phage clone 16 qualifies to become a candidate for a TB serodiagnostic test when applied at concentrations that ensure maximum plateau domain region binding signals.

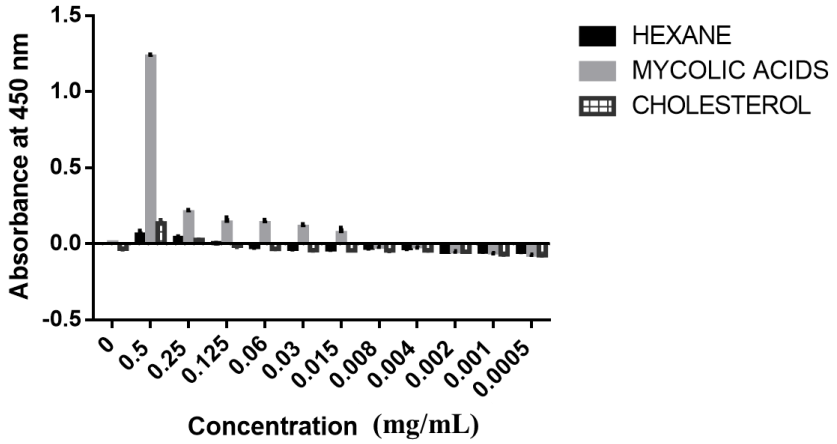

Figure 4-4: Indirect ELISA assay to determine the avidity of the anti-MA scFv SA from phage clone 12 for binding MA and cholesterol. ELISA plates were coated with either MA antigen or cholesterol. Hexane solvent was used as antigen control. Anti-MA scFv SA from phage clone 12 was applied unlabelled. Binding activity was indirectly measured by using a secondary anti-c-MYC mouse monoclonal antibody-HRP conjugate, of which the bound amount was quantified by the HRP enzyme reaction with colour indicator substrate. The anti-MA scFv SAs' binding signals were then corrected by subtracting the background signal generated by the binding of ELISA dilution buffer (antibody control) to hexane (antigen control). The data represents two biological repeats performed in triplicate. The error bars represent standard deviation and K_d represents the apparent dissociation constant, defined as the highest dilution of scFv multimer (expressed in mg/mL) that still gives a binding signal at or above 50% of the average plateau region achieved at higher scFv SA concentrations.

Figure 4-4 shows a high binding signal of anti-MA scFv SA from phage clone 12 at a scFv SA concentration as high as 0.5 mg/mL. The signal abates when the anti-MA scFv SA is diluted, demonstrating an unstable tetramer dissociating into monomers already upon slight dilution. The instability of anti-MA scFv SA from phage clone 12 is also seen in Figure 3-15 (Western Blot) in chapter 3, section 3.3. Figure 4-4 indicates that anti-MA scFv SA from phage clone 12 does not qualify to be utilized as a component of a lateral flow TB serodiagnostic test immunoassay, owing to instability.

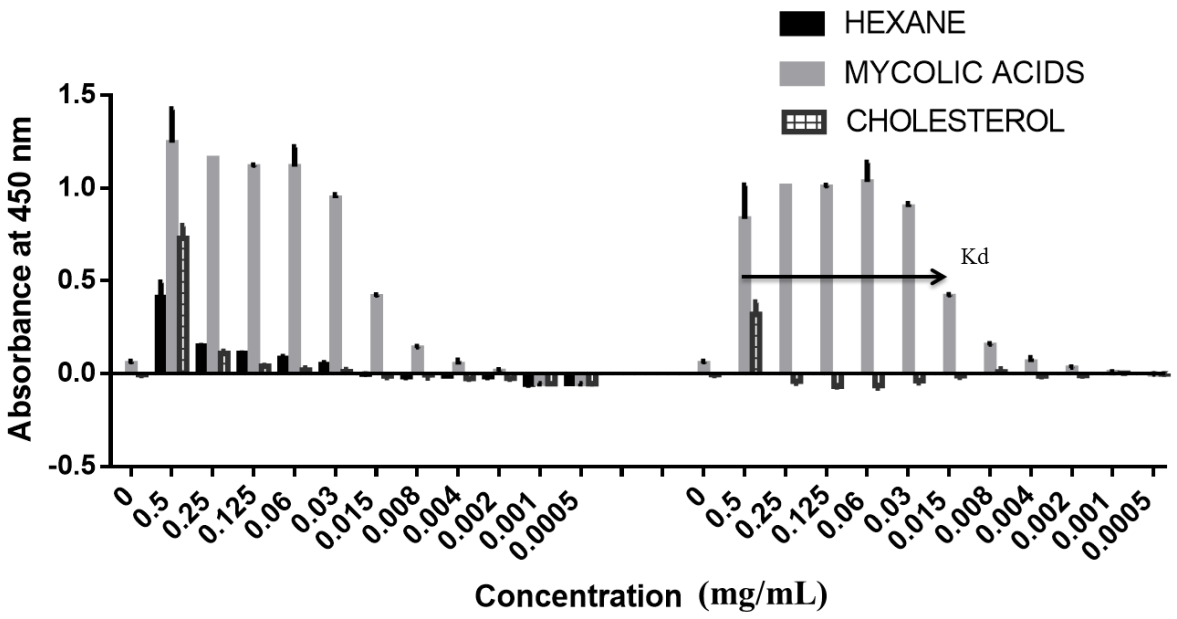

Figure 4-5: Indirect ELISA assay to determine the avidity of the anti-MA scFv SA from phage clone 16 for binding MA and cholesterol. ELISA plates were coated with either MA antigen or cholesterol. Hexane solvent was used as antigen control. Anti-MA scFv SA from phage clone 16 was applied unlabelled. Binding activity was indirectly measured by using a secondary anti-c-MYC mouse monoclonal antibody-HRP conjugate, of which the bound amount was quantified by the HRP enzyme reaction with colour indicator substrate. The anti-MA scFv SAs' binding signals were then corrected by subtracting the background signal generated by the binding of ELISA dilution buffer (antibody control) to hexane (antigen control). The data represents two biological repeats performed in triplicate. The error bars represent standard deviation and K_d represents the apparent dissociation constant, defined as the highest dilution of scFv multimer (expressed in mg/mL) that still gives a binding signal at or above 50% of the average plateau region achieved at higher scFv SA concentration. (Left graph) High background signals generated by anti-MA scFv SA from phage clone 16 (Right graph) Binding signals of anti-MA scFv SA from phage clone 16 after correcting for the high background signal.

Figure 4-5 shows a plateau domain of the binding of anti-MA scFv SA from clone phage 16 to MA from a scFv SA concentration of 0.5 mg/mL to 0.03 mg/mL. A decrease in the binding signal occurs from 0.015 mg/mL implying dissociation from the bound antigen. The calculated apparent K_d of anti-MA scFv SA from phage clone 16 is 0.02 mg/mL indicating sensitivity. The anti-MA scFv SA from phage clone 16 also generates high binding background signal as shown by the high hexane signals (left graph). After correcting for the background signals, anti-MA scFv SA 16 recognized cholesterol at scFv SA concentration as high as 0.5 mg/mL (see right graph). Figure 4-5 hereby provides evidence that the aim to increase functional binding avidity of anti-MA scFv SA was achieved, as a plateau ELISA binding signal was found to be maintained up to a scFv SA concentration of 0.03 mg/mL, and the apparent K_d registered at 0.02 mg/mL. From this it can be concluded that anti-MA scFv SA from phage clone 16 qualifies to become a candidate for a TB serodiagnostic test at concentrations up to 0.25 mg/mL, after which cholesterol cross-reactivity comes into play.

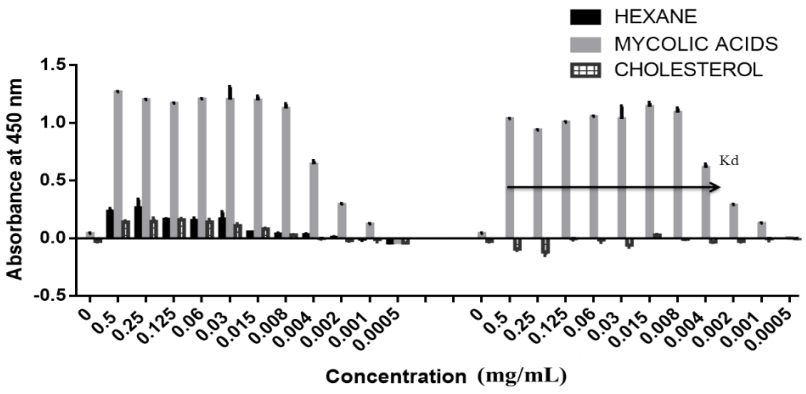

<u>Figure 4-6</u>: Indirect ELISA assay to determine the avidity of the anti-MA scFv SA from phage clone 18 for binding MA and cholesterol. ELISA plates were coated with either MA antigen or cholesterol. Hexane solvent was used as antigen control. Anti-MA scFv SA from phage clone 18 was applied unlabelled. Binding activity was indirectly measured by using a secondary anti-c-MYC mouse monoclonal antibody-HRP conjugate, of which the bound amount was quantified by the HRP enzyme reaction with colour indicator substrate. The anti-MA scFv SAs' binding signals were then corrected by subtracting the background signal generated by the binding of ELISA dilution buffer (antibody control) to hexane (antigen control). The data represents two biological repeats performed in triplicate. The error bars represent standard deviation and K_d represents the apparent dissociation constant, defined as the highest dilution of scFv multimer (expressed in mg/mL) that still gives a binding signal at or above 50% of the average plateau region achieved at higher scFv SA concentration. (Left graph) High background signals generated by anti-MA scFv SL from phage clone 16 (Right graph) Binding signals of anti-MA scFv SL from phage clone 16 after correcting for the high background signal.

Figure 4-6 shows a plateau domain of the binding of anti-MA scFv SA from clone phage 18 to MA from a scFv SA concentration of 0.5 mg/mL to 0.008 mg/mL. A decrease in the binding signal occurs from 0.004 mg/mL implying dissociation from the bound antigen. The calculated apparent K_d of anti-MA scFv SA from phage clone 18 is 0.0037 mg/mL indicating the highest sensitivity. The anti-MA scFv SA from phage clone 18 also generates high binding background signal as shown by the high hexane signals (left graph). However, after correcting for the background signals, anti-MA scFv SA 18 does not recognize cholesterol at any scFv SA concentration (see right graph) signifying specificity to MAs. Figure 4-6 hereby provides evidence that the aim to increase functional binding avidity of anti-MA scFv SA was achieved, as a plateau ELISA binding signal was found to be maintained up to a scFv SA concentration of 0.004 mg/mL, and the apparent K_d registered at a good 0.0037 mg/mL. From this it can be concluded that anti-MA scFv SA from phage clone 18 qualifies to become a candidate for a TB serodiagnostic test at any plateau signal concentrations. Moreover, this oligomer may be the best to use in MALIA due to its sensitivity and ability to resist cholesterol cross-reactivity.

Table 4-1 depicts the ranking of the anti-MA scFv oligomers according to sensitivity, stability and cholesterol cross-reactivity. The ranking is from the best multimer to the worst.

Table 4-1: Anti-MA scFv oligomer ranking from the best to the worst.

Rank	Phage clone	Anti-MA scFv oligomer	Sensitivity (K_d) mg/mL	Cross-reactivity
1	18	Anti-MA scFv SA	0.0037	✗
2	16	Anti-MA scFv SL	0.02	✗
3	12	Anti-MA scFv SL	0.006	✓
4	16	Anti-MA scFv SA	0.02	✓
5	12	Anti-MA scFv SA	-	✓

4.3.2 Comparing the performance of anti-MA scFv SL and anti-MA scFv SA in a typical lateral flow indirect immunoassay (LFIA)

The oligomerization strategies in chapters 2 and 3 yielded two multimer types from the same phage clone anti-MA scFv's, namely the short-linker (SL) and streptavidin (SA) recombinant products. For phage clone 16, both types could be generated in a functionally intact way, allowing these oligomers to be compared for their relative functionality in a lateral flow test with eventual potential application in an effective point of care (POC) TB diagnostic test. MAs dissolved in acetone were spotted on aluminium based TLC silica plates. The MAs were detected using two scFv multimer solutions diluted in blocking buffer that moved by capillary flow towards the MAs for binding. The scFv multimers were used at the lowest concentrations that still gave plateau maximum binding signals in ELISA. The anti-MA scFv SL from phage clone 16 was used at 0.06 mg/mL concentration (Figure 4-3) and the anti-MA scFv SA from phage clone 16 was used at a 0.03 mg/mL concentration (Figure 4-5). The binding of the oligomeric scFv's to MAs was then detected using anti-c-MYC conjugated HRP. The results are shown in Figure 4-7.

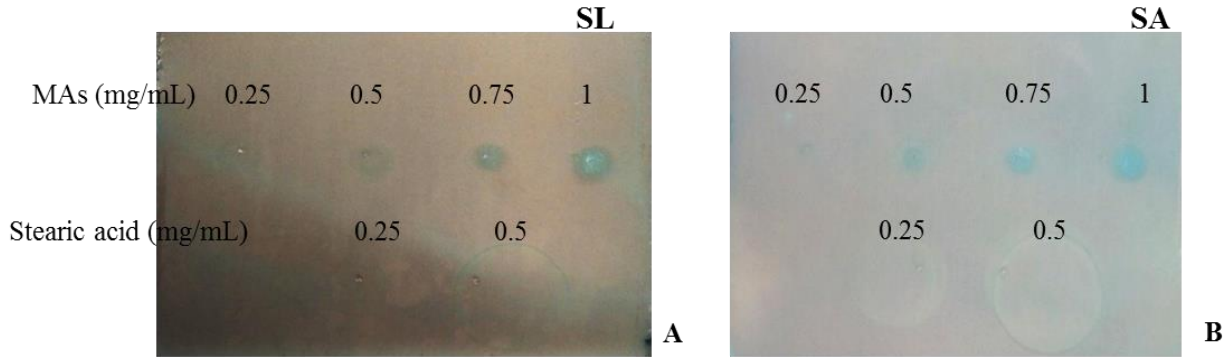

Figure 4-7: Comparing the performance of anti-MA scFv SL and anti-MA scFv SA from phage clone 16 in a lateral flow indirect immunoassay. The MAs and stearic acid were immobilized at the indicated concentrations in mg/mL. The MAs were detected by anti-MA scFv SL from phage clone 16 at a concentration of 0.06 mg/mL, and anti-MA scFv SA from phage clone 16 at a concentration of 0.03 mg/mL through capillary flow movement of the oligomer solutions in block buffer towards the MA spots. Spots of antigen-antibody complex were visualized indirectly using mouse anti-c-MYC monoclonal antibody-HRP conjugate. Blue colours indicate positive binding of scFv multimers to the MA antigen. White rings indicate no binding of scFv multimers.

Figure 4-7 demonstrates the activities of anti-MA scFv SL and anti-MA scFv SA from phage clone 16 to the spotted MAs. The blue spots become more pronounced on MA spot concentrations from 0.25 mg/mL to 1 mg/mL. The stearic acid (negative control) spots produce a whitish ring around the spots at all concentrations, indicating absence of binding of anti-MA scFv SA and anti-MA scFv SL to the stearic acid. Figure 4-7 shows that the two oligomer types bind equally well to the MAs in a lateral flow indirect immunoassay. Equally important, the TLC plates withstood the washing steps and provided clear decipherable results. From this, one may conclude that these two multimer types derived from phage clone 16 are also both suitable for further development of a MALIA POC TB diagnostic test.

4.4 DISCUSSION

The two scFv oligomerization strategies described in chapters 2 and 3 successfully yielded oligomers that could be characterized according to their cholesterol cross-reactivity, binding avidities to MAs and stability. The packed structures of cholesterol and MAs have been proven to provide similar antigenic surfaces as demonstrated by the indistinguishable binding of Amphotericin B (AmB) to both lipids (Benadie *et al*., 2008). Consequently, natural human anti-cholesterol antibodies are prone to recognizing the folded structure of MAs, thus the antibodies generate false positive results in serological tests for TB negative patients. It was therefore imperative to rule out cross-reactive multimers using the indirect ELISA assays shown in Figures 4-2 to 4-6. The coating concentration of cholesterol in the ELISA was 1 mg/mL as opposed to 0.25 mg/mL (MAs coating concentration), because all the anti-MA scFv clones have been shown to recognize cholesterol only at high concentrations (Ranchod *et al*., 2018). At higher concentrations, cholesterol crystallizes into antigenic structures that are not achieved at lower concentrations (Prinsloo, 2009). It was reported before that anti-MA scFv's from phage clone 18 were the only scFv's to not recognize cholesterol, however, the conclusion was reached based on the use of a low cholesterol concentration (Ndlandla *et al*., 2016). Therefore, a high coating concentration was utilized by Ranchod *et al.* (2018) in order to ensure that cholesterol was presented as a potentially cross-reactive antigen to the gallibodies. In the same manner, a high cholesterol coating concentration was used for detection by the oligomeric scFv's. Anti-MA scFv SLs from phage clone 12 and anti-MA scFv SAs from phage clones 12 and 16 are the scFv oligomers that recognized cholesterol as shown in Figures 4-2, 4-4 and 4-5 respectively, even at low avidities characterized by apparent K_d values higher than 0.5 mg/mL of the multimer. Once again, the results are comparable to what was observed in the study by Ranchod *et al.* (2018), where gallibodies 12CH2-4 and 16CH2-4 recognized cholesterol at apparent K_d values in excess of 0.25 mg/mL. Although anti-MA scFv SLs from phage clone 16 produced a high background signal, the oligomers did not recognize cholesterol as expected, indicating a deviation from what was observed with the parental gallibody constructs. Anti-MA scFv SAs from phage clone 18 did not recognize cholesterol as expected due to its V_H CDR3 that gives rise to specificity (Barrios *et al*., 2004). Therefore, anti-MA scFv SAs from phage clone 18 and anti-MA scFv SLs from phage clone 16 would be the best multimers to use in serological tests, including lateral flow immunoassays, as they appear not to cross-react with cholesterol.

The binding avidities to MAs were determined using indirect ELISA limiting dilution assays as shown in Figures 4-2 to 4-6. The multimer that possessed the greatest binding avidity to MAs was anti-MA scFv SA from phage clone 18 with an apparent K_d of 0.0037 mg/mL (Table 4-1). Conversely, other multimers exhibited somewhat weaker binding avidities ranging in apparent K_d values from 0.006 – 0.02 mg/mL. The binding avidity of anti-MA scFv SA from phage clone 18 compares well to the binding avidity of gallibody 18CH1-4 in a study where anti-MA scFv from phage clone 18 was grafted back onto its Fc domains to give a recombinant gallibody resembling a full divalent IgY gallibody 18CH1-4 (Ranchod *et al.*, 2018). The expected logarithmic increase in avidity of scFv SA due to its anticipated tetrameric nature, compared to the divalent nature of gallibody, was however not observed.

The greatest binding avidity of anti-MA scFv SA from phage clone 18 as compared to other oligomeric scFv's is explained by the longer variable heavy chain (V_H) complementarity determining region 3 (CDR3) that loops to form obtrusions and crevices imperative for antibody binding. Studies have evidenced that the specificity of the binding of an antibody to an antigen is chiefly affected by the sequence diversity and length of V_H CDR3 (Ranchod *et al.*, 2018, Rock *et al.*, 1994, Xu and Davis, 2000, Barrios *et al.*, 2004). Anti-MA scFv SA from phage clone 18 could therefore be the best candidate multimer for use in serological tests as it possesses the greatest sensitivity for binding to MAs even if only marginally better than that of scFv SA from phage clone 16.

The stability of multimers is also a determining factor for use in serological tests. Anti-MA scFv SA from phage clone 12 is the only multimer selected that did not exhibit stability. The SDS-PAGE under non-denaturing conditions shown in chapter 3, Figure 3-15 unexpectedly revealed only a 45 kDa band that represents a monomeric protein as opposed to an anticipated band at 180 kDa that represents a tetrameric scFv. Moreover, the ELISA limiting dilution assay in Figure 4-4 depicted that the binding signals did not follow a normal titration curve as expected but resulted in a sharp signal decrease from 0.5 mg/mL to 0.25 mg/mL of scFv multimer concentration which is not characteristic of stable multimeric proteins. The results therefore strongly suggest that anti-MA scFv SA monomers from phage clone 12 tend to multimerize into unstable non-covalent quaternary structures. The stability fostering properties of proteins have been shown to arise from either the intrinsic stability of any one of the domains or the interface

of the contacting domains (Wörn and Plückthun, 1999). Since anti-MA scFv SAs from phage clones 16 and 18 are stable, it is more likely that the instability arises from the interface of the domains of anti-MA scFv SA from phage clone 12 and not the subunit stability as such. In this situation, two stable domains are linked by a weak interface and the breaking up of the interface ensues at lower concentrations as the hydrophobic residues of the domains are exposed to water (Wörn and Plückthun, 1999). To ensure stability of the oligomeric scFv's over long-term storage and to prevent the loss of functionality of the scFv's over time, the storage buffer of the oligomeric scFv's will be changed. The use of PBS for long-term storage of proteins is fairly common. While PBS has been convenient and widely used, reports demonstrate that this buffer is not ideal for cryostorage of proteins. Freezing of PBS buffer leads to precipitation of dibasic sodium salts which in turn causes a significant drop of pH. A different storage buffer like borate buffer will therefore be used (Kubiak *et al.*, 2016).

Anti-MA scFv SAs and anti-MAs scFv SLs were purified using different methods, affording a comparison of the two methods for their utility in fast and affordable lateral flow immunoassays. Anti-MA scFv SLs were purified using the c-MYC tag while the anti-MA scFv SAs were purified using their His-tags on nickel affinity columns. The c-MYC tag is one of the epitope tags extensively used in detection as its sequence is absent in the host cell, However, it is expensive when used as a purification method owing to the cost of mouse IgG1 monoclonal antibody (clone 9E10) that recognizes the c-MYC epitope tag derived from the human c-MYC oncogene (p62 c-MYC) (Woodroffe and Wilson, 1977). In addition to being expensive, the c-MYC conjugated agarose resin is not rechargeable. Moreover, while eluting with sodium thiocyanate (NaSCN) results in high elution capacity and preservation of the resin binding capacity, NaSCN is a harsh solution and may cause denaturation of the scFv's (Woodroffe and Wilson, 1977). C-MYC tag purification costs approximately $950 per 50 mL unpurified protein per single use. On the other hand, the hexa-histidine tag is the most utilized affinity tag for high-throughput protein purification. The resin is inexpensive as compared to the c-MYC agarose resin and can withstand multiple regeneration cycles. Furthermore, the elution conditions are mild and can be easily optimized to increase the elution capacity (Malhotra, 2009). Hexa-histidine tag purification costs approximately $630 per 50 mL unpurified protein per single use. Therefore, incorporating a hexa-histidine tag in anti-MA scFv SLs could considerably reduce the purification costs. While the cost of producing anti-MA scFv SLs might have been more

expensive than the cost of producing anti-MA scFv SAs, the cost of producing the multimers was less than the cost of producing the gallibodies. Although the multimers gained the same functional binding avidity to MAs as the gallibodies, the multimers were successfully expressed in an inexpensive prokaryotic cell system, thus eliminating the need for a eukaryotic expression system that could increase the cost of the POC TB diagnostic test.

The anti-MA scFv SLs and anti-MA scFv SAs from phage clone 16 were used in a LFIA test for proof of concept (Figure 4-1) as this phage clone produced active and stable multimers from both oligomerization strategies that could be compared. The LFIA test results depicted in Figure 4-7 shows that both the oligomers when applied in a lateral flow test bind equally well to the MAs at the test spots. The comparable binding is explained by the binding avidities of the oligomers that were both calculated at approximately 0.02 mg/mL. Moreover, the multimers did not recognize the stearic acid – (18-carbon long fatty acid chain) - negative control, indicating specificity of binding to MAs. The ability of the multimers to specifically recognize MAs in a LFIA test demonstrates the feasibility of modifying the test into a competitive LFIA test. Introducing patient sera into the multimer solution used to detect MAs should allow for the competitive binding of MAs between the multimers from phage clone 16 and the human antibodies. For a TB positive patient, it is expected that the human anti-MA antibodies would outcompete the labelled multimers for binding to the MAs, consequently therefore not generating blue spots in the test at the same intensity than with non-TB positive patient serum sample. For a TB negative patient, it is expected that the multimers would outcompete the human anti-cholesterol antibodies for binding to the MAs, therefore, generating blue spots at similar intensity as seen in Figure 4-7. The LFIA also underlines the important discovery of partial solubility of MAs in acetone, subsequently leading to the prospect of TLC plates mounted on aluminium backing to replace the nitrocellulose paper as the TLC silica plates successfully remained intact for the short duration of the test. The aim to increase the functional binding avidities of anti-MA scFv's from the *Nkuku* library was not only achieved, but the practicality of using these multimers in a lateral flow test has been demonstrated and verified. This study has thus contributed oligomeric scFv's that recognize MAs, which can easily be upscaled for production to provide affordable anti-MA binding antibody type reagents that can be used labelled or unlabelled in future MALIA designs. Future work will therefore investigate the stability and functionality of the oligomeric scFv's after labelling for use in the MALIA POC TB diagnostic test.

The hypothesis that the prokaryotically expressed SL- and SA-oligomers of anti-MA scFv's derived from any of scFv phage clones 12, 16 and 18 can be applied in the prototype lateral flow immunoassay to recognise immobilised MA on the test spot is however, rejected. The hypothesis is only supported for stable multimers that do not recognize cholesterol. Only anti-MA scFv SL from phage clone 16 and anti-MA scFv SA from phage clone 18 complied with the criteria for potential utility in MALIA. To the best of our knowledge, this is the first study to increase the binding avidities of anti-MA scFv's using the two oligomerization strategies described in chapters 2 and 3. From this study therefore, anti-MA scFv SA from phage clone 18 appears to be the best candidate multimer to consider for use in a POC TB diagnostic test with respect to stability, high sensitivity, binding avidity to MAs, high specificity due to no cholesterol cross-reactivity and less production cost compared to eukaryotic expressed gallibodies. How amenable the oligomers are towards labelling with gold without loss of biological antigen binding activity remains to be determined.

4.5 CONCLUSION

In conclusion, this is the first study that resulted in the successful expression of multimeric scFv's against *Mycobacterium tuberculosis* MAs, using two different strategies of multimerization. In both strategies, individual anti-MA clones were found that did not give the desired products, usually due to an inability to form stable multimers, but also some that displayed cross-reactivity to cholesterol. The LFIA prototype test demonstrated the feasibility of using such scFv multimers in a lateral flow immunoassay from small blood samples. Of all the multimeric scFv's, anti-MA scFv SA from phage clone 18 appeared to be the best qualified to be used in the development of a cost-effective POC TB diagnostic test with regards to stability, high sensitivity towards binding MA, high specificity by not cross-reacting to cholesterol and affordable production. The aims to increase the functional binding avidities of the anti-MA scFv's from the *Nkuku* library and the demonstration of their successful detection in a lateral flow immunoassay were therefore achieved. This prepares the way for the development of such a much needed affordable POC test for TB diagnosis that is based on non-invasive blood sampling, and which may be used in an environment where there is no electricity. As such, this dissertation successfully addressed the technical aspects of the most pressing need that currently exists for the improved management of the global TB epidemic.

4.6 REFERENCES

ADAMS, G., SCHIER, R., MCCALL, A., CRAWFORD, R., WOLF, E., WEINER, L. & MARKS, J. 1998. Prolonged in vivo tumour retention of a human diabody targeting the extracellular domain of human HER2/neu. *British Journal of Cancer,* 77**,** 1405.

ADDINGTON, W. W. 1979. Patient compliance: the most serious remaining problem in the control of tuberculosis in the United States. *Chest,* 76**,** 741-743.

AHMED, N., MOHANTY, A. K., MUKHOPADHYAY, U., BATISH, V. K. & GROVER, S. 1998. PCR-based rapid detection of *Mycobacterium tuberculosis* in blood from immunocompetent patients with pulmonary tuberculosis. *Journal of Clinical Microbiology,* 36**,** 3094-3095.

ALVING, C. R. & WASSEF, N. M. 1999. Naturally occurring antibodies to cholesterol: a new theory of LDL cholesterol metabolism. *Immunology Today,* 20**,** 362-366.

ARGOS, P. 1990. An investigation of oligopeptides linking domains in protein tertiary structures and possible candidates for general gene fusion. *Journal of Molecular Biology,* 211**,** 943-958.

AZIZ, M. A., WRIGHT, A., LASZLO, A., DE MUYNCK, A., PORTAELS, F., VAN DEUN, A., WELLS, C., NUNN, P., BLANC, L. & RAVIGLIONE, M. 2006. Epidemiology of antituberculosis drug resistance (the Global Project on Anti-tuberculosis Drug Resistance Surveillance): an updated analysis. *The Lancet,* 368**,** 2142-2154.

BARRIOS, Y., JIRHOLT, P. & OHLIN, M. 2004. Length of the antibody heavy chain complementarity determining region 3 as a specificity-determining factor. *Journal of Molecular Recognition,* 17**,** 332-338.

BENADIE, Y., DEYSEL, M., SIKO, D. G. R., ROBERTS, V. V., VAN WYNGAARDT, S., THANYANI, S. T., SEKANKA, G., TEN BOKUM, A. M., COLLETT, L. A., GROOTEN, J., BAIRD, M. S. & VERSCHOOR, J. A. 2008. Cholesteroid nature of free mycolic acids from *M. tuberculosis. Chemistry and Physics of Lipids,* 152**,** 95-103.

BETTER, M., CHANG, C. P., ROBINSON, R. R. & HORWITZ, A. H. 1988. Escherichia coli secretion of an active chimeric antibody fragment. *Science,* 240**,** 1041-1043.

BEUKES, M., LEMMER, Y., DEYSEL, M., AL DULAYYMI J. R., BAIRD, M. S., KOZA, G., IGLESIAS, M. M., ROWLES, R. R., THEUNISSEN, C., GROOTEN, J., TOSCHI, G., ROBERTS, V. V., PILCHER, L., VAN WYNGAARDT, S., MATHEBULA, N., BALOGUN, M., STOLTZ, A. C. & VERSCHOOR, J. A. 2010. Structure–function relationships of the antigenicity of mycolic acids in tuberculosis patients. *Chemistry and Physics of Lipids,* 163**,** 800-808.

BHALLA, A. S., GOYAL, A., GULERIA, R. & GUPTA, A. K. 2015. Chest tuberculosis: Radiological review and imaging recommendations. *The Indian Journal of Radiology & Imaging,* 25**,** 213.

BIE, C.-Q., YANG, D.-H., LIANG, X.-J. & TANG, S.-H. 2010. Construction of non-covalent single-chain Fv dimers for hepatocellular carcinoma and their biological functions. *World Journal of Hepatology,* 2**,** 185.

BIRD, R. E., HARDMAN, K. D., JACOBSON, J. W., JOHNSON, S., KAUFMAN, B. M., LEE, S.-M., LEE, T., POPE, S. H., RIORDAN, G. S. & WHITLOW, M. 1988. Single-chain antigen-binding proteins. *Science,* 242**,** 423-426.

BURRILL, J., WILLIAMS, C. J., BAIN, G., CONDER, G., HINE, A. L. & MISRA, R. R. 2007. Tuberculosis: a radiologic review. *Radiographics,* 27**,** 1255-1273.

BUTLER, W. R. & GUTHERTZ, L. S. 2001. Mycolic acid analysis by high-performance liquid chromatography for identification of Mycobacterium species. *Clinical microbiology reviews,* 14**,** 704-726.

CASTELLANOS-MENDOZA, A., CASTRO-ACOSTA, R. M., OLVERA, A., ZAVALA, G., MENDOZA-VERA, M., GARCÍA-HERNÁNDEZ, E., ALAGÓN, A., TRUJILLO-ROLDÁN, M. A. & VALDEZ-CRUZ, N. A. 2014. Influence of pH control in the formation of inclusion bodies during production of recombinant sphingomyelinase-D in *Escherichia coli*. *Microbial Cell Factories,* 13**,** 137.

CASTRO, K. G., GOLDBERG, S., JEREB, J. A., LOBUE, P., MAZUREK, G. H. & VERNON, A. 2010. Updated guidelines for using interferon gamma release assays to detect *Mycobacterium tuberculosis* infection--United States, 2010.

CHAN, E. D., REVES, R., BELISLE, J. T., BRENNAN, P. J. & HAHN, W. E. 2000. Diagnosis of tuberculosis by a visually detectable immunoassay for lipoarabinomannan. *American Journal of Respiratory and Critical Care Medicine,* 161**,** 1713-1719.

CHEUNG, N.-K. V., MODAK, S., LIN, Y., GUO, H., ZANZONICO, P., CHUNG, J., ZUO, Y., SANDERSON, J., WILBERT, S. & THEODORE, L. J. 2004. Single-chain Fv-streptavidin substantially improved therapeutic index in multistep targeting directed at disialoganglioside GD2. *Journal of Nuclear Medicine,* 45**,** 867-877.

CHOI, J. & LEE, S. 2004. Secretory and extracellular production of recombinant proteins using Escherichia coli. *Applied Microbiology and Biotechnology,* 64**,** 625-635.

CHOPRA, I. & BRENNAN, P. 1998. Molecular action of anti-mycobacterial agents. *Tubercle and Lung Disease,* 78**,** 89-98.

CLOUTIER, S., COUTY, S., TERSKIKH, A., MARGUERAT, L., CRIVELLI, V., PUGNIERES, M., MANI, J.-C., LEISINGER, H.-J., MACH, J. & DEPERTHES, D. 2000. Streptabody, a high avidity molecule made by tetramerization of in vivo biotinylated, phage display-selected scFv fragments on streptavidin. *Molecular Immunology,* 37**,** 1067-1077.

COLDITZ, G. A., BERKEY, C. S., MOSTELLER, F., BREWER, T. F., WILSON, M. E., BURDICK, E. & FINEBERG, H. V. 1995. The efficacy of bacillus Calmette-Guerin vaccination of newborns and infants in the prevention of tuberculosis: meta-analyses of the published literature. *Pediatrics,* 96**,** 29-35.

COLE, S., BROSCH, R., PARKHILL, J., GARNIER, T., CHURCHER, C., HARRIS, D., GORDON, S., EIGLMEIER, K., GAS, S. & BARRY III, C. 1998. Deciphering the biology of *Mycobacterium tuberculosis* from the complete genome sequence. *Nature,* 393**,** 537.

CONNOLLY, L. E., EDELSTEIN, P. H. & RAMAKRISHNAN, L. 2007. Why is long-term therapy required to cure tuberculosis? *PLoS Medicine,* 4**,** e120.

COPP, B. 2006. The Global plan to Stop TB 2006-2015.

CROTHERS, D. M. & METZGER, H. 1972. The influence of polyvalency on the binding properties of antibodies. *Immunochemistry,* 9**,** 341-357.

CRUZ, A. T. & STARKE, J. R. 2007. Clinical manifestations of tuberculosis in children. *Paediatric Respiratory Reviews,* 8**,** 107-117.

CUESTA, Á. M., SAINZ-PASTOR, N., BONET, J., OLIVA, B. & ÁLVAREZ-VALLINA, L. 2010. Multivalent antibodies: when design surpasses evolution. *Trends in Biotechnology,* 28**,** 355-362.

DANNENBERG JR, A. M. & ROOK, G. A. 1994. Pathogenesis of pulmonary tuberculosis: an interplay of tissue-damaging and macrophage-activating immune responses—dual mechanisms that control bacillary multiplication. p 459-483 *In* Bloom B (ed), *Tuberculosis.* ASM Press, Washington, DC.

DATTA, S., SHAH, L., GILMAN, R. H. & EVANS, C. A. 2017. Comparison of sputum collection methods for tuberculosis diagnosis: a systematic review and pairwise and network meta-analysis. *The Lancet Global Health,* 5**,** e760-e771.

DE NORONHA, A. L., BAFICA, A., NOGUEIRA, L., BARRAL, A. & BARRAL-NETTO, M. 2008. Lung granulomas from *Mycobacterium tuberculosis*/HIV-1 co-infected patients display decreased in situ TNF production. *Pathology-Research and Practice,* 204**,** 155-161.

DENKINGER, C. M., DOLINGER, D., SCHITO, M., WELLS, W., COBELENS, F., PAI, M., ZIGNOL, M., CIRILLO, D. M., ALLAND, D. & CASENGHI, M. 2015a. Target product profile of a molecular drug-susceptibility test for use in microscopy centers. *The Journal of Infectious Diseases,* 211**,** S39-S49.

DENKINGER, C. M., KIK, S. V., CIRILLO, D. M., CASENGHI, M., SHINNICK, T., WEYER, K., GILPIN, C., BOEHME, C. C., SCHITO, M. & KIMERLING, M. 2015b. Defining the needs for next generation assays for tuberculosis. *The Journal of Infectious Diseases,* 211**,** S29-S38.

DOHERTY, T. M., DEMISSIE, A., OLOBO, J., WOLDAY, D., BRITTON, S., EGUALE, T., RAVN, P. & ANDERSEN, P. 2002. Immune responses to the *Mycobacterium tuberculosis*-specific antigen ESAT-6 signal subclinical infection among contacts of tuberculosis patients. *Journal of Clinical Microbiology,* 40**,** 704-706.

DOWDY, D. W., STEINGART, K. R. & PAI, M. 2011. Serological testing versus other strategies for diagnosis of active tuberculosis in India: a cost-effectiveness analysis. *PLoS Medicine,* 8**,** e1001074.

DÜBEL, S., BREITLING, F., KONTERMANN, R., SCHMIDT, T., SKERRA, A. & LITTLE, M. 1995. Bifunctional and multimeric complexes of streptavidin fused to single chain antibodies (scFv). *Journal of Imunological Methods,* 178**,** 201-209.

DYE, C., SCHEELE, S., PATHANIA, V. & RAVIGLIONE, M. C. 1999. Global burden of tuberculosis: estimated incidence, prevalence, and mortality by country. *JAMA,* 282**,** 677-686.

EWER, K., DEEKS, J., ALVAREZ, L., BRYANT, G., WALLER, S., ANDERSEN, P., MONK, P. & LALVANI, A. 2003. Comparison of T-cell-based assay with tuberculin skin test for diagnosis of *Mycobacterium tuberculosis* infection in a school tuberculosis outbreak. *The Lancet,* 361**,** 1168-1173.

FORBES, B. & HICKS, K. 1993. Direct detection of *Mycobacterium tuberculosis* in respiratory specimens in a clinical laboratory by polymerase chain reaction. *Journal of Clinical Microbiology,* 31**,** 1688-1694.

FÖRSTER, G. J., SANTOS, E. B., SMITH-JONES, P. M., ZANZONICO, P. & LARSON, S. M. 2006. Pretargeted radioimmunotherapy with a single-chain antibody/streptavidin construct and radiolabeled DOTA-biotin: strategies for reduction of the renal dose. *Journal of Nuclear Medicine,* 47**,** 140-149.

GEORGIOU, G. & VALAX, P. 1996. Expression of correctly folded proteins in *Escherichia coli*. *Current Opinion in Biotechnology,* 7**,** 190-197.

GENSCRIPT.COM. (2019). *pUC57 plasmid DNA Vector - GenScript*. [online] Available at: https://www.genscript.com/vector/SD1176-pUC57_plasmid_DNA.html [Accessed 15 Nov. 2019].

GHODBANE, R., RAOULT, D. & DRANCOURT, M. 2014. Dramatic reduction of culture time of *Mycobacterium tuberculosis*. *Scientific reports,* 4**,** 4236.

GOODRUM, M., SIKO, D. G. R., NIEHUES, T., EICHELBAUER, D. & VERSCHOOR, J. A. 2001. Mycolic acids from *Mycobacterium tuberculosis*: purification by countercurrent distribution and T-cell stimulation. *Microbios,* 106**,** 55-67.

GRANT, L. R., HAMMITT, L. L., MURDOCH, D. R., O'BRIEN, K. L. & SCOTT, J. A. 2012. Procedures for collection of induced sputum specimens from children. *Clinical Infectious Diseases,* 54**,** S140-S145.

GUIRADO, E. & SCHLESINGER, L. 2013. Modeling the *Mycobacterium tuberculosis* granuloma–the critical battlefield in host immunity and disease. *Frontiers in Immunology,* 4**,** 98.

GUPTA, R. K., LUCAS, S. B., FIELDING, K. L. & LAWN, S. D. 2015. Prevalence of tuberculosis in post-mortem studies of HIV-infected adults and children in resource-limited settings: a systematic review and meta-analysis. *AIDS (London, England),* 29**,** 1987.

HAMASUR, B., BRUCHFELD, J., HAILE, M., PAWLOWSKI, A., BJORVATN, B., KÄLLENIUS, G. & SVENSON, S. B. 2001. Rapid diagnosis of tuberculosis by detection of mycobacterial lipoarabinomannan in urine. *Journal of Microbiological Methods,* 45**,** 41-52.

HAMIDON, N. H., SURAIYA, S., SARMIENTO, M. E., ACOSTA, A., NORAZMI, M. N. & LIM, T. S. 2018. Immune TB antibody phage display library as a tool to study B cell immunity in TB infections. *Applied Biochemistry and Biotechnology,* 184**,** 852-868.

HASENWINKLE, D., JERVIS, E., KOPS, O., LIU, C., LESNICKI, G., HAYNES, C. A. & KILBURN, D. G. 1997. Very high-level production and export in *Escherichia coli* of a cellulose binding domain for use in a generic secretion-affinity fusion system. *Biotechnology and Bioengineering,* 55**,** 854-863.

HENDRICKSON, W. A., PÄHLER, A., SMITH, J. L., SATOW, Y., MERRITT, E. A. & PHIZACKERLEY, R. P. 1989. Crystal structure of core streptavidin determined from multiwavelength anomalous diffraction of synchrotron radiation. *Proceedings of the National Academy of Sciences,* 86**,** 2190-2194.

HOLLIGER, P., PROSPERO, T. & WINTER, G. 1993. " Diabodies": small bivalent and bispecific antibody fragments. *Proceedings of the National Academy of Sciences,* 90**,** 6444-6448.

HOLLIGER, P. & WINTER, G. 1997. Diabodies: small bispecific antibody fragments. *Cancer Immunology, Immunotherapy,* 45**,** 128-130.

HORVÁTH, A., BÁNHEGYI, D., BÍRÓ, A., UJHELYI, E., VERES, A., HORVÁTH, L., PROHÁSZKA, Z., BÁCSI, A., TARJÁN, V. & ROMICS, L. 2001. High level of anticholesterol antibodies (ACHA) in HIV patients. Normalization of serum ACHA concentration after introduction of HAART. *Immunobiology,* 203**,** 756-768.

HORVÁTH, A. & BíRÓ, A. 2003. Anti-cholesterol antibodies in human sera. *Autoimmunity Reviews,* 2**,** 272-277.

HORWITZ, A. H., CHANG, C. P., BETTER, M., HELLSTROM, K. E. & ROBINSON, R. R. 1988. Secretion of functional antibody and Fab fragment from yeast cells. *Proceedings of the National Academy of Sciences,* 85**,** 8678-8682.

HU, W.-G., ALVI, A. Z., FULTON, R. E., SURESH, M. R. & NAGATA, L. P. 2002. Genetic engineering of streptavidin-binding peptide tagged single-chain variable fragment antibody to Venezuelan equine encephalitis virus. *Hybridoma and Hybridomics,* 21**,** 415-420.

HUDSON, P. J. & KORTT, A. A. 1999. High avidity scFv multimers; diabodies and triabodies. *Journal of Immunological Methods,* 231**,** 177-189.

HUSTON, J. S., LEVINSON, D., MUDGETT-HUNTER, M., TAI, M.-S., NOVOTNÝ, J., MARGOLIES, M. N., RIDGE, R. J., BRUCCOLERI, R. E., HABER, E. & CREA, R. 1988. Protein engineering of antibody binding sites: recovery of specific activity in an anti-digoxin single-chain Fv analogue produced in *Escherichia coli*. *Proceedings of the National Academy of Sciences,* 85**,** 5879-5883.

IOANNIDIS, P., PAPAVENTSIS, D., KARABELA, S., NIKOLAOU, S., PANAGI, M., RAFTOPOULOU, E., KONSTANTINIDOU, E., MARINOU, I. & KANAVAKI, S. 2011. Cepheid GeneXpert MTB/RIF assay for *Mycobacterium tuberculosis* detection and rifampin resistance identification in patients with substantial clinical indications of tuberculosis and smear-negative microscopy results. *Journal of Clinical Microbiology,* 49**,** 3068-3070.

JAEGER, S., CANDEMIR, S., ANTANI, S., WÁNG, Y.-X. J., LU, P.-X. & THOMA, G. 2014. Two public chest X-ray datasets for computer-aided screening of pulmonary diseases. *Quantitative Imaging in Medicine and Surgery,* 4**,** 475.

JAENICKE, R. 1990. Protein structure and function at low temperatures. *Philosophical Transactions of the Royal Society of London. B, Biological Sciences,* 326**,** 535-553.

KAFWABULULA, M., AHMED, K., NAGATAKE, T., GOTOH, J., MITARAI, S., OIZUMI, K. & ZUMLA, A. 2002. Evaluation of PCR-based methods for the diagnosis of tuberculosis by identification of mycobacterial DNA in urine samples. *The International Journal of Tuberculosis and Lung Disease,* 6**,** 732-737.

KANE, J. F. & HARTLEY, D. L. 1988. Formation of recombinant protein inclusion bodies in *Escherichia coli*. *Trends in Biotechnology,* 6**,** 95-101.

KARDOS, M. & KIMBALL, A. B. 2012. Time for a change? Updated guidelines using interferon gamma release assays for detection of latent tuberculosis infection in the office setting. *Journal of the American Academy of Dermatology*, 66(1), 148-152.

KIPRIYANOV, S. M., LITTLE, M., KROPSHOFER, H., BREITLING, F., GOTTER, S. & DÜBEL, S. 1996. Affinity enhancement of a recombinant antibody: formation of complexes with multiple valency by a single-chain Fv fragment–core streptavidin fusion. *Protein Engineering, Design and Selection,* 9**,** 203-211.

KIPRIYANOV, S. M., MOLDENHAUER, G. & LITTLE, M. 1997. High level production of soluble single chain antibodies in small-scale *Escherichia coli* cultures. *Journal of Immunological Methods,* 200**,** 69-77.

KIVIHYA-NDUGGA, L., VAN CLEEFF, M., JUMA, E., KIMWOMI, J., GITHUI, W., OSKAM, L., SCHUITEMA, A., VAN SOOLINGEN, D., NGANGA, L. & KIBUGA, D. 2004. Comparison of PCR with the routine procedure for diagnosis of tuberculosis in a population with high prevalences of tuberculosis and human immunodeficiency virus. *Journal of Clinical Microbiology,* 42**,** 1012-1015.

KOCH, R. 1982. The etiology of tuberculosis. *Reviews of Infectious Diseases,* 4**,** 1270-1274.

KOO, K., FOEGEDING, P. M. & SWAISGOOD, H. E. 1998. Development of a Streptavidin-Conjugated Single-Chain Antibody That Binds Bacillus cereusSpores. *Applied Environmental Microbiology.,* 64**,** 2497-2502.

KORTT, A. A., DOLEZAL, O., POWER, B. E. & HUDSON, P. J. 2001. Dimeric and trimeric antibodies: high avidity scFvs for cancer targeting. *Biomolecular Engineering,* 18**,** 95-108.

KORTT, A. A., LAH, M., ODDIE, G. W., GRUEN, C. L., BURNS, J. E., PEARCE, L. A., ATWELL, J. L., MCCOY, A. J., HOWLETT, G. J. & METZGER, D. W. 1997. Single-chain Fv fragments of anti-neuraminidase antibody NC10 containing five-and ten-residue linkers form dimers and with zero-residue linker a trimer. *Protein Engineering,* 10**,** 423-433.

KUBIAK, R. J., LEE, N., ZHU, Y., FRANCH, W. R., LEVITSKAYA, S. V., KRISHNAN, S. R., ABRAHAM, V., AKUFONGWE, P. F., LARKIN, C. J. & WHITE, W. I. 2016. Storage conditions of conjugated reagents can impact results of immunogenicity assays. *Journal of Immunology Research,* 2016, 1-10.

LALVANI, A. & PAREEK, M. 2010. Interferon gamma release assays: principles and practice. *Enfermedades Infecciosas y Microbiologia Clinica,* 28**,** 245-252.

LAWN, S. D. 2012. Point-of-care detection of lipoarabinomannan (LAM) in urine for diagnosis of HIV-associated tuberculosis: a state of the art review. *BMC Infectious Diseases,* 12**,** 103.

LAWN, S. D., KERKHOFF, A. D., VOGT, M. & WOOD, R. 2012. Clinical significance of lipoarabinomannan detection in urine using a low-cost point-of-care diagnostic assay for HIV-associated tuberculosis. *AIDS,* 26**,** 1635-1643.

LAWN, S. D. & NICOL, M. P. 2011. Xpert® MTB/RIF assay: development, evaluation and implementation of a new rapid molecular diagnostic for tuberculosis and rifampicin resistance. *Future Microbiology,* 6**,** 1067-1082.

LEMMER, Y., THANYANI, S. T., VREY, P. J., DRIVER, C. H. S., VENTER, L., VAN WYNGAARDT, S., TEN BOKUM, A. M. C., OZOEMENA, K., PILCHER, L. A., FERNIG, D G., STOLTZ, A. C., SWAI, H. S. & VERSCHOOR, J. A. 2009. Detection of antimycolic acid antibodies by liposomal biosensors. *Methods in Enzymology,* 464**,** 79-104.

LI, J. Y., SUGIMURA, K., J. BOADO, R., LEE, H. J., ZHANG, C., DUEBEL, S. & M. PARDRIDGE, W. 1999. Genetically engineered brain drug delivery vectors: cloning, expression and in vivo application of an anti-transferrin receptor single chain antibody–streptavidin fusion gene and protein. *Protein Engineering,* 12**,** 787-796.

LIN, Y., PAGEL, J. M., AXWORTHY, D., PANTELIAS, A., HEDIN, N. & PRESS, O. W. 2006. A genetically engineered anti-CD45 single-chain antibody-streptavidin fusion protein for pretargeted radioimmunotherapy of hematologic malignancies. *Cancer Research,* 66**,** 3884-3892.

LUCA, S. & MIHAESCU, T. 2013. History of BCG Vaccine. *Journal of Clinical Medicine,* 8, 53-58.

MAKRIDES, S. C. 1996. Strategies for achieving high-level expression of genes in *Escherichia coli*. *Microbiolog &. Molecular Biology Reviews,* 60**,** 512-538.

MALHOTRA, A. 2009. Tagging for protein expression. *Methods in Enzymology,* 463, 239-258.

MARAKALALA, M. J., RAJU, R. M., SHARMA, K., ZHANG, Y. J., EUGENIN, E. A., PRIDEAUX, B., DAUDELIN, I. B., CHEN, P.-Y., BOOTY, M. G. & KIM, J. H. 2016. Inflammatory signaling in human tuberculosis granulomas is spatially organized. *Nature Medicine,* 22**,** 531.

NDLANDLA, F., EJOH, V., STOLTZ, A. C., NAICKER, B., CROMARTY, A. D., VAN WYNGAARDT, S., KHATI, M., ROTHERHAM, L., LEMMER, Y., NIEBUHR, J., BAUMEISTER, C. R., AL DULAYYMI, J. R., SWAI, H., BAIRD, M. S. & VERSCHOOR, J.A. 2016. Standardization of natural mycolic acid antigen composition and production for use in biomarker antibody detection to diagnose active tuberculosis. *Journal of Immunological Methods,* 435**,** 50-59.

OBERHELMAN, R. A., SOTO-CASTELLARES, G., GILMAN, R. H., CASTILLO, M. E., KOLEVIC, L., DELPINO, T., SAITO, M., SALAZAR-LINDO, E., NEGRON, E. & MONTENEGRO, S. 2015. A controlled study of tuberculosis diagnosis in HIV-infected and uninfected children in Peru. *PloS One,* 10**,** e0120915.

OKINO, L., OKINO, L., OKINO, L. AND TISONE, K. . 2019. *BioDot | Low Volume Precision Dispensing Equipment.* [Online]. Available: https://www.biodot.com/ [Accessed 18 November 2019].

PÄHLER, A., HENDRICKSON, W., KOLKS, M., ARGARANA, C. & CANTOR, C. 1987. Characterization and crystallization of core streptavidin. *Journal of Biological Chemistry,* 262**,** 13933-13937.

PAN, J., FUJIWARA, N., OKA, S., MAEKURA, R., OGURA, T. & YANO, I. 1999. Anti-cord factor (trehalose 6, 6'-dimycolate) IgG antibody in tuberculosis patients recognizes mycolic acid subclasses. *Microbiology and Immunology,* 43**,** 863-869.

PANDEY, A. K. & SASSETTI, C. M. 2008. Mycobacterial persistence requires the utilization of host cholesterol. *Proceedings of the National Academy of Sciences,* 105**,** 4376-4380.

PEARCE, L. A., ODDIE, G. W., COIA, G., KORTT, A. A., HUDSON, P. J. & LILLEY, G. G. 1997. Linear gene fusions of antibody fragments with streptavidin can be linked to biotin labelled secondary molecules to form bispecific reagents. *IUBMB Life,* 42**,** 1179-1188.

PEYRON, P., BORDIER, C., ELSA-NOAH, N. & MARIDONNEAU-PARINI, I. 2000. Nonopsonic phagocytosis of Mycobacterium kansasii by human neutrophils depends on cholesterol and is mediated by CR3 associated with glycosylphosphatidylinositol-anchored proteins. *The Journal of Immunology,* 165**,** 5186-5191.

PLÜCKTHUN, A. & PACK, P. 1997. New protein engineering approaches to multivalent and bispecific antibody fragments. *Immunotechnology,* 3**,** 83-105.

PRINSLOO, W. 2009. Computational models for conformations of cell wall mycolates from *Mycobacterium tuberculosis.* MSc dissertation, Faculty of Natural and Agricultural Sciences, University of Pretoria.

PUGSLEY, A. P. 1993. The complete general secretory pathway in gram-negative bacteria. *Microbiology and Molecular Biology Reviews,* 57**,** 50-108.

PUGSLEY, A. P., FRANCETIC, O., POSSOT, O. M., SAUVONNET, N. & HARDIE, K. R. 1997. Recent progress and future directions in studies of the main terminal branch of the general secretory pathway in Gram-negative bacteria–a review. *Gene,* 192**,** 13-19.

RAGAVALOO, A. 2019. Towards a rapid immuni-test for Tuberculosis: Immunochemical characterization of suitable mycolic acid antigen preparation. MSc dissertation, Faculty of Natural and Agricultural Sciences, University of Pretoria.

RANCHOD, H., NDLANDLA, F., LEMMER, Y., BEUKES, M., NIEBUHR, J., AL-DULAYYMI, J., WEMMER, S., FEHRSEN, J., BAIRD, M. & VERSCHOOR, J. 2018. The antigenicity and cholesteroid nature of mycolic acids determined by recombinant chicken antibodies. *PloS One,* 13**,** e0200298.

RAVIGLIONE, M. C. & UPLEKAR, M. W. 2006. WHO's new Stop TB Strategy. *The Lancet,* 367**,** 952-955.

ROBERTS, V. V. 2008. Immunochemistry of mycolic acid antigens in tuberculosis. MSc dissertation, Faculty of Natural and Agricultural Sciences, University of Pretoria.

ROCK, E. P., SIBBALD, P. R., DAVIS, M. M. & CHIEN, Y.-H. 1994. CDR3 length in antigen-specific immune receptors. *Journal of Experimental Medicine,* 179**,** 323-328.

ROSENTHAL, I. M., ZHANG, M., WILLIAMS, K. N., PELOQUIN, C. A., TYAGI, S., VERNON, A. A., BISHAI, W. R., CHAISSON, R. E., GROSSET, J. H. & NUERMBERGER, E. L. 2007. Daily dosing of rifapentine cures tuberculosis in three months or less in the murine model. *PLoS Medicine,* 4**,** e344.

ROULSON, J. A., BENBOW, E. & HASLETON, P. S. 2005. Discrepancies between clinical and autopsy diagnosis and the value of post mortem histology; a meta-analysis and review. *Histopathology,* 47**,** 551-559.

ROY, A., EISENHUT, M., HARRIS, R., RODRIGUES, L. C., SRIDHAR, S., HABERMANN, S., SNELL, L., MANGTANI, P., ADETIFA, I. & LALVANI, A. 2014. Effect of BCG vaccination against *Mycobacterium tuberculosis* infection in children: systematic review and meta-analysis. *British Medical Journal,* 349**,** g4643.

RUDOLPH, R. & LILIE, H. 1996. In vitro folding of inclusion body proteins. *The FASEB Journal,* 10**,** 49-56.

SADA, E., BRENNAN, P., HERRERA, T. & TORRES, M. 1990. Evaluation of lipoarabinomannan for the serological diagnosis of tuberculosis. *Journal of Clinical Microbiology,* 28**,** 2587-2590.

SALDARELLI, P., KELLER, H., DELL'ORCO, M., SCHOTS, A., ELICIO, V. & MINAFRA, A. 2005. Isolation of recombinant antibodies (scFvs) to grapevine virus B. *Journal of Virological Methods,* 124**,** 191-195.

SAMANICH, K., KEEN, M., VISSA, V., HARDER, J., SPENCER, J., BELISLE, J., ZOLLA-PAZNER, S. & LAAL, S. 2000. Serodiagnostic potential of culture filtrate antigens of *Mycobacterium tuberculosis*. *Clinical & Diagnostic Laboratory. Immunology.,* 7**,** 662-668.

SANO, T. & CANTOR, C. R. 1990. Expression of a cloned streptavidin gene in Escherichia coli. *Proceedings of the National Academy of Sciences,* 87**,** 142-146.

SANO, T., PANDORI, M. W., CHEN, X., SMITH, C. L. & CANTOR, C. R. 1995. Recombinant core streptavidins a minimum-sized core streptavidin has enhanced structural stability and higher accessibility to biotinylated macromolecules. *Journal of Biological Chemistry,* 270**,** 28204-28209.

SATO, N., HASSAN, R., AXWORTHY, D. B., WONG, K. J., YU, S., THEODORE, L. J., LIN, Y., PARK, L., BRECHBIEL, M. W. & PASTAN, I. 2005. Pretargeted radioimmunotherapy of mesothelin-expressing cancer using a tetravalent single-chain Fv-streptavidin fusion protein. *Journal of Nuclear Medicine,* 46**,** 1201-1209.

SCHLEICHER, G. K., FELDMAN, C., VERMAAK, Y. & VERSCHOOR, J. A. 2002. Prevalence of anti-mycolic acid antibodies in patients with pulmonary tuberculosis co-infected with HIV. *Clinical Chemistry and Laboratory Medicine,* 40**,** 882-887.

SCHOFIELD, L., MCCONVILLE, M. J., HANSEN, D., CAMPBELL, A. S., FRASER-REID, B., GRUSBY, M. J. & TACHADO, S. D. 1999. CD1d-restricted immunoglobulin G formation to GPI-anchored antigens mediated by NKT cells. *Science,* 283**,** 225-229.

SCHULTZ, J., LIN, Y., SANDERSON, J., ZUO, Y., STONE, D., MALLETT, R., WILBERT, S. & AXWORTHY, D. 2000. A tetravalent single-chain antibody-streptavidin fusion protein for pretargeted lymphoma therapy. *Cancer Research,* 60**,** 6663-6669.

SILVA MIRANDA, M., BREIMAN, A., ALLAIN, S., DEKNUYDT, F. & ALTARE, F. 2012. The tuberculous granuloma: an unsuccessful host defence mechanism providing a safety shelter for the bacteria? *Clinical and Developmental Immunology,* 2012, 1-14.

SIXHOLO, J. 2008. Engineering recombinant chicken antibodies for improved characteristics. MSc dissertation, Faculty of Veterinary Sciences, University of Pretoria.

SIXHOLO, J., VAN WYNGAARDT, W., MASHAU, C., FRISCHMUTH, J., DU PLESSIS, D. H. & FEHRSEN, J. 2011. Improving the characteristics of a mycobacterial 16 kDa-specific chicken scFv. *Biologicals,* 39**,** 110-116.

SKERRA, A. & PLUCKTHUN, A. 1988. Assembly of a functional immunoglobulin Fv fragment in Escherichia coli. *Science,* 240**,** 1038-1041.

SMITH, G. P. 1985. Filamentous fusion phage: novel expression vectors that display cloned antigens on the virion surface. *Science,* 228**,** 1315-1317.

SMITH, G. P. & PETRENKO, V. A. 1997. Phage display. *Chemical Reviews,* 97**,** 391-410.

SMITH, P. & MOSS, A. 1994. Epidemiology of tuberculosis. *Tuberculosis.* American Society of Microbiology. p47-59 *In* Bloom B (ed), Tuberculosis. ASM Press, Washington, DC.

SONG, S. H., PARK, K. U., LEE, J. H., KIM, E. C., KIM, J. Q. & SONG, J. 2009. Electrospray ionization-tandem mass spectrometry analysis of the mycolic acid profiles for the identification of common clinical isolates of mycobacterial species. *Journal of Microbiological Methods,* 77**,** 165-177.

STERLING, T. R., PHAM, P. A. & CHAISSON, R. E. 2010. HIV Infection—Related tuberculosis: Clinical manifestations and treatment. *Clinical Infectious Diseases,* 50**,** S223-S230.

SWARTZ, G. M., GENTRY, M. K., AMENDE, L. M., BLANCHETTE-MACKIE, E. J. & ALVING, C. R. 1988. Antibodies to cholesterol. *Proceedings of the National Academy of Sciences,* 85**,** 1902-1906.

THANYANI, S. T., ROBERTS, V., SIKO, D. G. R., VREY, P. & VERSCHOOR, J. A. 2008. A novel application of affinity biosensor technology to detect antibodies to mycolic acid in tuberculosis patients. *Journal of Immunological Methods,* 332**,** 61-72.

TODOROVSKA, A., ROOVERS, R. C., DOLEZAL, O., KORTT, A. A., HOOGENBOOM, H. R. & HUDSON, P. J. 2001. Design and application of diabodies, triabodies and tetrabodies for cancer targeting. *Journal of Immunological Methods,* 248**,** 47-66.

TRUYTS, A. 2019. Towards paper-based micro biosensing of biomarker anti-mycolic acid antibodies for TB diagnosis, MSc dissertation, Faculty of Natural and Agricultural Sciences, University of Pretoria.

VAN CLEEFF, M., KIVIHYA-NDUGGA, L., MEME, H., ODHIAMBO, J. & KLATSER, P. 2005. The role and performance of chest X-ray for the diagnosis of tuberculosis: a cost-effectiveness analysis in Nairobi, Kenya. *BMC Infectious Diseases,* 5**,** 111.

VAN WYNGAARDT, W., MALATJI, T., MASHAU, C., FEHRSEN, J., JORDAAN, F., MILTIADOU, D. & DU PLESSIS, D. H. 2004. A large semi-synthetic single-chain Fv phage display library based on chicken immunoglobulin genes. *BMC Biotechnology,* 4**,** 6.

VERMA, R., BOLETI, E. & GEORGE, A. 1998. Antibody engineering: comparison of bacterial, yeast, insect and mammalian expression systems. *Journal of Immunological Methods,* 216**,** 165-181.

VERSCHOOR, J. A., BAIRD, M. S. & GROOTEN, J. 2012. Towards understanding the functional diversity of cell wall mycolic acids of *Mycobacterium tuberculosis*. *Progress in lipid research,* 51**,** 325-339.

VERSCHOOR, J. A. & BEUKES, M. 2016. Method of detecting surrogate markers in a serum sample. Google Patents.

VILLENEUVE, M., KAWAI, M., KANASHIMA, H., WATANABE, M., MINNIKIN, D. E. & NAKAHARA, H. 2005. Temperature dependence of the Langmuir monolayer packing of mycolic acids from *Mycobacterium tuberculosis*. *Biochimica et Biophysica Acta (BBA)-Biomembranes,* 1715**,** 71-80.

VITI, F., TARLI, L., GIOVANNONI, L., ZARDI, L. & NERI, D. 1999. Increased binding affinity and valence of recombinant antibody fragments lead to improved targeting of tumoral angiogenesis. *Cancer Research,* 59**,** 347-352.

VOLMINK, J. & GARNER, P. 2007. Directly observed therapy for treating tuberculosis. Cochrane Database of Systematic Reviews, Issue 4. Art. No.: CD003343. DOI: 10.1002/14651858.CD003343.pub3.

WANG, W. W.-S., DAS, D., MCQUARRIE, S. A. & SURESH, M. R. 2007. Design of a bifunctional fusion protein for ovarian cancer drug delivery: single-chain anti-CA125 core-streptavidin fusion protein. *European journal of pharmaceutics and biopharmaceutics,* 65**,** 398-405.

WARSINSKE, H., VASHISHT, R. & KHATRI, P. 2019. Host-response-based gene signatures for tuberculosis diagnosis: A systematic comparison of 16 signatures. *PLoS Medicine,* 16**,** e1002786.

WAUGH, D. S. 2005. Making the most of affinity tags. *Trends in Biotechnology,* 23**,** 316-320.

WEMMER, S. 2008. *Expression and engineering of recombinant antibodies against a heat-shock protein of Mycobacterium bovis.* Master of Science in the Faculty of Veterinary Sciences University of Pretoria.

WHO 2014. High priority target product profiles for new tuberculosis diagnostics: report of a consensus meeting, 28-29 April 2014, Geneva, Switzerland. World Health Organization.

WHO 2015. The use of lateral flow urine lipoarabinomannan assay (LF-LAM) for the diagnosis and screening of active tuberculosis in people living with HIV: policy guidance. World Health Organization.

WHO 2017. Bending the curve–ending TB: annual report 2017. *Regional Office for South-East Asia, New Delhi, India*.

WHO 2018. *Global tuberculosis report 2018*, World Health Organization.

WINKLER, S., NECEK, M., WINKLER, H., ADEGNIKA, A. A., PERKMANN, T., RAMHARTER, M. & KREMSNER, P. G. 2005. Increased specific T cell cytokine responses in patients with active pulmonary tuberculosis from Central Africa. *Microbes and Infection,* 7**,** 1161-1169.

WINTER, G., GRIFFITHS, A. D., HAWKINS, R. E. & HOOGENBOOM, H. R. 1994. Making antibodies by phage display technology. *Annual Review of Immunology,* 12**,** 433-455.

WINTER, G. & MILSTEIN, C. 1991. Man-made antibodies. *Nature,* 349**,** 293.

WON, J.-S., KANG, H.-W., NAM, P.-W. & CHOE, M.-H. 2009. B3 (Fab)-streptavidin tetramer has higher binding avidity than B3 (scFv)-streptavidin tetramer. *Bulletin of the Korean Chemical Society,* 30**,** 1101-1106.

WOODROFFE, A. J. & WILSON, C. B. 1977. An evaluation of elution techniques in the study of immune complex glomerulonephritis. *The Journal of Immunology,* 118**,** 1788-1794.

WÖRN, A. & PLÜCKTHUN, A. 1999. Different equilibrium stability behavior of ScFv fragments: identification, classification, and improvement by protein engineering. *Biochemistry,* 38**,** 8739-8750.

WRIGHT, A., ZIGNOL, M., VAN DEUN, A., FALZON, D., GERDES, S. R., FELDMAN, K., HOFFNER, S., DROBNIEWSKI, F., BARRERA, L. & VAN SOOLINGEN, D. 2009. Epidemiology of antituberculosis drug resistance 2002–07: an updated analysis of the Global Project on Anti-Tuberculosis Drug Resistance Surveillance. *The Lancet,* 373**,** 1861-1873.

XU, J. L. & DAVIS, M. M. 2000. Diversity in the CDR3 region of VH is sufficient for most antibody specificities. *Immunity,* 13**,** 37-45.

YAJIMA, W., RAHMAN, M. H., DAS, D., SURESH, M. R. & KAV, N. N. 2008. Detection of Sclerotinia sclerotiorum using a monomeric and dimeric single-chain fragment variable (scFv) antibody. *Journal of agricultural and food chemistry,* 56**,** 9455-9463.

YOUNG, C. L., BRITTON, Z. T. & ROBINSON, A. S. 2012. Recombinant protein expression and purification: a comprehensive review of affinity tags and microbial applications. *Biotechnology Journal,* 7**,** 620-634.

ZHANG, Y., HEYM, B., ALLEN, B., YOUNG, D. & COLE, S. 1992. The catalase—peroxidase gene and isoniazid resistance of *Mycobacterium tuberculosis*. *Nature,* 358**,** 591.

ZHANG, Z., PEN, Y., EDYVEAN, R. G., BANWART, S. A., DALGLIESH, R. M. & GEOGHEGAN, M. 2010. Adhesive and conformational behaviour of mycolic acid monolayers. *Biochimica et Biophysica Acta (BBA)-Biomembranes,* 1798**,** 1829-1839.

4.7 APPENDIX

The sephadex 75 10/300 GL column was calibrated using two proteins of known molecular weight, casein (24 kDa) and BSA (67 kDa) in order to determine the degree of oligomerization of the anti-MA scFv SLs. The elution profiles of the BSA and casein are depicted in Figure A-1.

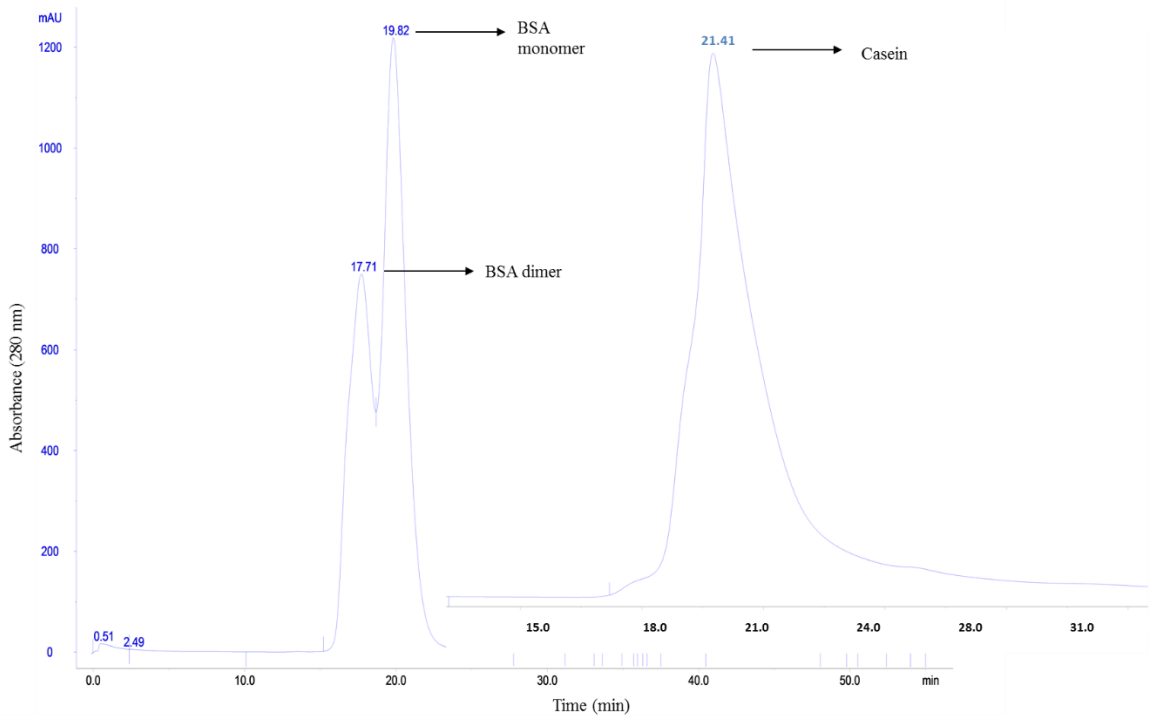

Figure A-1: SEC profiles of bovine serum albumin (BSA) and casein proteins for the calibration of the sephadex column. A volume of 25 µL of 0.5 mg/mL concentrated sample was loaded on the column, the flow rate of the column was 0.5 mL/min and the SEC was carried out until all fractions were eluted.

Figure A-1 shows that BSA possesses two peaks, one that is monomeric (19.82 min) and the other dimeric (17.71 min). Casein eluted at 21.41 min depicting a monomeric peak. The elution profile of BSA shows that the protein eluted in the void volume.

The Western blot analysis in Figure 2-12 for the analysis of unpurified and purified anti-MA scFv SLs from phage clones 12 and 16 was constructed using the Western blot assays as depicted by Figure A-2.

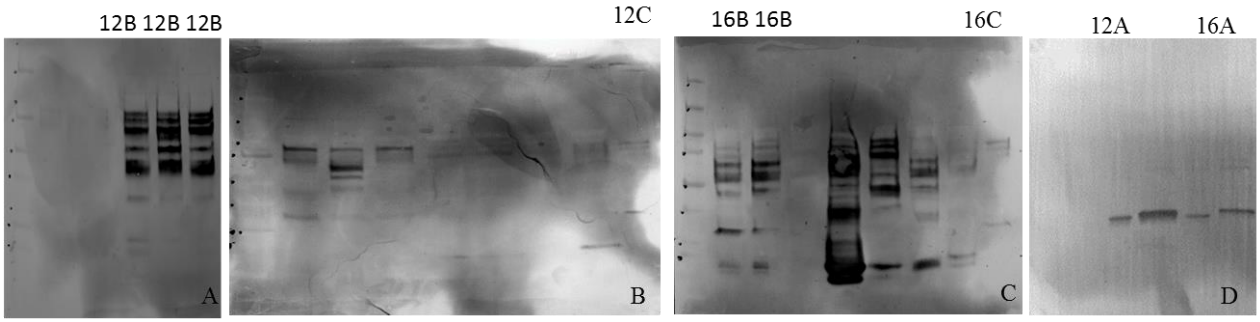

<u>Figure A-2:</u> Original Western blot assays for the analysis of unpurified and purified anti-MA scFv SLs from phage clones 12 and 16. (A) Three samples of anti-MA scFv SL from phage clone 12 before purification (12B). (B) One sample of the control anti-MA scFv from phage clone 12. (C) Two samples of anti-MA scFv SL from phage clone 16 before purification (16B) and one sample of the control anti-MA scFv from phage clone 16 (16C). (C) One sample of anti-MA scFv SL from phage clone 12 after purification (12A) and one sample of anti-MA scFv SL from phage clone 16 after purification (16A).